



UNIVERSITY OF
KWAZULU-NATAL

INYUVESI
YAKWAZULU-NATALI

**QUADRATURE SPATIAL MODULATION AIDED SINGLE-
INPUT MULTIPLE-OUTPUT-MEDIA BASED
MODULATION: APPLICATION TO COOPERATIVE
NETWORK AND GOLDEN CODE ORTHOGONAL SUPER-
SYMBOL SYSTEMS**

By

Bamisaye, Ayodeji James

A Thesis submitted in fulfilment of the academic requirements for the degree of

Doctor of Philosophy in Electronic Engineering

at the School of Engineering,

University of KwaZulu-Natal

South Africa

Supervisor: Dr Tahmid Quazi

February, 2022

As the candidate's supervisor, I agree with the submission of this thesis.

Signed:

Date.....

Supervisor: Dr Tahmid Quazi

DECLARATION 1 – PLAGIARISM

I, Ayodeji James Bamisaye, declare that:

1. The research reported in this thesis, except where otherwise indicated, is my original research.
2. This thesis has not been submitted for any degree or examination at any other university.
3. This thesis does not contain other persons' data, pictures, graphs, or other information unless specifically acknowledged as being sourced from other persons.
4. This thesis does not contain other persons' writing, unless specifically acknowledged as being sourced from other researchers. Where other written sources have been quoted, then:
 - a. Their words have been re-written, but the general information attributed to them has been referenced
 - b. Where their exact words have been used, then their writing has been placed in italics and inside quotation marks and referenced.
5. This thesis does not contain text, graphics or tables copied and pasted from the Internet, unless specifically acknowledged, and the source being detailed in the thesis and in the References sections.

Signed:

January 24, 2022
Date

Ayodeji James Bamisaye

DECLARATION 2 – PUBLICATIONS

This section includes details of publications that form part of the research presented in this thesis. These manuscripts include published and submitted manuscripts. All publications are written by the student, Ayodeji James Bamisaye, and by the research supervisor, Dr. Tahmid Quazi.

Publication 1: A. J Bamisaye, T. Quazi “Quadrature spatial modulation-aided single-input multiple output- media-based modulation”. International Journal of Communication Systems. Vol.34, Iss 11, 2021; e4883. <https://doi.org/10.1002/dac.4883> (*Published*)

Publication 2: A. J Bamisaye, T. Quazi “Two-Way Decode and Forward Quadrature Media-Based Modulation for Single-Input Multiple-Output Scheme” International Journal of Communication Systems. Vol.35, Iss 11, 2022; e5186. doi:10.1002/dac.5186 (*Published*)

Publication 3: A. J Bamisaye, T. Quazi “Application of Golden Code Orthogonal Super-Symbol in Media-Based Modulation for Single-Input Multiple-Output Schemes” Journal of Telecommunications and information Technology. 2/2022, pp 43-48. <https://doi.org/10.26636/jtit.2022.158921> (*published*)

Signed:

January 24, 2022
Date

Ayodeji James Bamisaye

ACKNOWLEDGEMENTS

First and foremost, I give glory to my Maker, my Sustainer, and my Keeper for HIS mercy, protection, provision, and guidance throughout this study, may HIS name be praised forever.

It is with immense gratitude that I acknowledge the support and help of my supervisor, Dr Tahmid Quazi, for his selfless research guidance, dedication, invaluable advice, and support that led to the success of my PhD thesis submission. I consider it an honor to work with him.

I am indebted to my many research colleagues with whom I enjoyed discussing problems and sharing ideas. Notably include Shaheen Solwa, Segun Oladoyinbo, and Olawoye Taiwo. I cannot find words to express my gratitude to Tertiary Education Trust Fund (TETFUND) and Federal Polytechnic, Ado-Ekiti, for financing my PhD programme.

I also thank all the Electrical & Electronics Engineering staff, Federal Polytechnic, Ado-Ekiti for their support and encouragement.

I owe my deepest gratitude to my mother, Mrs. Juliana Aduke Bamisaye, my wife, Funmilola Bamisaye, and my children, Oluwadamilola, Oyindamola, and Oluwafisayomi Bamisaye. God bless you all.

DEDICATION

This thesis is dedicated to:

- Almighty God, my Glory, the Bishop of my soul and Lifter of my head.
- My wife: Funmilola Aduke Bamisaye: - for your Love, prayers, support, and belief that I could do it.
- Daughters of Zion: Oluwadamilola Opeyemi Bamisaye, Oyindamola Hephzibah Bamisaye, and Oluwafisayomi Greatness Bamisaye:- for their Prayers, Love, and being an encouragement to me.
- Loving memory of my Dad: Chief Michael Omodara Bamisaye:- you are so loved and missed.

Abstract

SIMO-MBM (single-input multiple-output media-based modulation) overcomes the limitations of SIMO (single-input multiple-output) systems by reducing the number of antennas required to achieve a high data rate and improved error performance. In this thesis, the quadrature dimension of the spatial constellation is used to improve the overall error performance of the conventional SIMO-MBM and to achieve a higher data rate by decomposing the amplitude/phase modulation (APM) symbol into real and imaginary components, similar to quadrature spatial modulation (QSM).

The average bit error probability of the proposed technique is expressed using a lower bound approach and validated using the results of Monte Carlo simulation (MCS). The proposed system also investigates the effect of antenna correlation in combination with channel amplitude to select a sub-optimal mirror activation pattern. The results of MCS show a 3.5dB improvement at 10b/s/Hz with $m_{rf} = 2$ and a 7dB improvement at 12b/s/Hz with $m_{rf} = 2$ over the traditional SIMO-MBM scheme. The effect of imperfect channel estimation on the proposed scheme is investigated, with a trade-off of 2dB in coding gain due to channel estimation errors.

Cooperative Networking (CN) improves wireless network reliability, link quality, and spectrum efficiency by collaborating among nodes. The decode and forward relaying technique is used in this thesis to investigate the performance of QSM aided SIMO-MBM in a Cooperative Network (CN). This technique uses two source nodes that simultaneously transmit a unique message block on the same time slot to the relay node, which then decodes the received message block from both transmitting nodes before re-encoding and re-transmitting the decoded message block in the next time slot to the destinations in order to significantly improve the QSM aided SIMO-MBM's error performance.

Using network coding (NC) techniques, each Node can decode the data of the other Node. To enhance network performance, complexity, robustness, and minimize delays, data is encoded and decoded in NC; algebraic techniques are applied to the detected message to collect the various transmissions. The proposed scheme's theoretical average error probability was defined using a lower bound technique, and the results of Monte Carlo simulation (MCS) validated the result. The MCS results achieved exhibit a significant improvement of 8 dB at 6 b/s/Hz and 12 dB at 8 b/s/Hz over the conventional QSM aided SIMO-MBM scheme.

The media-based modulation (MBM) technique can achieve significant throughput, increase spectrum efficiency, and improve bit-error-rate performance (BER). In this thesis, the use of MBM in single-input multiple-output systems is examined using radio frequency (RF) mirrors and Golden code (GC-SIMO). The goal is to lower the system's hardware complexity by maximizing the linear relationship between RF mirrors and spectral efficiency in MBM in order to achieve a high data rate with less hardware complexity. The GC scheme's encoder uses orthogonal pairs of the super-symbol, each transmitted via a separate RF mirror at a different time slot to achieve full rate full diversity.

In the results of MCS obtained, at a BER of 10^{-5} , the GC-SIMO-MBM exhibits a significant performance of approximately 7dB and 6.5 dB SNR gain for 4 b/s/Hz and 6 b/s/Hz, respectively, compared to GC-SIMO. The proposed scheme's derived theoretical average error probability is validated by the results of the Monte Carlo simulation.

Table of Contents

Declaration 1- Plagiarism	ii
Declaration 2-Publication	iii
Acknowledgements	iv
Dedication	v
Abstract	vi
List of Figures	xi
List of Tables	xiii
List of Abbreviations	xiv
Notation	xvii
1. Research Background of the Study	1
1.1 Introduction	2
1.1.1 Review of Basic Communication systems.	2
1.1.1.1 Transmitter.	3
1.1.1.2 Channel.	3
1.1.1.3 Receiver	3
1.1.2 Wireless Communication Transmission Schemes.	4
1.1.2.1 Single Input Single Output Systems (SISO).	4
1.1.2.2 Single Input Multiple Output Systems (SIMO).	5
1.1.2.3 Multiple Input Single Output Systems (MISO).	5
1.1.2.4 Multiple Input Multiple Output Systems (MIMO).	6
1.2 Research Objectives	7
1.2.1 Enhanced wireless Communication Techniques.	8
1.2.1.1 Spatial Modulation (SM).	8
1.2.1.2 Quadrature Spatial Modulation (QSM).	9
1.2.1.3 Media-Based Modulation (MBM).	10
1.2.2 Cooperative Communications.	12
1.2.2.1 Network Coding.	13

1.2.3	Golden Code.	15
1.3	Research Motivation and Contributions.	16
1.3.1	Journal Article 1.	18
1.3.2	Journal Article 2.	19
1.3.3	Journal Article 3.	19
1.4	Structure of the thesis.	20
1.5	References.	21
2.	Journal Article 1	32
2.1	Abstract	33
2.2	Introduction.	34
2.3	The System Model of QSM Aided SIMO-MBM.	37
2.3.1	The System Model of QSM.	37
2.3.2	System Model for the Proposed Scheme.	38
2.4	Maximum Likelihood (ML) Detector.	39
2.5	Average BER Analysis for The Proposed Scheme.	40
2.6	MAP Selection for QSM Aided SIMO-MBM System.	41
2.6.1	Norm-based MAP selection.	41
2.6.2	Channel amplitude and antenna correlation MAP selection.	41
2.7	Effect of Imperfect Channel Estimation (IChE) on the proposed Scheme.....	42
2.8	Numerical Analysis and Discussion.	44
2.8.1	Average BER performance of the QSM aided SIMO-MBM scheme. . . .	44
2.8.2	Average BER performance of QSM aided SIMO-MBM scheme with MAP selection.	48
2.8.3	Average BER performance of QSM aided SIMO-MBM scheme with imperfect channel Estimation (IChE).....	50
2.9	Conclusion.	51
2.10	References.	53
3.	Article Journal 2	57
3.1	Abstract.	58
3.2	Introduction.	59
3.3	System Model.	62
3.3.1	Phase 1: Transmission Phase.	63

3.3.2	Phase 2: Relaying Phase.	64
3.4	Performance Analysis.	65
3.5	Numerical Analysis and Discussion.	67
3.6	Conclusion.	70
3.7	References.	71
4.	Journal Article 3	76
4.1	Abstract.	77
4.2	Introduction.	78
4.3	System Model.	81
4.3.1	A. Golden Code.	81
4.3.2	B. Proposed GC-SIMO-MBM.	81
4.4	Maximum Likelihood (ML) Detector.	83
4.5	Performance Analysis of GC-SIMO-MBM	83
4.6	Numerical Analysis and Discussion.	84
4.7	Conclusion.	86
4.8	References.	88
5.	Conclusion	92
5.1	Conclusion.	93
5.2	Summary of contributions and Results.	96
5.3	Suggestion for further research.	98

List of Figures

Figure 1.1. Components of communication system.	2
Figure 1.2 Single Input Single Output Model.	4
Figure 1.3: Single Input Multiple Output Model.	5
Figure 1.4: Multiple Input Single Output System Model.	6
Figure 1.5: Multiple Input Multiple Output System model.	7
Figure 1.6. Diagram of in-phase and quadrature components that are added to the spatial constellation symbols.	10
Figure 1.7. MBM with constellation $\mathbb{H}_{mbm} = h_1, h_2, \dots, h_{2^{m_{rf}}}$	12
Figure 1.8: Network coding is a notion in which network nodes can compute functions from input messages.	13
Figure 1.9 (a) Without network coding.	14
Figure 1.9 (b) With network coding.	14
Figure 2.1 System model of the proposed QSM aided SIMO-MBM scheme.	38
Figure 2.2 BER performance of QSM aided SIMO-MBM.	45
Figure 2.3 BER performance comparison of QSM aided SIMO-MBM ($m_{rf} = 2$) for 6, 8 and 10 b/s/Hz, respectively.	46
Figure 2.4 BER performance comparison of QSM aided SIMO-MBM ($m_{rf} = 4$) for 10 b/s/Hz and 12 b/s/Hz, respectively.	47
Figure 2.5 BER performance comparison of QSM aided SIMO-MBM for $m_{rf} = 2$ and $m_{rf} = 4$, respectively.	48
Figure 2.6 BER performance comparison of SIMO-MBM, QSM aided SIMO-MBM and QSM aided SIMO-MBM with MAP algorithm for 6 b/s/Hz and 8 b/s/Hz.	50
Figure 2.7: Effect of Imperfect Channel Estimation on QSM-SIMO-MBM scheme	51
Figure 3.1 The System model of the proposed two-way DF-QSM-SIMO-MBM	

relaying system.	63
Figure 3.2 Flow chart for the two-way DF-QSM aided SIMO-MBM Implementation	66
Figure 3.3 BER performance of 2W-DF-QSM-SIMO-MBM.	68
Figure 3.4 BER performance comparison of 2W-DF-QSM-MBM-SIMO for $m_{rf} = 2$ and $m_{rf} = 4$, respectively.	68
Figure 3.5 BER performance comparison of 2W-DF-QSM-MBM-SIMO and QSM aided SIMO-MBM.	69
Figure 4.1 System Model of the Proposed GC-SIMO-MBM	82
Figure 4.2 Performance analysis validation for GC-SIMO-MBM for 4 b/s/Hz, 6 b/s/Hz and 8 b/s/Hz, respectively.	84
Figure 4.3 BER performance comparison of GC-SIMO-MBM, GC-SIMO and SIMO-MBM for 4 b/s/Hz and 6 b/s/Hz, respectively.	86

List of Tables

Table 2.1: Mapping process for the QSM aided SIMO-MBM system	
using 4 QAM.	39
Table 2.2: SNR gain (dB) obtained for the QSM aided SIMO-MBM with $m_{rf} = 2$. . .	47
Table 2.3: SNR gain (dB) achieved for the QSM aided SIMO-MBM	
with $m_{rf} = 4$	47

List of Abbreviations

ABEP	Average B it Error P robability
AF	A mplify-and- F orward
APM	A mplitude/ P hase M odulation
AWGN	A dditive W hite G aussian N oise
BER	B it Error R ate
CC	C omputational C omplexity
CN	C ooperative N etwork
DF	D ecode-and- F orward
EDAS	E uclidean D istance- B ased A ntenna S election
FD	F requency D omain
GC-SIMO	G olden C ode S ingle- I nput M ultiple O utput
GSM	G eneralized S patial M ultiplexing
GSSK	G eneralized S pace S hift K eying
GSTSK	G eneralized S pace- T ime S hift K eying
IAI	I nter- A ntenna I nterference
i.i.d.	i ndependent and i dentically d istributed
ICI	I nter- C hannel I nterference
ICH _E	I mperfect C hannel E stimation
IM	I ndex M odulation
LC	L ow C omplexity

LD-STBC	Linear Dispersion Space-Time Block Code
MAP	Mirror Activation Pattern
MBM	Media-Based Modulation
MIMO	Multiple Input Multiple Output
MISO	Multiple Input Single Output
ML	Maximum Likelihood
MRC	Maximum Ratio Combining
NC	Network Coding
OIQSM	Optical Improved Quadrature Spatial Modulation
PEP	Pairwise Error Probability
QAM	Quadrature Amplitude Modulation
QSM	Quadrature Spatial Modulation
RF	Radio Frequency
SD-IM	Space Domain Index Modulation
SIMO	Single Input Multiple Output
SIMO-MBM	Single-Input-Multiple-Output Media-Based Modulation
SISO	Single Input Single Output
SM	Spatial Multiplexing
SNR	Signal-to-Noise Ratio
SSD	Signal Space Diversity
STBC	Space-Time Block Code

STC	Space Time Coding
STLD	Space-Time Labeling Diversity
TD-IM	Time Domain Index Modulation
MCS	Monte Carlo Simulation

Notation

Bold italic lowercase/uppercase symbols	Vectors/matrices
Regular letters	Scalar quantities.
$\ \cdot\ _F$	Frobenius norm
$Q(\cdot)$	Gaussian Q-function
$\underset{w}{\operatorname{Argmin}}(\cdot)/\underset{w}{\operatorname{argmax}}(\cdot)$	Minimum/maximum value of an argument with respect to w
$\binom{\cdot}{\cdot}$ represents	Binomial coefficient
i	Complex number
$R\{\cdot\}$	Real component of the complex number
$E\{\cdot\}$	Expectation operator
$ \cdot $	Euclidean norm,
$[\cdot]^T$	Transpose
$\lfloor \cdot \rfloor$	Nearest integer less than the input argument
\oplus	XOR operator

Chapter 1

Research Background of the Study

1.1 Introduction

1.1.1 Review of Basic Communication Systems

The transmission and receiving of data through a medium or channel are the foundation of a communication system. A transmitter, a receiver, and a channel, which is often a radio link, copper, or fiber, make up the system, which can be wired or wireless, as shown in Figure 1.1. Because low frequencies, such as human voice, cannot be transmitted directly via radio, the contents of the information must be overlaid over a carrier signal with a higher frequency at the source transmitter through a technique known as modulation [1-4].

Modulation allows many information signals to employ the same radio channel, each with a unique carrier frequency. To restore the original information, the receiver performs demodulation, which is the inverse of modulation. The message signal, also known as the baseband signal or modulating signal, is a type of information signal [1]. A transducer is used to convert the output of a source into an electrical signal that can be conveyed. At the receiving end, a comparable transducer is necessary to translate the electrical impulses received into a form that the user can understand, such as auditory signals, images, and so on [2]. In an ideal communication system, the exact information will be produced at the receiver except for the unavoidable delay in time and/or change in amplitude, phase and noise as it moves between transmitter and receiver; these changes are known as distortion, and any real system will have distortion; therefore, dealing with managing this distortion is one of the most important factors in the communication design process. Figure 1.1 depicts the components of a communication system.

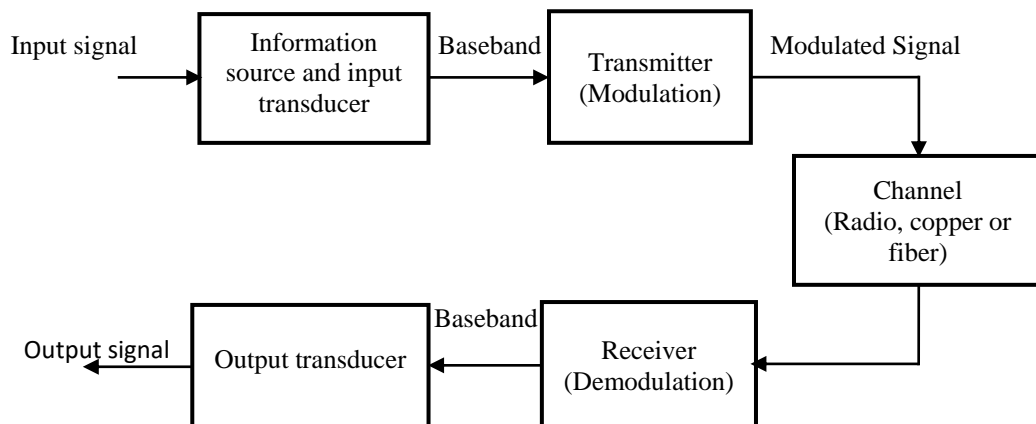


Figure 1.1. Components of communication system.

1.1.1.1 The Transmitter

The transmitter translates the electrical signal into a transmittable form through the physical channel or transmission medium. It makes use of modulation process to execute the information signal-to-channel matching. This procedure entails the usage of the baseband signal to vary either the amplitude, frequency, or phase of a sinusoidal signal. Several factors determine the choice of the nature of modulation, such as the types of distortions, amount of bandwidth and the available electronic devices for signal amplification preceding transmission [1-2]. Regardless, accommodating the transmission of several messages from various users over the same physical channel is made possible through modulation process [1-2]. Along with modulation, other functions implemented at the transmitter include amplification of the modulated signal, filtering of the information-bearing signal and in wireless transmission case, radiation of the signal with the help of a transmitting antenna [1-2].

1.1.1.2 The Channel.

In a communication system, a channel refers to the physical medium that is used to transport signals from the transmitter to the receiver. [1-2]. In wireless transmission, the channel is often free space. Regardless of the physical media used for signal transmission, the signal gets distorted at random by a number of causes. Additive noise, also known as thermal noise, is a type of signal degradation that occurs when signal amplification is performed at the receiver's front end [2]. Multipath propagation is another type of signal degradation that occurs and is classified as a nonadditive signal disturbance manifesting as time variations in signal amplitude, commonly referred to as fading [1-3]. Both additive and nonadditive signal distortions are statistically described and are commonly referred to as random events [4]. The impact of these signal distortions must be considered during the communication system design process.

1.1.1.3 The Receiver.

The receiver's purpose is to regain the information signal enclosed in the received signal. The receiver executes carrier demodulation on the transmitted message signal in order to extract the information from the sinusoidal carrier [1]. The demodulated information signal is usually degraded by the existence of these distortions in the received signal since the demodulation of the signal is performed in the presence of additive noise and perhaps in the presence of other signal distortions [2]. The reliability of the received information is determined by the strength of the

additive noise, type of modulation, type of any non-additive interference and type and strength of any other additive interference [1-3]. Receiver also accomplishes a few peripheral functions, such as noise suppression and signal filtering.

1.1.2 Wireless communication Transmission Schemes

In a wireless antenna communication system, information can be wirelessly transported from one location to another without the usage of electrical cables. The transmitter and receiver are the components of this system, and data is sent from the transmitter's antenna to the receiver's antenna. Single Input Single Output systems (SISO), Single Input Multiple Output systems (SIMO), Multiple Input Single Output systems (MISO), and Multiple Input Multiple Output systems (MIMO) are the four types of wireless communication transmission schemes. [5,6].

1.1.2.1 Single Input Single Output systems (SISO)

One antenna is used at both ends of the transmission in a SISO system, i.e. one at the transmitter and one at the receiver, therefore data transmission is through a single radio frequency (RF) signal chain. The channel capacity is the smallest when compared to other transmission schemes with simple design model as shown in figure 1.2. The SISO system capacity can be expressed as [7]

$$C_{SISO} = B \log_2(1 + S/N) \tag{1.1}$$

Where C and B are the channel capacity and Bandwidth of the signal respectively, S/N represent the signal to noise ratio.

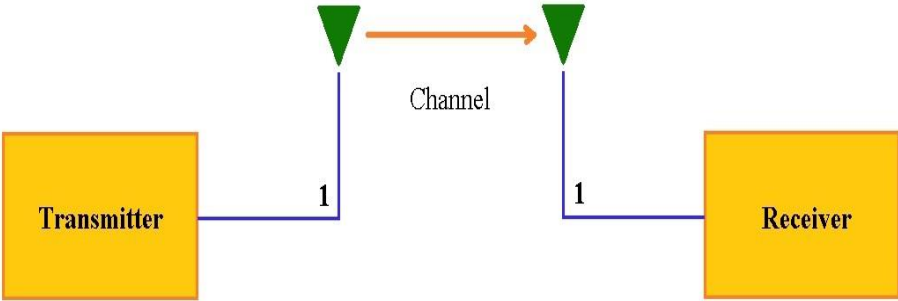


Figure. 1.2 Single Input Single Output Model [7]

1.1.2.2 Single Input Multiple Output systems (SIMO)

A SIMO system contains one transmitter antenna and numerous receiver antennas, each with its own RF chain. Consider a system with two receivers and two different fading channel coefficients, h_1 and h_2 (Figure 1.3). y_1 and y_2 are two possible values for the received signal.

The receiver selects the best antenna for receiving a stronger signal from the transmitter in a selection diversity or switched diversity implementation, whereas the receiver combines signals from all of its antennas for SNR maximization in a maximal ratio combining (MRC) implementation. [3]. Although channel capacity will not grow, the use of numerous antennas and diversity will result in a strong signal. The capacity of the SIMO system channel is [7]:

$$C_{SIMO} = N_r B \log_2(1 + S/N) \quad (1.2)$$

where N_r represent the number of receiving antenna, C and B are the channel capacity and Bandwidth of the signal respectively, S/N signify the signal to noise ratio

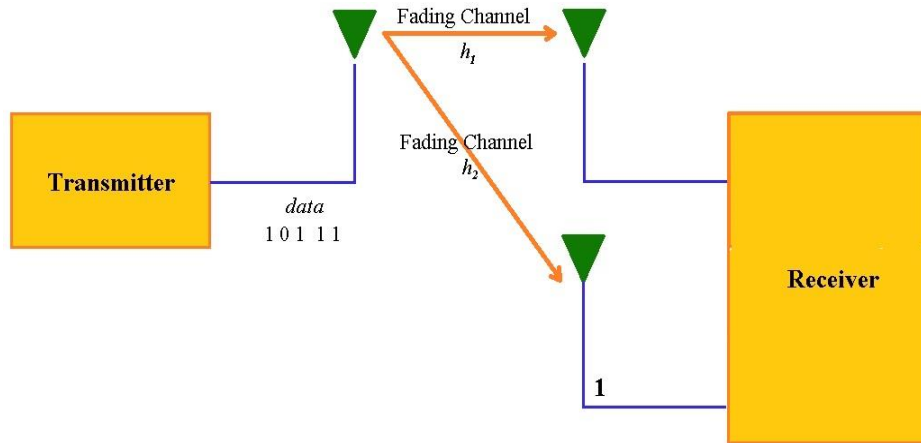


Figure 1.3: Single Input Multiple Output Model [7]

1.1.2.3 Multiple Input Single Output System (MISO)

MISO used a number of antennas at the transmitter or input end, each with its own RF chain, and one antenna at the receiver or output end. Figure 1.4 depicts a MISO model with two sending antennas and one receiving antenna, each with two fading channels, h_1 and h_2 . Y_1 and Y_2 represent the send signal. The Alamouti Space Time Coding (STC) technology, which used two antennas at the transmitter and allowed the transmitter to send signals in both time and space—that is, data is

transmitted via the two antennas at two separate successive times is an example of MISO. The MISO channel capacity can be expressed as [7]:

$$C_{MISO} = N_t B \log_2(1 + S/N) \quad (3)$$

N_t denotes the number of transmitting antennas, C and B denote the signal's channel capacity and bandwidth, respectively, and S/N denotes the signal-to-noise ratio.

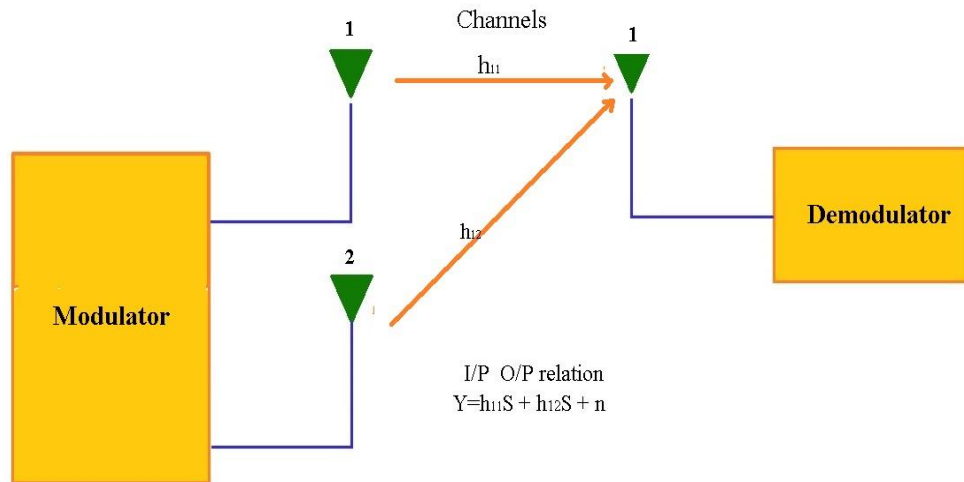


Figure 1.4: Multiple Input Single Output System Model [7]

1.1.2.4 Multiple Input Multiple Output System (MIMO)

For transmission purposes in spatial diversity, MIMO employs at both transmitting and receiving ends, numerous antennas and RF chains, resulting in numerous copies of the same signal at the receiver [8]. Because of its capacity and high data rate, this approach is widely used in wireless technology such as WiMAX, WiFi, 802.11n, and LTE. In a point-to-point (PTP) link, a MIMO scheme with the same number of antennas at the transmitting and receiving ends can increase the system reliability with each additional antenna (Figure 1.5). A good example is a 2x2 MIMO, which doubles the throughput. $r = hx + n$ where r , h , x and n represents the signal vector received, channel matrix, signal vector transmitted, and complex additive white Gaussian noise, respectively, in the MIMO signal model.

More antenna at both ends of the transmitter and receiver are required to increase capacity, maintain bandwidth, and transmit power. To approximate a channel in the frequency domain (FD), a complex matrix with Rayleigh model of random channel that has identically independent

distributed elements with unit variance and zero mean is utilized [9]. MIMO System capacity is given by [7] $C_{MIMO} = N_t N_r B \log_2(1 + S/N)$ (4)

where N_t and N_r denote the number of transmitting and receiving antennas respectively, C and B denote the signal's channel capacity and bandwidth, and S/N denotes the signal-to-noise ratio. The spatial multiplexing technology is used to increase data capacity by transmitting signals over many spatial domains.

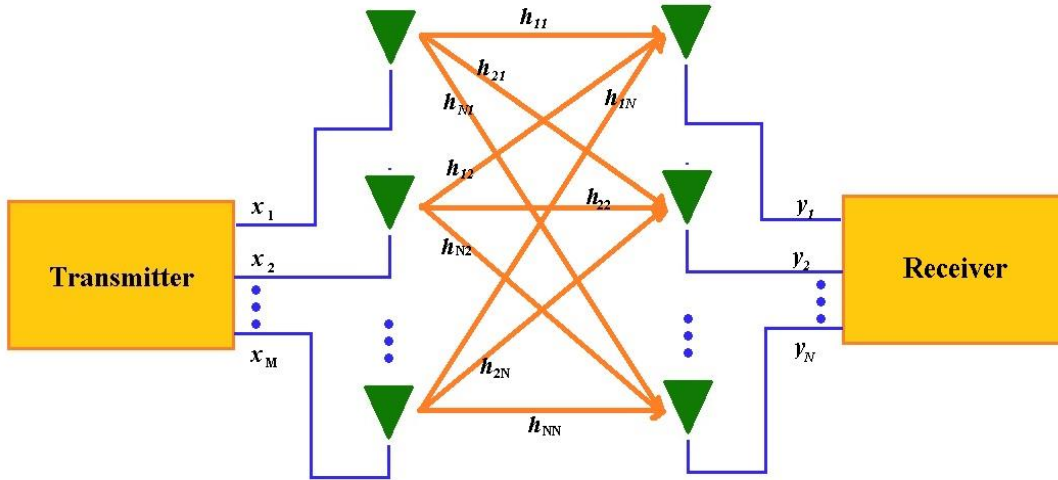


Figure 1.5: Multiple Input Multiple Output System model [7]

1.2 Research objectives

The objectives of the works are to:

- i. Enhance the overall error performance of the conventional SIMO-MBM and to achieve a higher data rate by employing the quadrature dimension of the spatial constellation.
- ii. Formulate the average bit error probability of the proposed QSM aided SIMO-MBM scheme using a lower bound approach, to be validated by the Monte Carlo simulations.
- iii. Examine the effect of the sub-optimal mirror activation pattern selection using channel amplitude coupled with antenna correlation for the proposed QSM aided SIMO-MBM system.
- iv. Investigate the impact of imperfect channel estimation on the proposed QSM aided SIMO-MBM.
- v. Investigate the performance of QSM aided SIMO-MBM in Cooperative Network (CN) by employing the two-way decode and forward relaying technique.

- vi. Formulate the theoretical average error probability of QSM aided SIMO-MBM in Cooperative Network, to be validated by the Monte Carlo simulations.
- vii. Investigate the application of MBM, employing radio frequency (RF) mirrors and Golden code in the single-input multiple-output (GC-SIMO-MBM).
- viii. Derive theoretical average error probability of the proposed GC-SIMO-MBM, to be validated by Monte Carlo simulation.

1.2.1 Enhanced wireless communication techniques.

1.2.1.1 Spatial Modulation (SM)

The requirement for a high data throughput and a good spectral efficiency are the essential fundamentals upon which the future wireless communication is based.[10]. The use of multiple antenna transmission technique i.e MIMO system enhances spectral efficiency because of its simultaneous transmission of data to the receiver [11-14]. Numerous challenges exist in the improvement of a transmission scheme using multiple antennas [15-18]. These challenges originated from different sources, which includes:

- high inter-channel interference (ICI) due to simultaneous occurrence of transmission from numerous antennas on the same frequency
- complex receiver algorithm is required to improve ICI which result in increment in the overall system complexity
- Performance of the system is traded off with receiver complexity, etc.

Spatial Modulation (SM) deals with these limitations [19-21] when at any given time only one transmit antenna is active. SM differs from other MIMO schemes as in the case space-time bit interleaved coded modulation [22] where the antenna pattern is identified as a spatial constellation but not utilized as a source of information. Therefore, Spatial Modulation (SM) is a transmission system that utilizes numerous antennas. The main concept is using a chosen symbol from a constellation diagram and a chosen transmit antenna number from a set of transmit antennas, and convert a block of information bits to two information carrying units. [23].

A single transmit antenna will be active, while null power will be transmitted by the other ones, hence the need for transmit antenna synchronization and ICI at the receiver are avoided completely. Utilizing each antenna index to convey additional information bits and a base-two logarithm of spatial multiplexing gain of the quantity of transmit antennas enhance the system's

spectral efficiency. This has gained substantial attention in literature as reported in Generalized SM(GSM), Generalized space shift keying modulation SSK(GSSK) and Generalized space–time shift keying *STSK(GSTSK)* [24-26]. Maximum receive ratio combining (MRRC) algorithm is adopted to determine the number of transmit antenna, and thereafter, estimate the transmitted symbol. Spatial demodulators make use of the two estimates to recover the block of information bits.

1.2.1.2 Quadrature Spatial Modulation (QSM)

By employing an additional modulation spatial dimension, QSM improves the throughput of the SM scheme. The SM method just uses the real part of the SM constellation, whereas QSM employs in-phase and quadrature dimensions [27]. In comparison to other MIMO schemes, SM schemes improve error performance by deploying a moderate number of transmit antennas, robustness to channel imperfections, such as spatial channel correlation, and estimation errors, because the SM system's error probability is determined by the differences in channels associated with the various antennas for each channel [27-37]. QSM is a signal processing technique used before transmission. It improves the SM system's spectrum efficiency while keeping nearly all of the system's benefits.

In-phase and quadrature components are now included in the spatial constellation symbols (figure 1.6). The real and imaginary halves of a signal constellation symbol are conveyed by the first and second dimensions, respectively, as shown in [38, Fig 1.6]. Because the two sent data are orthogonal and modulated on the carrier signal's real and imaginary components, ICI is abolished in QSM. The sine carrier transmits one component, and the cosine carrier transmits the other. As a result, in QSM, the number of transmit antenna bits can be increased by a base-two logarithm.

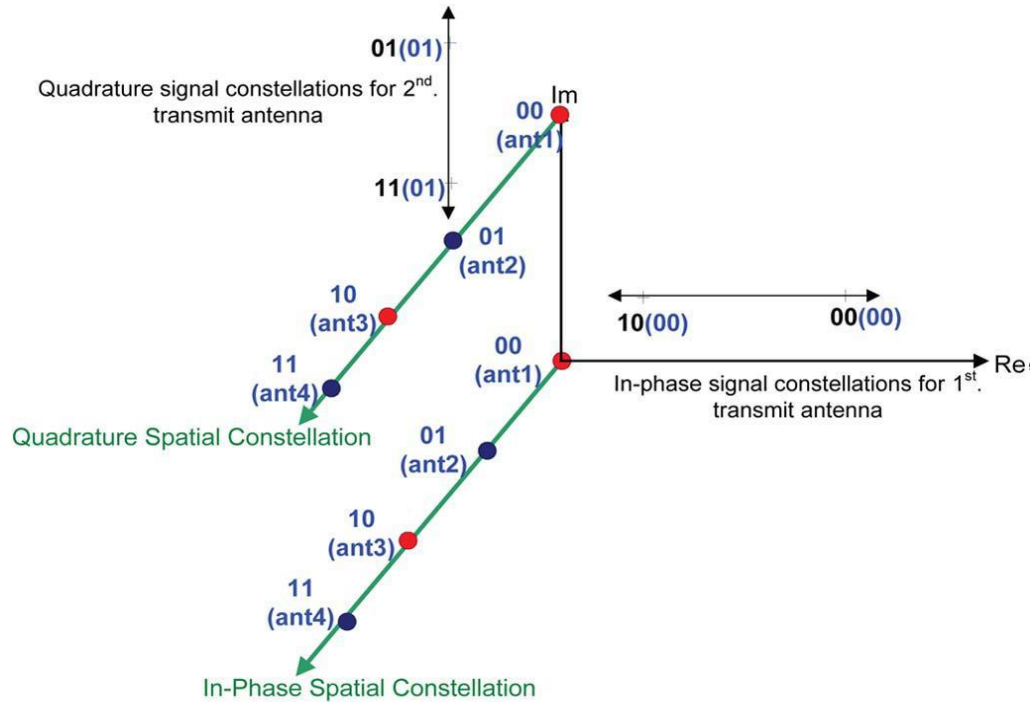


Figure. 1.6. This diagram shows the in-phase and quadrature components are added to the spatial constellation symbols. The in-phase portion of a signal constellation symbol is transmitted by one component, while the quadrature portion is transmitted by the other. As instances, the first transmit antenna's in-phase signal constellation symbols and the second transmit antenna's quadrature signal constellation points are displayed.[27]

1.2.1.3 Media-based Modulation (MBM). MBM is a way of modulating the wave after it leaves the transmit antenna(s) [39]. MBM can be achieved by altering the RF parameters of the transmitter's propagation environment, such as permittivity, permeability, and/or resistivity [40]. As a result, the end-to-end channel is affected, received signal's magnitude and phase will change. In a rich scattering environment, a tiny environmental perturbation near the transmitter will be enhanced by multiple random reflections across the propagation path, culminating in an end-to-end channel realization that is completely independent. MBM sends out a tone and then different channel fading realizations are provided by RF mirrors at the transmit antenna(s) depending on their ON/OFF condition. The modulation alphabet [40-42] is made up of these sophisticated fade realizations. While the intricate fade symbols of the alphabet need the use of numerous transmit antennas, MBM uses multiple RF mirrors with a single transmit antenna to create the complex fade symbols of the alphabet [43]. A number of RF mirrors are placed near the tone-transmitting transmit antenna to achieve this. In the propagation environment, the placement of RF mirrors near a transmit antenna is similar to the placement of scatterers near the transmitter.

An ON/OFF control signal provided to each of these scatterers (i.e., RF mirrors) can modify its radiation characteristics; depending on whether it is OFF or ON, it reflects or passes the incoming wave emanating from the transmit antenna. The "mirror activation pattern (MAP)" refers to the ON/OFF condition of the mirrors [39]. From one MAP to the next, the positions of the ON and OFF mirrors change, resulting in a change in the propagation environment around the transmitter. Because multiple random reflections in a rich scattering environment will reinforce a modest change in the propagation environment, therefore, an independent channel will emerge [39].

By serving as regulated scatterers, the RF mirrors produce such disturbances, which result in independent fading realizations for different MAPs [43]. M_{rf} is the total number of RF mirrors in the antenna's vicinity. The "MBM transmit unit (MBMTU)" (Figure. 1.7) is a unit that includes a transmit antenna as well as a set of M_{rf} RF mirrors. Let m_{rf} be the number of RF mirrors employed out of M_{rf} total RF mirrors, with $1 \leq m_{rf} \leq M_{rf}$. Based on a single information bit on a given channel, each of these m_{rf} mirrors are turned ON or OFF. The ON/OFF status of all m_{rf} mirrors as determined by m_{rf} information bits is represented by a MAP. As a result, $2^{m_{rf}}$ MAPs are feasible. Each of these patterns produces a unique channel fade and MBM alphabet with a size of $|\mathbb{H}| = 2^{m_{rf}}$. MBM can transmit m_{rf} data bits in a single channel, where m_{rf} is the number of RF mirrors employed in MBM which has a linear relationship with the spectral efficiency. The alphabet \mathbb{H} must also be recognized at the receiver, not at the transmitter, in MBM. MBM has been demonstrated to significantly improve the system performance when compared to traditional modulation systems [40-42]. MBM has also been demonstrated to save energy significantly even with a single transmit antenna and N_r reception antennas when compared to a standard $N_r \times N_t$ MIMO system with $N_r = N_t$ [41]. Its ability to save energy by picking only a channel configurations subset, resulting in greater overall performance for the same amount of energy and spectral efficiency. [40].

Over a static multipath channel with 1 transmit and N_r receive antennas, MBM has also been proven to asymptotically attain the capacity of N_r parallel AWGN channels [40]. [44] demonstrates how to construct an MBM-TU using $M_{rf} = 14RF$ mirrors in a dense cylinder structure at the centre of which is a dipole transmit antenna element

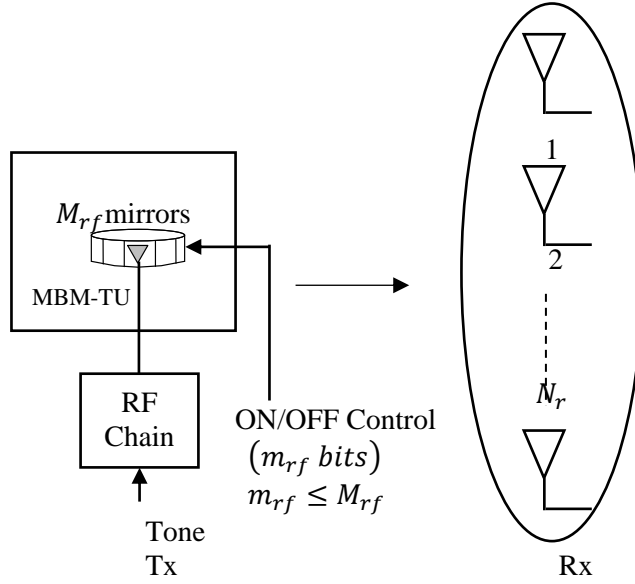


Figure 1.7. MBM with constellation $\mathbb{H}_{mbm} = h_1, h_2, \dots, h_{2^{m_{rf}}}$ [39]

1.2.2 Cooperative Communications

Wireless users not only send their own data to a common destination, but also repeat the data of other users in cooperative communications. Furthermore, the resulting diversity is referred to as transmit or receive diversity when several antennas are used just at the transmitting or receiving ends. To gain the benefits of broadcast diversity, multiple antennas on the transmitting side are required [45]. However, having many antennas at the user terminal in some wireless networks, such as mobile communications, is difficult due to the size of the devices utilized or the mobile in emerging wireless networks, such as Ad hoc networks. The concept of cooperative communications was first offered as a solution to this problem by [46]. Cooperative communication is a type of wireless communication in which each user not only sends and receives data but also acts as a relay for other users [46-47].

Cooperative communications can be thought of as a subset of the relay channel, which consists of three nodes: relay, receiver and transmitter. A relay receives a signal from a source and transfer it to a destination, such as a repeater. In cooperative communications, on the contrary, the node functioning as a relay, it not only forwards the information of other users, but it also has its own information to share. Similarly, a source has its own data and serves as a conduit for other users. [48] was the first to introduce the relay channel. [49] went on to describe that a relay can assist the source in a variety of ways. They also provide capacity results for specific relay channel situations,

such as degraded relay channels. Relaying protocols are the methods through which a relay can assist a source in sending information reliably to a destination. Following that, numerous separate researchers researched on different features of relay channels, such as capacity [50], diversity [51], and diversity multiplexing tradeoff [52]. After its initial introduction by [46], [53], cooperative communications drew a lot of interest from the research community, and several papers were published to demonstrate its possibilities and techniques to attain them [54], [51], [55], [56].

1.2.2.1 Network Coding

The concept of network coding allows a node to generate output data by mixing (that is, computing certain functions of) its incoming input. The transmission of a combination of data collected from many source nodes at the same time slot, on the other hand, enhances the network's flow rate [57]. The basic goal of network coding is to make the most efficient use of network resources.[58]. Because of the unique properties of the wireless medium, network coding is especially advantageous. In a wireless ad hoc network, network coding can be utilized to provide the lowest energy-per-bit for multicasting, however the network coding-based solution has only polynomial time complexity. The use of network coding as a link layer enhancement strategy is another example [59]. The network coding engine on the link layer can opportunistically bundle outbound packets to minimize air transfers.

Routing, which entails having intermediate routers store and forward data, is used to transmit information in today's actual communication networks, such as the Internet and wireless networks. Nodes generate output data by encoding previously received input data in network coding, which is a recent extension of routing. As seen in Figure 1.8, each node in a network can do some computations in network coding, whereas in routing, the output messages can only be duplicates of the received messages. On the surface, network coding allows information to be "mixed" at a node .

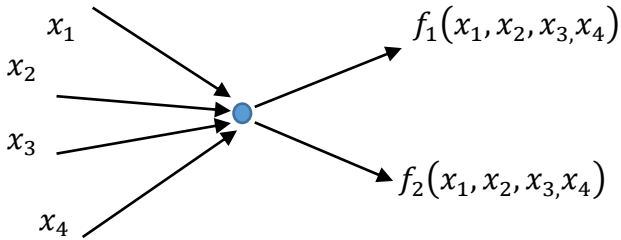


Figure 1.8: Network coding is a notion in which network nodes can compute functions from input messages.

Network coding has potential advantages over routing in terms of resource efficiency (e.g., bandwidth and power), processing efficiency, and network dynamics robustness. [57] showed that network coding can increase network throughput and, in the case of multicast, can achieve the theoretical maximum data rate.

We may assume error-free transmissions in wired networks [60], but multi-path fading of signals in wireless networks can drastically decrease link quality and cause transmission mistakes. The ever-increasing data rate demands in wireless networks with limited resources such as frequency spectrum and system power are a problem that can be solved or at least mitigated by employing network coding in conjunction with cooperative communication [58].

Another challenge in wireless channels is interference, which traditional setups attempt to address by choosing proper link scheduling, selecting optimal routes, and modifying signal modulation of a node and its neighbors (closest nodes), as in the OFDMA technique [61-68]. The effect of interference is turned into a benefit via network coding, which makes use of it in terms of bandwidth utilization.

Node A delivers the message m_A to the relay R (first time slot) in the traditional setup shown in Figure 1.9(a), which forwards it to node B. (second time slot). Similarly, node B sends m_B to node A via the relay R in two time slots (TS). Both transmissions have a total duration of four TS. In the network coding scenario shown in Figure 1.9(b), node A sends m_A to R in the first TS, node B sends m_B to R in the second TS, and then the relay R performs a basic coding operation using the exclusive OR (XOR) denoted \oplus on the received messages m_A and m_B , broadcasting the result $m_R = m_A \oplus m_B$ to both nodes in the third TS. As a result, the total transmission time is three TS [58].

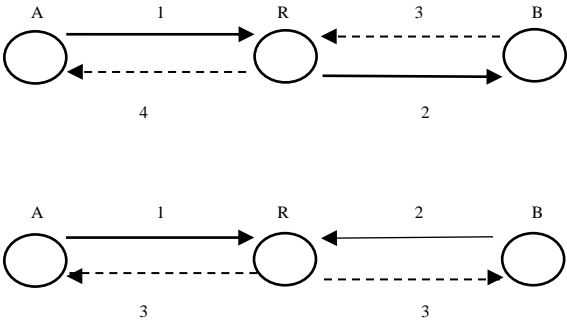


Figure. 1.9 The relay network (a) Without coding (b) With coding

Each node recovers the message transmitted to it by employing the XOR operator to combine the received encoded message mR with the message it delivered. As a result, node A recovers mB by carrying out the operation $mB = mA \oplus mR = mA \oplus (mA \oplus mB)$. As a result, we can see that by combining a basic XOR coding procedure (network coding) with the advantageous broadcast attribute of the wireless medium (cooperation), we may save $\frac{1}{4}$ of transmission time, implying a throughput gain of $\frac{4}{3}$, as well as $\frac{1}{4}$ watts of transmitting power [69-75].

1.2.3 Golden Code

Data transmission rate and communication dependability are top priorities in next-generation wireless communication technologies. The use of multiple-input multiple-output (MIMO) techniques is the key to such progress [76]. However, in MIMO systems, there is a trade-off between rate and reliability when it comes to the diversity-multiplexing advantage [77]. The Golden code, which is a linear dispersion space-time block code (LD-STBC) that requires two transmit antennas [78 - 81], achieves both full rate and full diversity and is employed in the widely used WiMAX standard on this point. SIMO (single-input multiple-output) systems have recently been examined using the Golden code [82].

The traditional Golden encoder accepts four complex symbols, $x_i, i \in [1: 4]$, and creates two pairs of super-symbols $(x_{2i-1} + x_{2i}\theta, x_{2i-1} + x_{2i}\bar{\theta}), i \in [1: 2], \theta$ and $\bar{\theta}$ are real-valued constants. In one pair, two super-symbols are rotated by angles φ_1 and φ_2 , whereas in another pair, two super-symbols are rotated by angles φ_1 and $\varphi_2 + 90^\circ$. Both φ_1 and φ_2 are precise angles that may be calculated using product distance requirements for signal space diversity (SSD) systems [83], [84]. Independent fading affects the in-phase and quadrature parts of a complex symbol in the SSD system, which is accomplished through signal rotation and component interleaving. Component interleaving directly between two Golden code super-symbol pairs to achieve SSD can be performed and hence improve error performance because the two pairs of super-symbols in the Golden code have already been rotated [76].

In wireless communications, there is an ever-increasing demand to boost data transfer rates and enhance communication dependability. Multiplexing is a data transmission rate enhancement technology, while diversity is a communication reliability improvement system [85]. Multiple copies of a transmitted signal arriving at the receiver over various channels is used in receive

diversity approaches for single-input multiple-output (SIMO) systems. Receiving diversity is easily achieved by having multiple independent receive antennas on the receiver [85].

Another way for achieving diversity is signal space diversity (SSD). [86] Signal diversity is produced in SSD systems by broadcasting the rotating multidimensional signal in phase and quadrature on an independent fading channel. There is no need for increased bandwidth, broadcast power, or receive antennas with SSD systems. The Golden code is a linear dispersion space-time block code (LD-STBC) that uses two broadcast antennas and two or more reception antennas [87 and 88]. The Golden encoder takes four symbols and generates two pairs of super symbols, or Golden codewords, which are then sent out in two time slots by two separate transmit antennas. Because two transmit antennas send four symbols in two time slots, the Golden code reaches full rate.

Furthermore, the Golden Code encompasses all aspects of diversity. The Golden code might be considered one sort of space-time labeling diversity (STLD) based on the principle of diversity in space-time labeling. [89] This is due to the fact that each pair of super symbols conveys the same information. The IEEE 802.16e WiMAX standard includes a significant application of the Golden codes. [90] Trellis-coded modulation and space-time block-coded modulation has also been applied to the Golden code. [91-92]. For multiple-input multiple-output (MIMO) systems, the Golden code has been proposed in the literature. To the best of the authors' knowledge, the Golden code has never been applied to Media-Based Modulation for Single-Input Multiple-Output. The bandwidth efficiency of a SIMO system when a pair of super symbols is conveyed in two time slots is the same as in a conventional SIMO system. In a SIMO system, however, a pair of super symbols broadcast in two time slots provides an additional diversity gain [85].

1.3 Research Motivation and Contributions

QSM is a scheme that conveys information by extending its spatial dimension to the in-phase and quadrature dimensions [27]. In QSM, the APM symbols are decomposed into its real and imaginary components, which are respectively modulated into cosine and sine carriers. Hence, it made a single RF chain requirement possible, which is more energy-efficient than GSM and exhibits an improved error performance than SM and GSM.

Also, Media-based modulation (MBM) has been proven as a more efficient technique to achieve a high data rate at the cost of low hardware complexity [39]. This is accomplished by utilizing RF mirrors to produce various channel fade realizations, classified as mirror activation patterns

(MAPs). In MBM, a subset of channel realizations may be chosen from the unique channel perturbations. Also, the received constellation size is independent of the transmit power. An additional advantage of the MBM scheme is that placement of RF mirrors side-by-side is achievable

Likewise, in MBM-QSM, Single RF chain's requirement is achieved by modulating the decomposed APM symbol into in-phase and quadrature components which are respectively transmitted via the sine and cosine carriers [93].

Considering the benefits of QSM stated above over SM and conventional MIMO schemes coupled with improved error performance, it reveals that QSM exhibits superior error performance and is more desirable. Thus, this motivates me to investigate the application of the quadrature dimension in the SIMO-MBM scheme similar to conventional QSM scheme termed QSM aided SIMO-MBM scheme.

Furthermore, cooperative relay-based communication systems have shown tremendous promise in enhancing wireless link quality, reliability, and spectral efficiency. This is achieved by employing multiple relay nodes (active or passive nodes) as a virtual antenna to re-transmit user information [46-47]. Its primary objective is to achieve optimum utilization of network resource efficiency, computational efficiency, and robustness to network dynamics

Hence, two-way DF-QSM aided SIMO-MBM is expected to outperform SIMO-MBM coupled with QSM aided SIMO-MBM with reference to error performance. This motivates me to examine a novel two-way DF-QSM aided SIMO-MBM.

Considering MBM achieves a high data rate at a reduced hardware complexity. Therefore, incorporating the MBM technique in the GC-SIMO scheme employs only the super-symbol orthogonal pairs, i.e., only two symbols as against 4 in [98] in the encoder will achieve a high data rate similar to [82], at a reduced hardware complexity. This motivates me to propose media-based Golden codeword modulation for SIMO system termed GC-SIMO-MBM.

This thesis contributions are as follows:

- a) Investigation of RF mirror-based MBM in a SIMO-based QSM system, decomposing the APM symbol prior to transmission and employing unique (different) RF mirrors to transmit the decomposed APM symbol in a SIMO scheme as compared to SIMO-MBM.

- b) The theoretical ABEP is formulated for QSM aided SIMO-MBM to be validated by the simulation results.
- c) To further improve QSM aided SIMO-MBM error performance, the impact of MAP selection based on processing the channel amplitude and antenna correlation to remove the imperfect channel(s) at each transmission instance is studied on the QSM aided SIMO-MBM scheme.
- d) Investigation of the effect of imperfect channel Estimation on the QSM aided SIMO-MBM scheme.
- e) Investigation of the two-way DF-QSM aided SIMO-MBM relaying technique with two source nodes.
- f) Formulation of the theoretical analysis for DF-QSM aided SIMO-MBM and validation of the results with the Monte Carlo simulation results obtained.
- g) Investigation of RF mirror-based MBM in a GC-SIMO system.
- h) The theoretical average bit error probability (ABEP) formulation for GC-SIMO-MBM to be validated by the simulation results obtained.

The research conducted in the course of preparation of this thesis has contributed to three Journal Papers. The authors, title, publication status and a brief summary of each article is provided.

1.3.1 Journal Article 1

A. J Bamisaye and T. Quazi ‘‘Quadrature Spatial Modulation Aided Single-Input Multiple-Output-Media Based Modulation’’ International Journal of Communication Systems. Vol.34, Iss 11, 2021; e4883. <https://doi.org/10.1002/dac.4883> (Published).

Single-input multiple-output media-based modulation (SIMO-MBM) improves the limitation of single-input multiple-output (SIMO) systems by minimizing the required number of antennas to achieve a high data rate and enhanced error performance. In this paper, we employ the quadrature dimension of the spatial constellation by decomposing the amplitude/phase modulation (APM) symbol into real and imaginary components similar to quadrature spatial modulation (QSM) to enhance the overall error performance of the conventional SIMO-MBM and to achieve a higher data rate. The average bit error probability of the proposed scheme is formulated using a lower bound approach and validated by the Monte Carlo simulation (MCS) results obtained. Furthermore, the effect of the sub-optimal mirror activation pattern selection using channel amplitude coupled with antenna correlation is examined for the proposed system. Also examined, is the effect of imperfect Channel Estimation on the proposed scheme. The Monte Carlo simulation

results achieved demonstrate a substantial improvement of 3.5dB at 10b/s/Hz with $m_{rf} = 2$ and 7dB at 12b/s/Hz with $m_{rf} = 4$ over the conventional SIMO-MBM scheme.

1.3.2 Journal Article 2

A. J Bamisaye and T. Quazi ‘Two-way Decode and Forward Quadrature Media-based Modulation for Single-Input Multiple-Output Scheme’ International Journal of Communication Systems. Vol.35, Iss 11, 2022, e5186. Doi:101002/dac.5186 (published)

In the proposed system in Journal Article 1, Quadrature spatial modulation aided single-input multiple-output media-based modulation (QSM aided SIMO-MBM) improves the spectral efficiency, achieves a high data rate, and overall system error performance when compared with conventional SIMO media-based modulation (SIMO-MBM) and single-input multiple-output (SIMO) schemes. Cooperative Network (CN) involves collaboration among nodes to improve wireless network reliability, link quality, and spectral efficiency. This Paper investigates the performance of QSM aided SIMO-MBM in Cooperative Network (CN) by employing the decode and forward relaying technique, which utilizes two source nodes that simultaneously transmit a unique message block on the same time slot to the relay node, the relay node decodes the received message block from both transmitting nodes, before re-encoding and re-transmitting the decoded message block in the next time slot to the destinations in order to enhance the error performance of the QSM aided SIMO-MBM further. Each Node can decode the data of the other Node using network coding (NC) techniques. In NC, data is encoded and decoded to improve network throughput, complexity, robustness and lower delays; algebraic algorithms are applied to the detected message to accumulate the various transmissions. The theoretical average error probability of the proposed scheme was formulated using a lower bound technique, and the Monte Carlo simulation (MCS) results obtained validated the result. The MCS results achieved exhibit a significant improvement of 8 dB at 6 b/s/Hz for a BER of 10^{-5} , and 12 dB at 8 b/s/Hz for a BER of 10^{-5} over the conventional QSM aided SIMO-MBM scheme.

1.3.3 Journal Article 3

A. J Bamisaye and T. Quazi ‘Application of Golden Code Orthogonal Super-Symbol in Media-Based Modulation for Single-Input Multiple-Output Schemes’ Journal of Telecommunications and Information Technology. 2/2022, pp 43-48. <https://doi.org/10.26636/jtit.2022.158921> (published).

The media-based modulation (MBM) scheme can achieve significant throughput, increase spectrum efficiency, and enhance the performance of bit-error-rate (BER). In this paper, the application of MBM, employing radio frequency (RF) mirrors and Golden code, is investigated in the single-input multiple-output (GC-SIMO). The purpose is to lessen the system's hardware complexity, maximizing the linear relationship between RF mirrors and the spectral efficiency in MBM to obtain a high data rate at a lower hardware complexity. The orthogonal pairs of the super-symbol in the GC scheme's encoder are employed, transmitted via different RF mirror at a different time slot to achieve full rate full diversity. In the results of MCS obtained, at a BER of 10^{-5} , the GC-SIMO-MBM exhibits a significant performance of approximately 7dB and 6.5 dB SNR gain for 4 b/s/Hz and 6 b/s/Hz, respectively, compared to GC-SIMO. The derived theoretical average error probability of the proposed scheme is validated by the results of the Monte Carlo simulation

1.4 Structure of the Thesis

The research presented in this thesis has been published in journal article 1, journal article 2 and journal article 3 which are presented in chapter 2, chapter 3, and chapter 4 respectively. The conclusion and recommendations for future study work are presented in Chapter 5.

1.5 References

- [1] K.R. Rao, Z. S. Bojkovic, D. A. Milovanovic “Wireless Multimedia Communications” CRC Press Taylor & Francis Group, New York, 2009.
- [2] J. G. Proakis and M. Salehi Communication Systems Engineering” Upper Saddle River, New Jersey 07458, 2002.
- [3] A. Goldsmith, *Wireless Communications*: Cambridge university press, 2005.
- [4] Theodore S. Rappaport, “Wireless Communication: Principles and Practice”, Prentice-Hall, 2nd Edition, India. 2010.
- [5] B.P. Lathi, ZhiDing—Modern Digital and Analog Communication System”, 4th Ed., page no. 9-15, 1998.
- [6] John G. Proakis, Masoud S., “Communication System Engineering”, 2nd Ed., PHI learns private limited, 2009.
- [7] A. Kumar, A. Datta, “Capacity Comparison of SISO, SIMO, MISO &MIMO Systems ,” Proceedings of the Second International Conference on Computing Methodologies and Communication (ICCMC 2018) IEEE Conference Record pp 798-801.
- [8] G. J. Foschini and M. J. Gans, “On limits of wireless communications in a fading environment when using multiple antennas,” *Wireless Personal Communications*, vol. 6, pp. 311–335, March, 1998.
- [9] W. Son, H. S. Jang, and B. C. Jung. "A pseudo-random beamforming technique for improving physical-layer security of MIMO cellular networks Entropy” (Basel, Switzerland), vol 21, no 11, Oct. 2019.
- [10] H. Haas and S. McLaughlin, eds., *Next Generation Mobile Access Technologies: Implementing TDD*. Cambridge, U.K.: Cambridge Univ. Press, Jan. 2008.
- [11] E. Telatar, “Capacity of multi-antenna Gaussian channels,” *Eur. Trans. Telecommun.*, vol. 10, no. 6, pp. 558–595, Nov./Dec. 1999.

- [12] G. J. Foschini and M. J. Gans, "On limits of wireless communications in a fading environment when using multiple antennas," in *Wirel. Pers. Commun.*, vol. 1, no.6, pp. 311–335, March, 1998
- [13] G. J. Foschini, "Layered space-time architecture for wireless communication in a fading environment when using multi-element antennas," *Bell Labs Tech. J.*, vol. 1, no. 2, pp. 41–59, Sep. 1996.
- [14] Y. J. Zhang and K. Letaief, "Adaptive resource allocation for multiaccess MIMO/OFDM systems with matched filtering," *IEEE Trans. Commun.*, vol. 53, no. 11, pp. 1810–1816, Nov. 2005.
- [15] A. Goldsmith, S. Jafar, N. Jindal, and S. Vishwanath, "Capacity limits of MIMO channels," *IEEE J. Sel. Areas Commun.*, vol. 21, no. 5, pp. 684–702, Jun. 2003.
- [16] M. Damen, A. Abdi, and M. Kaveh, "On the effect of correlated fading on several space-time coding and detection schemes," in *Proc. IEEE 54th Veh. Technol. Conf.*, vol. 1, pp. 13–16, Oct. 7–11, 2001.
- [17] M. Chiani, M. Win, and A. Zanella, "On the capacity of spatially correlated MIMO Rayleigh-fading channels," *IEEE Trans. Inf. Theory*, vol. 49, no. 10, pp. 2363–2371, Oct. 2003.
- [18] T. Svantesson and A. Ranheim, "Mutual coupling effects on the capacity of multielement antenna systems," in *Proc. IEEE ICASSP*, vol. 4, pp. 2485–2488, May 7–11, 2001.
- [19] S. Ganesan, R. Mesleh, H. Haas, C. W. Ahn, and S. Yun, "On the performance of spatial modulation OFDM," in *Proc. 40th Asilomar Conf. Signals, Syst. Comput.*, pp. 1825–1829, Oct. 29–Nov. 1, 2006.
- [20] R. Mesleh, H. Haas, C. W. Ahn, and S. Yun, "Spatial modulation—A new low-complexity spectral efficiency enhancing technique," in *Proc. CHINACOM*, pp. 1–5, Oct. 25–27, 2006.
- [21] R. Mesleh, H. Haas, C. W. Ahn, and S. Yun, "Spatial modulation—OFDM," in *Proc. 11th InOWo*, pp. 288–292, Aug. 30–31, 2006.
- [22] A. Tonello, "Space-time bit-interleaved coded modulation with an iterative decoding strategy," in *Proc. IEEE 52nd Veh. Technol. Conf.*, 24–28 Sept. 2000.

- [23] R. Y. Mesleh, H Haas, S. Sinanovic, C.W Ahn and S. Yun, “Spatial Modulation” *IEEE Transactions on Vehicular Technology*, vol. 57, no. 4, pp. 2228-2241, July 2008.
- [24] J. Jeganathan, A. Ghayeb, and L. Szczecinski, “Generalized space shift keying modulation for MIMO channels,” in *Proc. IEEE 19th Int. Symp. PIMRC*, Cannes, France, pp. 1–5, Sep. 15–18, 2008
- [25] A. Younis, S. Sinanovic, M. Di Renzo, R. Mesleh, and H. Haas, “Generalised sphere decoding for spatial modulation,” *IEEE Trans. Commun.*, vol. 61, no. 7, pp. 2805–2815, Jul. 2013.
- [26] S. Sugiura, C. Sheng, and L. Hanzo, “Generalized space–time shift keying designed for flexible diversity-, multiplexing- and complexitytradeoffs,” *IEEE Trans. Wireless Commun.*, vol. 10, no. 4, pp. 1144–1153, Apr. 2011.
- [27] R. Mesleh, S. S. Ikki, and H. M. Aggoune, “Quadrature spatial modulation system,” U.S. Patent 61/897 894, Oct. 31, 2013.
- [28] H. Yonghong, W. Pichao, W. Xiang, Z. Xiaoming, and H. Chunping, “Ergodic capacity analysis of spatially modulated systems,” *Commun. China*, vol. 10, no. 7, pp. 118–125, Jul. 2013.
- [29] J. Wang, S. Jia, and J. Song, “Generalised spatial modulation system with multiple active transmit antennas and low complexity detection scheme,” *IEEE Trans. Wireless Commun.*, vol. 11, no. 4, pp. 1605–1615, Apr. 2012.
- [30] J. Wang, S. Jia, and J. Song, “Signal vector based detection scheme for spatial modulation,” *IEEE Commun. Lett.*, vol. 16, no. 1, pp. 19–21, Jan. 2012.
- [31] M. Maleki, H. Bahrami, S. Beygi, M. Kafashan, and N. Tran, “Space modulation with CSI: Constellation design and performance evaluation,” *IEEE Trans. Veh. Technol.*, vol. 62, no. 4, pp. 1623–1634, May 2013.
- [32] M. Maleki, H. Bahrami, A. Alizadeh, and N. Tran, “On the performance of spatial modulation: Optimal constellation breakdown,” *IEEE Trans. Commun.*, vol. 62, no. 1, pp. 144–157, Jan. 2014.

- [33] S. Sugiura, S. Chen, and L. Hanzo, "Coherent and differential space–time shift-keying: A dispersion matrix approach," *IEEE Trans. Commun.*, vol. 58, no. 11, pp. 3219–3230, Nov. 2010.
- [34] S. Sugiura, S. Chen, and L. Hanzo, "Coherent and differential space–time shift keying: A dispersion matrix approach," *IEEE Trans. Commun.*, vol. 58, no. 11, pp. 3219–3230, Nov. 2010.
- [35] S. S. Ikki and R. Mesleh, "A general framework for performance analysis of Space Shift Keying (SSK) modulation in the presence of Gaussian imperfect estimations," *IEEE Commun. Lett.*, vol. 16, no. 2, pp. 228–230, Feb. 2012.
- [36] A. Younis, N. Serafimovski, R. Mesleh, and H. Haas, "Generalized spatial modulation," in *Conf. Rec. Asilomar Conf. Signals, Syst., Comput.*, Pacific Grove, CA, USA, pp. 1498–1502, Nov.7-10, 2010.
- [37] J. Jeganathan, A. Ghayeb, and L. Szczecinski, "Generalized space shift keying modulation for MIMO channels," in *Proc. IEEE 19th Int. Symp. PIMRC*, Cannes, France, pp. 1–5, Sep. 15–18, 2008.
- [38] R. Mesleh, I. Stefan, H. Haas, and P. Grant, "On the performance of trellis coded spatial modulation," in *Proc. ITG Int. WSA*, Berlin, Germany, pp. 235–241, Feb. 16–19, 2009.
- [39] Y. Naresh, and A. Chockalingam, "On Media-Based Modulation Using RF Mirrors" *IEEE Transactions on Vehicular Technology*, Vol. 66, No. 6, pp 4967-4983, June 2017
- [40] A. K. Khandani, "Media-based modulation: A new approach to wireless transmission," 2013 *IEEE International Symposium on Information Theory*, pp. 3050-3054, July 7-12, 2013.
- [41] Y. Naresh and A. Chockalingam. "Performance Analysis of Media-Based Modulation With Imperfect Channel State Information" *IEEE Trans. Veh. Technol.*, vol.67, no. 5, pp. 4192–4207, Jan. 2018.
- [42] A. K. Khandani, "Media-based modulation: Converting static Rayleigh fading to AWGN," in *Proc. IEEE Int. Symp. Inf. Theory*, pp. 1549–1553, Jun./Jul. 2014.

- [43] L. Zheng and D. Tse, "Diversity and Multiplexing: A Fundamental Tradeoff in Multiple Antenna Channels, *IEEE Transactions on Information Theory*, vol. 49, pp. 1073-96, May 2003.
- [44] E. Seifi, M. Atamanesh, and A. K. Khandani, "Media-based modulation: A new frontier in wireless communications," Oct. 7, 2015. [Online]. Available: <https://arxiv.org/abs/1507.07516>
- [45] G. Das Menghwar and C. F. Mecklenbrauker, "Cooperative versus non-cooperative communications," *2009 2nd International Conference on Computer, Control and Communication*, pp. 1-3, Feb. 2009.
- [46] A. Sendonaris, E. Erkip, and B. Aazhang, "User cooperation diversity Part I: System description," *IEEE Trans. Commun.*, vol. 51, no. 11, pp. 1927–1938, Nov 2003.
- [47] J. N. Laneman, "Cooperative diversity in wireless networks: Algorithms and architectures," Ph.D. dissertation, Massachusetts Institute of Technology, Cambridge, MA, Aug 2002.
- [48] E. Van Der Meulen, "Three-terminals communication channels," *Adv. Appl. Prob.*, vol. 3, no. 1, pp. 120–154, 1971.
- [49] A. E. G. T Cover, "Capacity theorems for the relay channel," *IEEE Trans. Inf. Theory*, vol. IT-25, no. 5, pp. 572–584, Sep 1979.
- [50] A. El Gamal and S. Zahedi, "Capacity of a class of relay channels with orthogonal components," *IEEE Transactions on Information Theory*, vol. 51, no. 5, pp. 1815-1817, May 2005.
- [51] J. N. Laneman, D. N. C. Tse, and G. W. Wornell, "Cooperative diversity in wireless networks: efficient protocols and outage behavior," *IEEE Trans. Inf. Theory*, vol. 50, no. 12, pp. 3062–3080, Dec 2004.
- [52] M. Yuksel and E. Erkip, "Multi-antenna cooperative wireless systems: A diversity-multiplexing tradeoff perspective," *IEEE Trans on Inf Theory*, vol. 53, no. 10, pp. 3371–3393, Oct 2007.
- [53] A. Sendonaris, E. Erkip, and B. Aazhang, "User cooperation diversity Part II: Implementation aspects and performance analysis," *IEEE Trans. Commun.*, vol. 51, no. 11, pp. 1939–1948, Nov 2003.

- [54] G. Kramer, M. Gastpar and P. Gupta, "Cooperative strategies and capacity theorems for relay networks," *IEEE Transactions on Information Theory*, vol. 51, no. 9, pp. 3037-3063, Sept. 2005, doi: 10.1109/TIT.2005.853304.
- [55] P. Razaghi and W. Yu, "Bilayer LDPC codes for the relay channel," *IEEE International Conference on Communications*, 2006, vol. 4, pp. 1574–1579, Jun 2006.
- [56] G. D. Menghwar and C. F. Mecklenbrauker, "Network coding for cooperative communications," *Proceedings of Junior Scientist Conference 2008*, Vienna, Austria, pp. 105–106, Nov 2008.
- [57] R. Ahlswede, N. Cai, S.-Y. R. Li, and R.W. Yeung, "Network information flow," *IEEE Trans. Inform. Theory*, vol. 46, no. 4, pp. 1204–1216, Jul. 2000.
- [58] E. Benamira, F. Merazka "Application of Cooperative Communication and Network Coding on Wireless Network Topologies' Conference: ICNAS 2017, uploaded June 2021.
- [59] Yunnan Wu "Network Coding for Wireless Networks" Microsoft Research, One Microsoft Way, Redmond, WA 98052-6399 USA, pp 1-25, July 2007.
- [60] R. Koetter and M. Médard, "An algebraic approach to network coding," *IEEE/ACM Trans. Netw.*, vol. 11, no. 5, pp. 782-795, Oct. 2003.
- [61] S. Katti, D. Katabi, W. Hu, H. Rahul, M. Médard, "The Importance of Being Opportunistic: Practical Network Coding for Wireless Environments," in *Proc. 43rd Annual Allerton Conference on Communication, Control, and Computing*, June 2005.
- [62] S. Katti, H. Rahul, W. Hu, D. Katabi, M. Médard, J. Crowcroft, "XOR in The Air: Practical Wireless Network Coding," *IEEE/ACM Transactions on Networking*, vol. 16, no. 3, pp. 497–510, June 2008.
- [63] Y. Chen, S. Kishore, and J. Li, "Wireless diversity through network coding," in *Proc. IEEE WCNC*, pp. 1681–1686, Apr. 2006.
- [64] J. Zhang and Q. Zhang, "Cooperative Network Coding-Aware Routing for Multi-Rate Wireless Networks," in *Proc. Infocom*, pp. 181-189., Apr. 2009.

- [65] A. Nasri, R. Schober, and M. Uysal, "Error rate performance of network-coded cooperative diversity systems," in Proc. IEEE GLOBECOM, pp. 1–6, Dec. 2010.
- [66] L. Zheng and D. Tse, "Diversity and multiplexing: a fundamental tradeoff in multiple-antenna channels," *IEEE Trans. Inf. Theory*, vol. 49, no. 5, pp. 1073–1096, May 2003.
- [67] M. Di Renzo, M. Iezzi, and F. Graziosi, "On diversity order and coding gain of multisource multirelay cooperative wireless networks with binary network coding," *IEEE Trans. Veh. Technol.*, vol. 62, no. 3, pp. 1138–1157, Mar. 2013.
- [68] S. Rouayheb, A. Sprintson, and C. Georghiadis, "Robust network codes for unicast connections: A case study," *IEEE/ACM Trans. Netw.*, vol. 19, no. 3, pp. 644–656, Jun. 2011.
- [69] A. Pašić, "Survivable routing meets diversity coding," in *Proc. IFIP Netw.*, pp. 1–9, May 2015.
- [70] B. Ladóczki, "Robust network coding in transport networks," in Proc. IEEE Conf. Comput. Commun. Workshops (INFOCOM WKSHPs), pp. 27–28, May 2015.
- [71] F. Rossetto and M. Zorzi, "Mixing network coding and cooperation for reliable wireless communications," *IEEE Wireless Commun.*, vol. 18, no. 1, pp. 15–21, Feb. 2011.
- [72] M. Médard and A. Sprintson, *Network Coding: Fundamentals and Applications*. Academic Press, 2012.
- [73] T. Ho and D. Lun, *Network Coding: An Introduction*. New York, NY, USA: Cambridge University Press, 2008.
- [74] Y. Hong, W. Huang, and C. Kuo, *Cooperative Communications and Networking: Technologies and System Design*. Springer US, 2010.
- [75] L. Dai, and K. B. Letaief, "Throughput maximization of Ad-hoc wireless networks using adaptive cooperative diversity and truncated ARQ," *IEEE Trans. Wireless Comm.*, vol. 56, no. 11 pp. 1907-1918, Nov. 2008.
- [76] H. Xu and N. Pillay, "The Component-Interleaved Golden Code and Its Low-Complexity Detection," *IEEE Access*, vol. 8, pp. 59550-59558, Mar. 2020.

- [77] L. Zheng and D. N. C. Tse, "Diversity and multiplexing: A fundamental tradeoff in multiple-antenna channels," *IEEE Trans. Inf. Theory*, vol. 49, no. 5, pp. 1073–1096, May 2003.
- [78] J. C. Belfiore, G. Rekaya, and E. Viterbo, "The golden code: A 2×2 fullrate space-time code with nonvanishing determinants," *IEEE Trans. Inf. Theory*, vol. 51, no. 4, pp. 1432–1436, Apr. 2005.
- [79] M. Sinnokrot and J. Barry, "Fast maximum-likelihood decoding of the golden code," *IEEE Trans. Wireless Commun.*, vol. 9, no. 1, pp. 26–31, Jan. 2010.
- [80] S. Sirinaunpiboon, A. R. Calderbank, and S. D. Howard, "Fast essentially maximum likelihood decoding of the golden code," *IEEE Trans. Inf. Theory*, vol. 57, no. 6, pp. 3537–3541, Jun. 2011.
- [81] E. Viterbo and Y. Hong, "On the performance of golden space-time trellis coded modulation over MIMO block fading channels," *IEEE Trans. Wireless Commun.*, vol. 8, no. 6, pp. 2737–2741, Jun. 2009.
- [82] H. Xu and N. Pillay, "Golden codeword-based modulation schemes for single-input multiple-output systems," *Int. J. Commun. Syst.*, vol. 32, no. 10, Jul. 2019, Art. no. e3963.
- [83] J. Boutros and E. Viterbo, "Signal space diversity: A power- and bandwidth-efficient diversity technique for the Rayleigh fading channel," *IEEE Trans. Inf. Theory*, vol. 44, no. 4, pp. 1453–1467, Jul. 1998.
- [84] G. Taricco and E. Viterbo, "Performance of component interleaved signal sets for fading channels," *Electron. Lett.*, vol. 32, no. 13, p. 1170, Oct. 1996.
- [85] H. Xu and N. Pillay "Golden codeword-based modulation schemes for single-input multiple output systems" *International Journal of Communication system* Volume 32, Issue 10 e.3963, April 2019. <https://doi-org.ukzn.idm.oclc.org/10.1002/dac.3963>
- [86] J. Boutros and E. Viterbo, "Signal space diversity: a power- and bandwidth-efficient diversity technique for the Rayleigh fading channel," *IEEE Transactions on Information Theory*, vol. 44, no. 4, pp. 1453–1467, July 1998.

- [87] J. Belfiore, G. Rekaya and E. Viterbo, "The golden code: a $2/\text{spl times}/2$ full-rate space-time code with nonvanishing determinants," *IEEE Transactions on Information Theory*, vol. 51, no. 4, pp. 1432-1436, April 2005.
- [88] Sinnokrot MO, Barry JR. Fast maximum-likelihood decoding of the Golden code. *IEEE Trans Wireless Commun.* 9(1): 26- 31, 2010.
- [89] H. Xu, K. Govindasamy and N. Pillay, "Uncoded Space-Time Labeling Diversity," *IEEE Communications Letters*, vol. 20, no. 8, pp. 1511-1514, Aug. 2016.
- [90] S. Sirinaunpiboon, A. R. Calderbank and S. D. Howard, "Fast Essentially Maximum Likelihood Decoding of the Golden Code," *IEEE Transactions on Information Theory*, vol. 57, no. 6, pp. 3537-3541, June 2011.
- [91] E. Viterbo and Y. Hong, "On the performance of golden space-time trellis coded modulation over MIMO block fading channels," *IEEE Transactions on Wireless Communications*, vol. 8, no. 6, pp. 2737-2741, June 2009.
- [92] L. Luzzi, G. R. Othman, J. Belfiore and E. Viterbo, "Golden Space–Time Block-Coded Modulation," *IEEE Transactions on Information Theory*, vol. 55, no. 2, pp. 584-597, Feb. 2009.
- [93] N. Pillay and H. Xu, "Quadrature spatial media-based modulation with RF mirrors," *IET Communication*, vol. 11, pp. 2440 - 2448, Nov.2017.
- [94] R. Pillay, N. Pillay, and H. Xu, "A Study of Single-Input Multiple-Output Media-based Modulation with RF Mirrors," presented at the SATNAC, Spain, Sept. 2017.
- [95] Li Y, Daneshmand M, and Duan W. "A cooperative relay method and performance for wireless networks," In: Proc. 2nd international symposium on intelligence information processing and trusted computing, Hubei, pp. 31-34, Dec. 2011.
- [96] Althunibat S, Mesleh R. "Performance analysis of quadrature spatial modulation in two-way relaying cooperative networks," *IET Communications*, vol. 12, no. 4, pp. 466-472, Mar. 2018.
- [97] A. J Bamisaye and T. Quazi, "Quadrature Spatial Modulation-aided Single-Input Multiple-Output media-based Modulation," *International Journal of Communication Systems*.vol. 34, no.11, May 2021;e4883. <https://doi.org/10.1002/dac.4883>.

- [98] N. Pillay, and H. Xu, "RF Mirror Media-based Modulation for Golden Codes," *Journal of telecommunication electronic and computer engineering*, vol. 10, pp. 21-24, Aug.2018.

Chapter 2

Journal Article 1

Journal Article 1

**Quadrature Spatial Modulation Aided Single-Input Multiple-
Output-Media Based Modulation**

Ayodeji James Bamisaye and Tahmid Quazi

Published: International Journal of Communication Systems

Vol.34, Iss 11, 2021; e4883. <https://doi.org/10.1002/dac.4883>

2.1 Abstract

Single-input multiple-output media-based modulation (SIMO-MBM) improves the limitation of single-input multiple-output (SIMO) systems by minimizing the required number of antennas to achieve a high data rate and enhanced error performance. In this paper, we employ the quadrature dimension of the spatial constellation by decomposing the amplitude/phase modulation (APM) symbol into real and imaginary components similar to quadrature spatial modulation (QSM) to improve the overall error performance of the conventional SIMO-MBM and to achieve a higher data rate. The average bit error probability of the proposed scheme is formulated using a lower bound approach and validated by the Monte Carlo (MC) simulation results obtained. Furthermore, the effect of the sub-optimal mirror activation pattern selection using channel amplitude coupled with antenna correlation is examined for the proposed system. The Monte Carlo simulation results achieved demonstrate a substantial improvement of 3.5dB at 10b/s/Hz with $m_{rf} = 2$ and 7dB at 12b/s/Hz with $m_{rf} = 4$ over the conventional SIMO-MBM scheme. The effect of imperfect channel estimation on the proposed scheme is investigated, with a trade-off of 2dB in coding gain due to channel estimation errors.

2.2 Introduction

Multiple-input multiple-output (MIMO) systems [1] have shown tremendous promise over the years as the future of wireless communication regarding improved system performance and high transmission capacity [2-4]. However, some significant drawbacks to the practical realization of MIMO systems, such as inter-antenna synchronization (IAS) and inter-channel interference (ICI) due to multi-active transmit antennas [5,6], are experienced in MIMO systems.

These drawbacks experienced in MIMO systems are eliminated in spatial modulation (SM) [7-10]. SM is an innovative MIMO scheme, which requires a single radio frequency (RF) chain. The SM system's basic idea is to use both the amplitude/phase modulation (APM) and transmit antenna index to convey information. Improvements achieved in SM have spawned a wealth of research in MIMO systems [11,12].

Achieving a high data rate in SM systems requires a large number of transmit antennas. Considering the logarithmic relationship between the total number of transmit antennas and the spectral efficiency, this limits its practical implementation due to the hardware cost, leading to the investigation of quadrature spatial modulation (QSM) [13].

QSM [13] is an SM-based scheme, which extends its spatial constellation to the quadrature dimension. The APM constellation symbol is decomposed into real and imaginary components. Two transmit antennas are selected based on the input bits; one transmits the decomposed APM symbol's real component while the other transmits the imaginary component to the receiver. In QSM, ICI and IAS are avoided completely. The decomposed APM symbol is modulated into the cosine and sine carriers, respectively [13], enabling the use of a single RF chain similar to SM. Thus, it eliminates the setback of SM by employing additional $\log_2 N_T$ transmit antenna bits to relay the second component of the decomposed symbol. In addition, the error performance of QSM and optical improved quadrature spatial modulation (OIQSM) are superior to SM and conventional MIMO schemes [13-16] due to the full utilization of the transmit diversity in QSM. Recently, media-based modulation (MBM) [17] has been introduced in the research community as an efficient technique for achieving high data rate with a lower cost in terms of hardware complexity. MBM employs the linear relationship between the number of RF mirrors and the achieved spectral efficiency to reduce the imposed hardware complexity compared to SM and QSM. This is achieved by employing RF mirrors to create different channel fade realizations, known as mirror activation patterns (MAPs) [17].

Also, in MBM [18], a subset of channel realizations may be selected from the distinct channel perturbations that result in superior error performance. The received constellation size is independent of the transmit power. Hence, a substantial increase in spectral efficiency is easily realizable. Likewise, transmit antennas in SM systems must have a minimum distance between them to achieve an independent fading, while RF mirrors can be positioned alongside each other.

In [17,18], MBM was proposed for generalized SM (MBM-GSM) and quadrature SM (MBM-QSM), respectively. The MBM-GSM scheme [17] employs the conventional GSM scheme, utilizing the transmit antenna combination to activate two transmit units at every transmission instant with the spatial dimension to convey information similar to [7]. In the MBM-SM scheme, the APM symbol is not decomposed and an additional m_{rf} bits is employed to activate a single RF mirror in one transmit units, which is employed for transmission. However, in the MBM-GSM scheme, the additional $2m_{rf}$ bits employed activates two RF mirrors, each in a unique transmit unit, i.e. two transmit units coupled with two RF mirrors are employed in total for transmission.

Similarly, in MBM-QSM [18], the decomposed APM symbol is modulated into in-phase and quadrature components transmitted via the sine and cosine carriers, respectively. Therefore, achieving the requirement of a single RF chain. However, MBM-GSM requires multiple RF chains. In the MBM-QSM scheme, an additional $2m_{rf}$ bits are employed to activate two RF mirrors, each in a unique transmit unit provided the transmit antenna indices are different. However, if the transmit antenna indices are the same, a single transmit unit is employed with a larger number of RF mirrors available within the transmit unit, employing only a single RF mirror.

In [19], a single-input multiple-output-MBM (SIMO-MBM) system was investigated to achieve a high data rate at lower hardware cost than SM and the conventional SIMO schemes. SIMO-MBM employs the linear relationship between the number of RF mirrors (m_{rf}) to achieve high data rate with few numbers of transmit antennas. Considering an example of an SM system with four transmits antennas coupled with 4-QAM, which will yield 4 b/s/Hz. However, SIMO-MBM with one transmit antenna, 4 RF mirrors and 4-QAM, will generate 6 b/s/Hz. Therefore, SIMO-MBM is more desirable than SM in terms of data rate. In the SIMO-MBM scheme, the APM symbol is not decomposed and an additional m_{rf} bits is employed to activate a single RF mirror in the only available transmit units (as only one is available in SIMO schemes), which is employed for transmission. Considering the benefits of QSM stated earlier over SM and conventional MIMO schemes coupled with improved error performance, it reveals that QSM exhibits superior error performance and is more desirable. Thus, this motivates us to investigate the application of the

quadrature dimension in the SIMO-MBM scheme similar to conventional QSM scheme termed QSM aided SIMO-MBM scheme.

Furthermore, transmit antenna selection is an efficient technique to improve the error performance of index modulation schemes [20, 21]. The most efficient transmit antenna selection mostly used in index modulation schemes are the Euclidean distance antenna selection technique, norm-based transmit antenna selection technique, and norm-correlation-based transmit antenna selection technique. In [22], the transmit antenna selection method was utilized to enhance the system's reliability, based on maximizing the minimum Euclidean distance between transmission vectors.

Also, in [23, 24], a sub-optimal transmit antenna selection algorithm is employed to maximize the channel amplitude and minimize the antenna correlation, reducing computational complexity (CC). However, applying a Euclidean distance-based antenna selection (EDAS) to the proposed scheme, it imposes a very high CC and demands an excessive amount of memory. Hence, limiting practical implementation. Considering an example of a system configuration with $m_{rf} = 5$, i.e. $N_m = 2^5 = 32$. Therefore, for each transmission interval, the EDAS technique requires 2×2^5 floating points of operations and additional $\binom{32}{4}$ enumerations to find the optimal 4 MAPs required at every transmission interval. These enumerations require storage for comparison purposes. Hence, the EDAS MAP selection technique for the proposed scheme is both computationally expensive and memory intensive.

This paper's contributions are as follows: a) we investigate RF mirror-based MBM in a SIMO-based QSM system, decomposing the APM symbol prior to transmission and employing unique (different) RF mirrors to transmit the decomposed APM symbol in a SIMO scheme as compared to SIMO-MBM [19]. b) The theoretical average bit error probability (ABEP) is formulated for the proposed scheme (QSM aided SIMO-MBM) to be validated by the simulation results. c) To further improve the proposed scheme's error performance, the impact of MAP selection based on processing the channel amplitude and antenna correlation to remove the imperfect channel(s) at each transmission instance is studied on the proposed scheme. The optimal transmit antenna selection (Euclidean distance-based transmit antenna selection EDAS) is not considered in this paper. The application of EDAS requires high memory and imposes high computational complexity (CC), limiting practical implementation.

The structure of the remainder of the paper is as follows. In Section 2, the proposed QSM aided SIMO-MBM system model is described. Analysis of the proposed scheme is presented in Section 3. In Section 4, the effect of transmit antenna selection is examined. Performance analysis in terms

of error rate achieved for the proposed scheme and conclusions are presented in sections 5 and 6, respectively.

Notation: Bold italic lowercase/uppercase symbols indicate vectors/matrices, while the scalar quantities are represented by regular letters. $\|\cdot\|_F$ represents Frobenius norm, $Q(\cdot)$ signifies the Gaussian Q-function, $E\{\cdot\}$ is the expectation operator, $\underset{w}{\operatorname{argmin}}(\cdot)/\underset{w}{\operatorname{argmax}}(\cdot)$ depicts the minimum or maximum value of an argument with respect to w , while $R\{\cdot\}$ and i portrays the real and complex number, respectively.

2.3 The System Model of QSM Aided SIMO-MBM

In this section, we first introduce the system model of QSM; after that, the proposed scheme's system model is presented.

2.3.1 The System Model of QSM

QSM achieves a spectral efficiency m of $\log_2 MN_T^2$ b/s/Hz. [13], where M represent the modulation order and N_T the number of transmit antennas. In QSM, the APM symbol x_q is decomposed into real and imaginary components and mapped into the $\log_2 M$ bits. The transmit antenna required to transmit the real part of the modulated symbol is activated by $\log_2 N_T$, while an additional $\log_2 N_T$ bits activate the second transmit antenna required to transmit the imaginary component.

An example of a QSM scheme with 2 transmit antennas and 4-QAM APM symbol yields 4 b/s/Hz. The first two bits modulate the 4-QAM symbol x_q , the third bit activates the transmit antenna index ℓ_R and the fourth bit activates the second transmit antenna index ℓ_I , which are used to transmit the real and imaginary components of the decomposed APM symbol and modulated in sine and cosine carriers, respectively.

The decomposed symbol x_q is transmitted via a channel \mathbf{H} with additive white gaussian noise (AWGN) \mathbf{n} and $CN(0,1)$ distribution. Thus, the received vector \mathbf{y} becomes:

$$\mathbf{y} = \mathbf{h}_{\ell_R} x_{Re}^q + i \mathbf{h}_{\ell_I} x_{Im}^q + \mathbf{n} \quad (2.1)$$

where $x_q = x_{Re}^q + i x_{Im}^q$, ℓ_R and ℓ_I is the corresponding transmit antenna employed to transmit the decomposed symbol.

2.3.2 System Model for the Proposed Scheme

The system model of the proposed QSM aided SIMO-MBM scheme is illustrated in Figure 2.1. A single transmit antenna with m_{rf} RF mirrors located around the transmit antenna and N_R receive antennas are assumed.

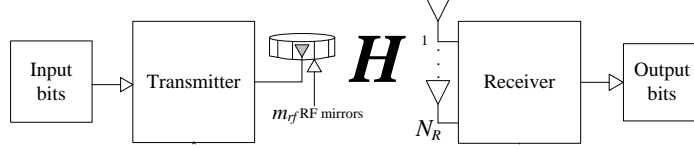


Figure 2.1 System model of the proposed QSM aided SIMO-MBM scheme.

The spectral efficiency of the proposed QSM aided SIMO-MBM is presented as $m = \log_2(M) + 2m_{rf}$ b/s/Hz, where M , N_T , and m_{rf} denotes the APM constellation size, total number of transmit antennas, and RF mirrors, respectively.

Considering the example of a system with the following settings: $M = 4$, $N_T = 1$, and $m_{rf} = 2$, i.e. $N_m = 2^{m_{rf}} = 4$. It produces a spectral efficiency of 6 b/s/Hz. Consequently, each transmitting unit's unique MAP indices are used in activating the RF mirrors, which will send the decomposed modulated symbol.

The modulated symbol is transmitted via the channel $\mathbf{H}_j = [\mathbf{h}_1 \mathbf{h}_2 \cdots \mathbf{h}_{N_m}]$, $j \in [1: N_m]$, which is independent and identically distributed (i.i.d) as $CN(0, 1)$ with $N_R \times N_m$ dimension with additive white Gaussian noise (AWGN) \mathbf{n} of dimension $N_R \times 1$. Therefore, the $N_R \times 1$ received signal vector \mathbf{y} can be written as:

$$\mathbf{y} = \sqrt{\rho}(\mathbf{H}_j \mathbf{e}_{\ell_R} x_{Re}^q + \mathbf{H}_j \mathbf{e}_{\ell_I} x_{Im}^q) + \mathbf{n} \quad (2.2)$$

where ρ represent the signal-to-noise ratio (SNR), $x_q = x_{Re}^q + ix_{Im}^q$, $q \in [1: M]$ signifies the APM symbol, ℓ_R and ℓ_I is the corresponding active RF mirror employed to transmit the decomposed symbol, \mathbf{e}_{ℓ_R} and \mathbf{e}_{ℓ_I} is an $N_m \times 1$ vector with ℓ^{th} the non-zero position equivalent to the selected MAP, set to unity.

Table 2.1 shows an example of the mapping process, the input bits [1 0 1 0 0 0] are partitioned into three segments; one segment modulates the APM symbol [1 0] based on $\log_2 M$, the next segment [1 0] selects the RF mirror to transmit the real component of the APM symbol, while the third segment [0 0] chooses the second RF mirror to be utilized in transmitting the imaginary part of the decomposed APM symbol, each based on m_{rf} .

2.4 Maximum Likelihood (ML) Detector

Maximum Likelihood (ML) detector detects optimally the received signal \mathbf{y} , which explores M constellation points' entire signal space, all possible transmit antenna index combinations, and MAP indices. The ML detector can be described as [17]:

$$[\hat{\ell}, \hat{j}, x_{\hat{R}e}^q, x_{\hat{I}m}^q] = \underset{\substack{q \in [1:M] \\ \ell \in [1:N_m]}}{\operatorname{argmin}} \left(\|\mathbf{y} - \sqrt{\rho}(\mathbf{H}_j \mathbf{e}_{\ell_R} x_{Re}^q + \mathbf{H}_j \mathbf{e}_{\ell_I} x_{Im}^q)\|_F^2 \right) \quad (2.3)$$

Table 2.1 illustrates the mapping procedure for the QSM aided SIMO-MBM scheme.

Table 2.1: Mapping process for the QSM aided SIMO-MBM system using 4-QAM

Configuration	Input bits $m = \log_2(M) + 2m_{rf}$	Symbol bits $\log_2 M$ bits	MAP index m_{rf} bits	MAP index m_{rf} bits
		$\log_2 M$ bits	m_{rf} bits $m_{rf} = 2$	m_{rf} bits $m_{rf} = 2$
$M = 4$ $N_T = 1$ $N_R = 4$	1 0 1 0 0 0	[1 0] x_q $= 1 + 1i$	[1 0] e_{ℓ_R} $= [0 \ 1 \ 0 \ 0]^T$	[0 0] e_{ℓ_I} $= [1 \ 0 \ 0 \ 0]^T$
$M = 4$ $N_T = 1$ $N_R = 4$	1 1 0 1 1 1	[1 1] x_q $= 1 - 1i$	[0 1] e_{ℓ_R} $= [0 \ 0 \ 1 \ 0]^T$	[1 1] e_{ℓ_I} $= [0 \ 0 \ 0 \ 1]^T$

2.5 Average BER Analysis for the Proposed Scheme

The average BER analysis for the proposed QSM aided SIMO-MBM scheme is based on the average BER analysis for SIMO-MBM in [19], with minor adjustments to formulate the theoretical bound for the proposed system. The average BER is given as:

$$\begin{aligned} P_e &\geq 1 - ((1 - P_a)(1 - P_b)) \\ &= P_a + P_b - P_a P_b \end{aligned} \quad (2.4)$$

where P_e is sectioned into two; P_a being the bit error probability of the antenna index estimation provided the APM symbol is correctly detected, while P_b the bit error probability of the estimated symbol provided the antenna index is correctly detected.

For the proposed scheme, the system is considered as if a single antenna was utilized, like SM. Yet, the antenna error requires adjustment since multiple transmit antennas convey the APM symbol. Based on active antennas, the error is modified as $P_a = m_{rf} P_a$ using an average SNR $\frac{\rho}{4}$. Thus, utilizing a union bound on PEP, P_a can be computed as [19]:

$$P_a \leq \sum_{q=1}^M \sum_{j=1}^{N_m} \sum_{\hat{j}=1}^{N_m} \frac{N(j, \hat{j}) \mu^{N_R} \sum_{k=0}^{N_R-1} \binom{N_R-1+k}{k} [1-\mu]^k}{N_m M} \quad (2.5)$$

where $\mu = \frac{1}{2} \left(1 - \sqrt{\frac{\gamma}{\gamma+1}} \right)$, $N(j, \hat{j})$ is the number of bit errors between the transmit antenna j and the estimated transmit antenna \hat{j} . $\gamma = \frac{\rho}{2} |x_q|^2$.

Employing square M -QAM, P_b is computed similar to [8] and [22] as:

$$\begin{aligned} P_b &= \frac{1}{\log_2 M} \left(\frac{a}{c} \left[\frac{1}{2} \left(\frac{2}{b\rho + 2} \right)^{N_R} - \frac{a}{2} \left(\frac{1}{b\rho + 1} \right)^{N_R} + (1 \right. \right. \\ &\left. \left. - a) \sum_{i=1}^{c-1} \left(\frac{2\sin^2 \theta}{b\rho + 2\sin^2 \theta} \right)^{N_R} + \sum_{i=c}^{2c-1} \left(\frac{2\sin^2 \theta}{b\rho + 2\sin^2 \theta} \right)^{N_R} \right] \right) \end{aligned} \quad (2.6)$$

where $a = 1 - \frac{1}{\sqrt{M}}$, $b = \frac{3}{M-1}$, $\theta = \frac{i\pi}{4c}$ and c is the number of summations $c > 10$, for convergence of the trapezoidal approximation of the Q-function [22].

2.6 MAP Selection for QSM Aided SIMO-MBM System

Like Fig. 1, a system model with a transmit antennas surrounded with M_{rf} RF mirrors, $M_{rf} > m_{rf}$, which creates $N_{m_{total}} = 2^{M_{rf}}$ distinct MAPs. However, the required MAPs is only $2^{m_{rf}}$ MAPs out of the total $2^{M_{rf}}$ at every transmission interval. Employing the channel knowledge at the receiver, a MAP selection algorithm is used in selecting $2^{m_{rf}}$ MAPs out of $2^{M_{rf}}$ MAPs. The index of the selected MAPs is sent to the transmitter via a perfect feedback link for the next transmission.

For the proposed scheme, we study the impact of sub-optimal MAP selection algorithms by employing the following techniques

- a) MAP selection based on channel amplitude (norm-based).
- b) MAP selection based on channel amplitude and antenna correlation.

Since the CC and memory requirements of $m_{rf} > 4$ are incredibly high when applied to the proposed scheme, which makes the approach impracticable. $m_{rf} = 4$ are examined for all MAP selection algorithm studied in this paper.

2.6.1 Norm-based MAP selection

This section investigates the impact of maximizing the channel amplitude based on the channel that shows the highest energy. The channel vectors are arranged in ascending order such that the channel corresponding to each transmit antenna set with the highest power is utilized for the next transmission interval, such that:

$$\|\mathbf{h}_1\|_F^2 \geq \|\mathbf{h}_2\|_F^2 \geq \dots \geq \|\mathbf{h}_{N_m}\|_F^2 \geq \dots \geq \|\mathbf{h}_{N_{mT}}\|_F^2 \quad (2.7)$$

The selected N_m MAPs are then utilized in the subsequent transmission interval.

2.6.2 Channel amplitude and antenna correlation MAP selection

[23] investigated a low-complexity antenna sub-optimal technique for the SM system, demonstrating a low CC compared to the EDAS approach of [25].

The combination of channel amplitude and antenna correlation is utilized, discarding transmit antennas based on low amplitude and high correlation similar to [23], [26]. An algorithm based on the channel amplitude and antenna correlation as applied to QSM aided SIMO-MBM is as follows:

Algorithm 1

Step 1: Construct an $N_R \times N_{m_{Total}}$ channel matrix, where $N_{m_{Total}} > N_m$:

$$\mathbf{H} = [\mathbf{h}_1 \quad \mathbf{h}_2 \quad \cdots \quad \mathbf{h}_{N_{m_{Total}}}] \quad (2.8)$$

Step 2: Sort the vectors in (8) by computing the vector norm and arrange them in ascending order.

Step 3: Select the first $N_m + 1$ vectors from the sorted vector, to form the matrix \mathbf{H} :

$$\mathbf{H} = [\mathbf{h}_1 \quad \mathbf{h}_2 \quad \cdots \quad \mathbf{h}_{N_m+1}] \quad (2.9)$$

Step 4: Compute the angle of correlation [15, 16] for all possible pairs of the MAP combinations $(\mathbf{h}_{k_1}, \mathbf{h}_{k_2})$:

$$\theta = \arccos\left(\frac{|\mathbf{h}_{k_1}^H \mathbf{h}_{k_2}|}{\|\mathbf{h}_{k_1}\|_F \|\mathbf{h}_{k_2}\|_F}\right) \quad (2.10)$$

where $\binom{N_m+1}{2}$ represent the number of combinations

Step 5: Select the channel gain vector corresponding to the largest correlation (smallest angle) and remove the channel gain vector with the smallest vector norm.

The selected channel vector is then conveyed to the transmitter through the perfect feedback link and utilized in the next transmission interval.

2.7 Effect of Imperfect Channel Estimation (IChE) on the Proposed Scheme

Most previous performance analyses of coherent diversity systems assume that the receiver has perfect knowledge of the fading channels. However, effect of Imperfect Channel Estimation is applied to the proposed scheme by taking into consideration the statistics of channel estimation errors [27].

The error probability performance with the repetition code can serve as a lower bound for systems employing spectral-efficient precoding schemes [28]. After precoding, equally-spaced pilots are inserted among the data symbols.

There is always a non-negligible loss in performance in terms of the error probability due to channel estimation errors. This performance loss can be quantified in term of the loss in coding gain. For the high mobility system with imperfect CSI, the coding gain can be defined as [29]

$$C = \lim_{\substack{\gamma_0 \rightarrow \infty \\ N \rightarrow \infty}} \frac{(E)^{\frac{-1}{D_0}}}{\gamma_0} \quad (2.11)$$

where $D_0 = NT_p D$ is the diversity order of the high mobility system. Equivalently, the coding gain can be represented in the log domain as [29]:

$$\log C = \lim_{\substack{\gamma_0 \rightarrow \infty \\ N \rightarrow \infty}} \left[\frac{1}{NT_p D} \log P(E) + \log \gamma_0 \right] \quad (2.12)$$

where $T_p = 1/R_p$ is the space between two consecutive pilot symbols. Thus R_p , the number of pilots per unit time. The coding gain in (2.12) is lower bounded by $\log C \geq \log C_L$, where

$$\log C_L = 1 - \log(2\pi f_D T_p) + 2 \log \left(\sin \frac{\pi}{M} \right) - \log \left[\frac{(K+b)(b+1)}{Kb} \right] \quad (2.13)$$

The loss in coding gain due to channel estimation can be quantified as [29]

$$\begin{aligned} \gamma_{Loss}(dB) &= 10 \log_{10} C_L^i - 10 \log_{10} C_L \\ &= 10 \log_{10} \left[\frac{(K+b)(b+1)}{Kb} \right] \end{aligned} \quad (2.14)$$

The coding gain loss represents the extra SNR required by a system with imperfect Channel State Information (CSI) to achieve the same performance as its perfect CSI counterpart, when both systems have the same diversity gain. In addition, the coding gain loss is strictly greater than 0 dB.

The coding gain loss can be further decomposed into two components as

$$\gamma_{Loss}(dB) = 10 \log_{10} \left(1 + \frac{b}{K} \right) + 10 \log_{10} \left(1 + \frac{1}{b} \right) \quad (2.15)$$

The first term, $10 \log_{10} \left(1 + \frac{b}{K} \right)$, is the loss caused by the extra energy allocated for pilot symbols in systems with imperfect CSI. Therefore it increases in b , which is the ratio between the energy allocated for pilot and coded symbols, respectively. The second term, $10 \log_{10} \left(1 + \frac{1}{b} \right)$ is due

to channel estimation error, and it decreases in b because a larger b means more energy for pilots thus more accurate channel estimations.

Under a fixed K , the optimum b that can minimize the coding gain loss is [29]

$$\gamma_{Loss}(dB) = 20 \log_{10} \left(1 + \frac{1}{\sqrt{K}} \right) dB \quad (2.16)$$

2.8 Numerical Analysis and Discussion

This section presents the MC simulation results achieved for the proposed scheme. A Flat-fading Rayleigh channel is assumed. Likewise, the average BER versus SNR in dB is considered, and the ML detection technique is employed. A system configuration setting of 4 receive antennas with 4-QAM, 16-QAM, and 64-QAM is utilized, coupled with 2 and 4 RF mirrors.

2.8.1 Average BER performance of the QSM aided SIMO-MBM scheme

The system performance of the proposed scheme is presented in this section. The theoretical ABER results formulated above is also shown in this section. Figure 2.2 shows the MC simulation results obtained for the proposed scheme coupled with the theoretical ABER. In each setting, unique MAP indices are utilized to activate the required RF mirrors. The MC simulation results achieved show a tight fit in the higher SNR region with the average theoretical result (2.6) obtained validating the theoretical expression.

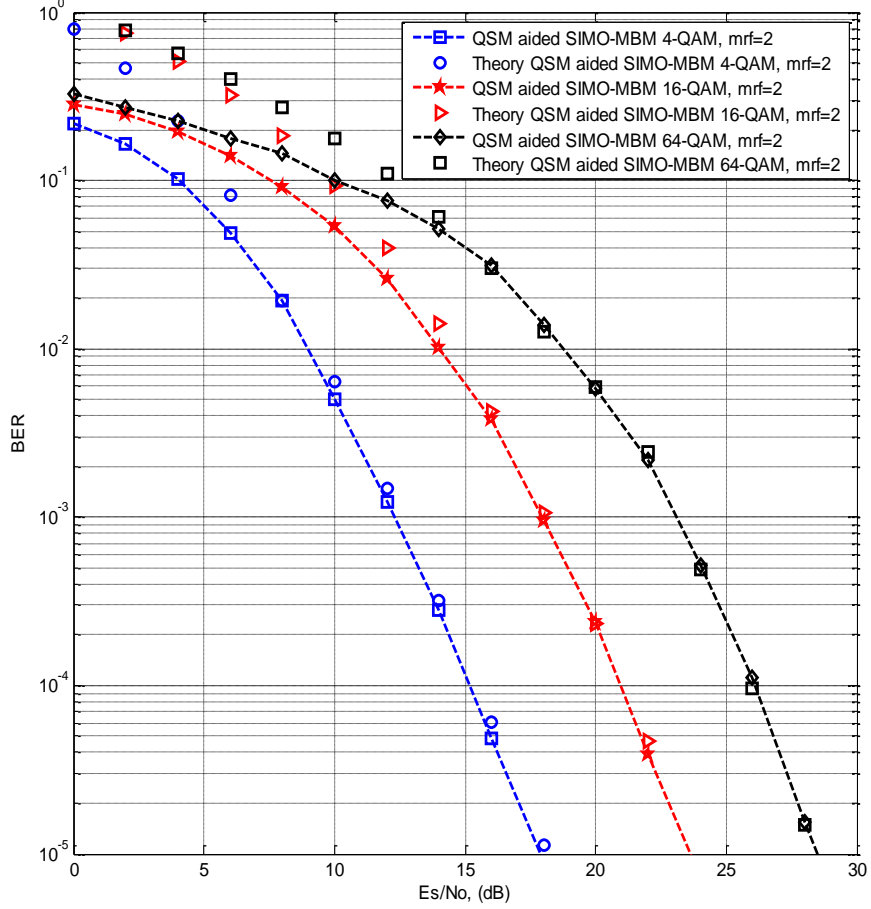


Figure 2.2 BER performance of QSM aided SIMO-MBM.

In Figure 2.3 and 2.4, the system configurations with $m_{rf} = 2$ and $m_{rf} = 4$ are considered, respectively. i.e., taking QSM aided SIMO-MBM with two and four RF mirrors as the reference point to compute the SNR gain obtained is presented in Table 2.2 and Table 2.3, respectively.

From the MC simulation results achieved, it is apparent that utilizing the quadrature dimension of the spatial constellation improves the scheme's system performance. At a BER of 10^{-5} , an SNR gain of approximately 3.5 dB is achieved when compared to the SIMO-MBM [19] with 6 b/s/Hz coupled with 2.5 dB SNR gain when compared to the SIMO-MBM [19] with 8 b/s/Hz and 3.5 dB SNR gain when compared to the SIMO-MBM [19] with 10 b/s/Hz, with two RF mirrors, i.e. $m_{rf} = 2$, respectively. Thus, this is achieved by maximizing the system's transmit diversity via employing the quadrature dimension of the APM symbol.

Likewise, in Figure 2.5, an SNR gain of approximately 6.5 dB is achieved when compared to the SIMO-MBM of [19] with 10 b/s/Hz and 7dB SNR gain when compared to the SIMO-MBM [19] with 12 b/s/Hz, with four RF mirrors, i.e. $m_{rf} = 4$, respectively.

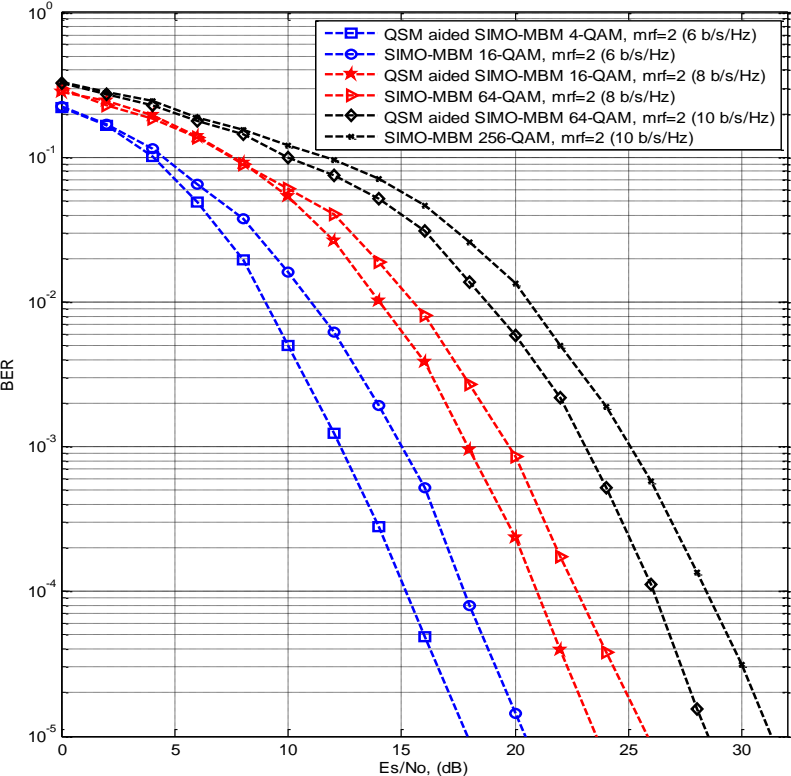


Figure 2.3 BER performance comparison of QSM aided SIMO-MBM ($m_{rf} = 2$) for 6, 8 and 10 b/s/Hz, respectively

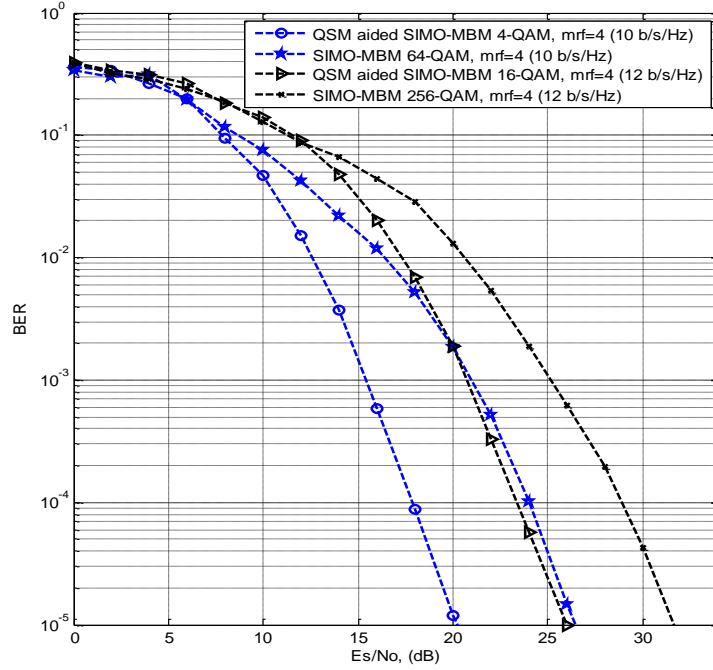


Figure 2.4 BER performance comparison of QSM aided SIMO-MBM ($m_{rf} = 4$) for 10 b/s/Hz and 12 b/s/Hz, respectively.

Table 2.2: SNR gain (dB) obtained for the QSM aided SIMO-MBM with $m_{rf} = 2$

Systems (b/s/Hz)	6	8	10
QSM aided SIMO-MBM	3.5 dB	2.5 dB	3.5 dB

Table 2.3: SNR gain (dB) achieved for the QSM aided SIMO-MBM with $m_{rf} = 4$

Systems (b/s/Hz)	10	12
QSM aided SIMO-MBM	6.5 dB	7dB

In Figure 2.5, the performance comparison between the proposed scheme (QSM aided SIMO-MBM) with different configuration settings ($m_{rf} = 2$ and $m_{rf} = 4$) are considered, respectively.

The MC simulation results revealed that the configuration settings with $m_{rf} = 2$ exhibits an improved system performance compared with its counterparts. The proposed system equipped with $m_{rf} = 2$ outperforms its counterpart equipped with $m_{rf} = 4$ by an SNR gain of approximately 3dB for 4-QAM, 2dB for 16-QAM and 1dB for 64-QAM, respectively.

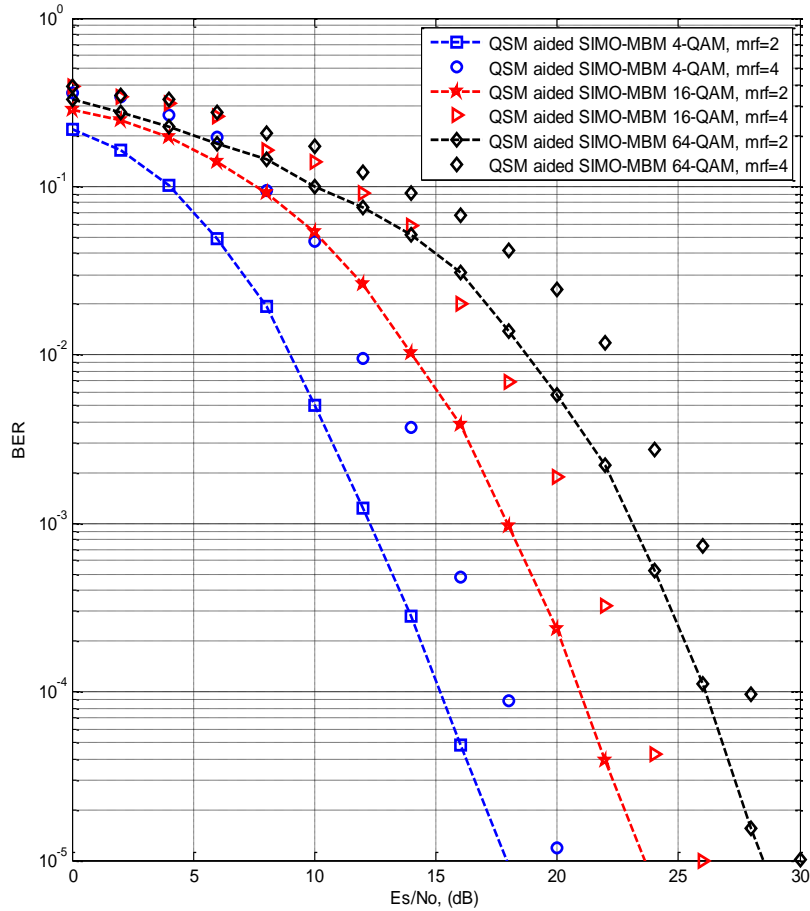


Figure 2.5 BER performance comparison of QSM aided SIMO-MBM for $m_{rf} = 2$ and $m_{rf} = 4$, respectively.

2.8.2 Average BER performance of QSM aided SIMO-MBM scheme with MAP selection

Figure 2.6 shows the MC simulation results for the QSM aided SIMO-MBM scheme equipped with the MAP selection algorithm. In this algorithm, we considered $m_{rf} = 2$ and $M_{rf} = 4$ with spectral efficiency of 6 and 8 b/s/Hz, respectively. The norm-correlation antenna selection technique is considered due to its less impose complexity and less memory requirement with a

considerable error performance where the norm-based antenna selection technique is used as a benchmark.

Considering a similar example mentioned above with $m_{rf} = 5$, i.e. $N_m = 2^5 = 32$ at each transmission interval the sub-optimal technique requires 2^5 floating points of operations as against 2×2^5 in the case of EDAS and requires additional $\binom{32}{2}$ enumerations as against $\binom{32}{4}$ In EDAS, finding the optimal MAPs required at every transmission interval and the enumerations do not need storage as it just a selector. Hence, this imposes a less CC as compared to EDAS.

The performance comparison between the conventional SIMO-MBM and QSM aided SIMO-MBM with the MAP selection algorithm is shown in Figure 2.6. The MC simulation results obtained for the QSM aided SIMO-MBM scheme with the MAP selection algorithm exhibit better performance than the conventional SIMO-MBM system. However, QSM aided SIMO-MBM with the MAP selection algorithm based on antenna norm-correlation outperforms every other scheme considered with approximately 4dB and 5.5dB with respect to conventional QSM aided SIMO-MBM and SIMO-MBM, respectively. This is due to the maximization of the MAPs amplitude and the minimization of the correlations between the MAPs.

The performance improvement between the two sub-optimal techniques considered (norm correlation MAP selection and norm MAP selection) is approximately 0.5dB SNR gain, which is small. This is due to the antenna correlation between the available MAPs that has already been maximized during the mapping process to fully maximize the transmit diversity before introducing the MAP selection technique.

Similarly, QSM aided SIMO-MBM with norm MAP selection algorithm outperforms the conventional SIMO-MBM scheme.

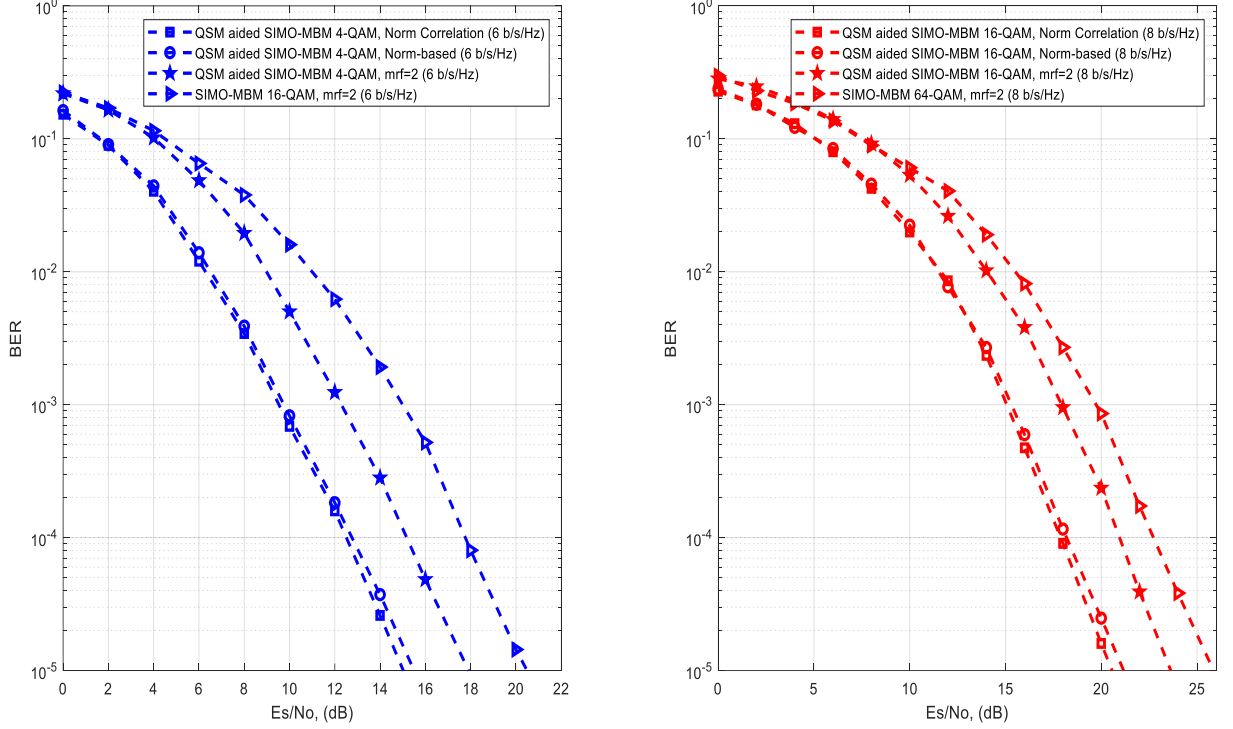


Figure 2.6 BER performance comparison of SIMO-MBM, (a) QSM aided SIMO-MBM with MAP algorithm for 6 b/s/Hz and (b) QSM aided SIMO-MBM with MAP algorithm for 8 b/s/Hz.

2.8.3 Average BER performance of QSM aided SIMO-MBM scheme with imperfect channel Estimation (IChE).

The analytical results are obtained by analyzing and quantifying the impacts of channel estimation errors on the system performance.

Figure 2.7 illustrates the loss in coding gain due to channel estimation errors. The parameters are $N^R = 4$, $M = 4, 16, 64$ and fixed $K = 15$. The BER curves with perfect and imperfect CSI have the same slope, which indicates that they have the same diversity order. The space between the BER curves with perfect and imperfect CSI corresponds to the loss in coding gain. Based on (2.16), the coding gain loss is $20 \log_{10} \left(1 + \frac{1}{\sqrt{K}} \right) \text{ dB} = 1.99$. This result is verified in Figure 2.7. For example, at $\text{BER} = 10^{-5}$ the required SNRs for system with imperfect and perfect CSI are 18dB and 20dB, 23.5dB and 25.5dB, and 28.5dB and 30.5dB for QSM-SIMO-MBM 4-QAM, QSM-SIMO-MBM 16-QAM and QSM-SIMO-MBM 64-QAM, respectively, which corresponds to a loss of 2.0dB.

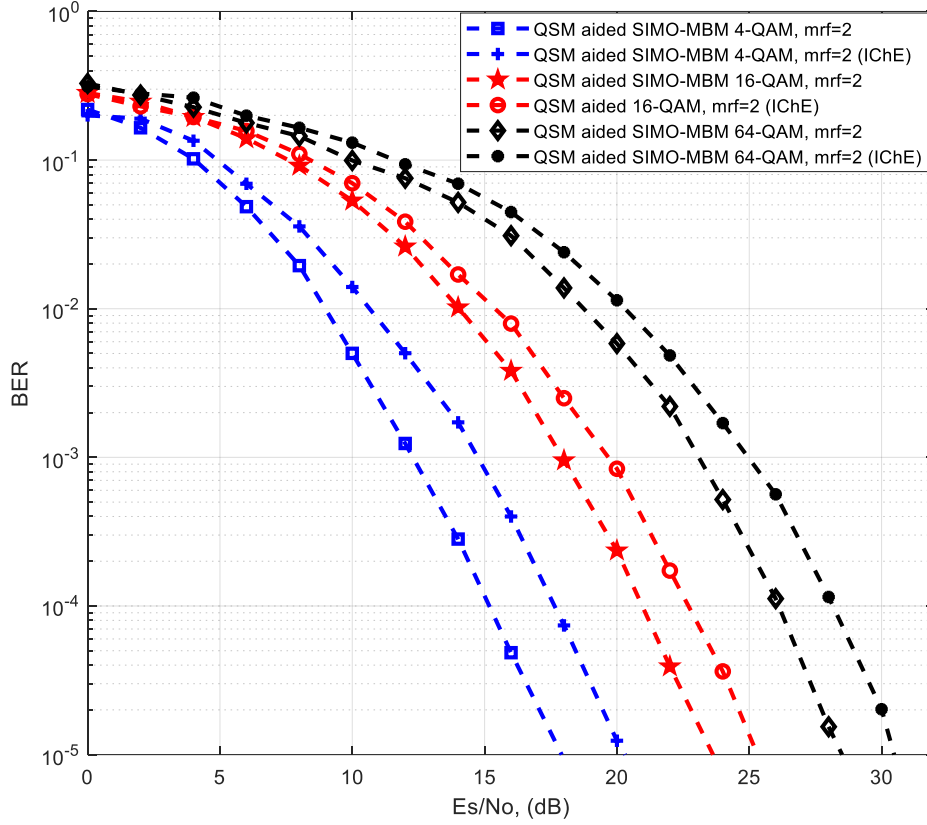


Figure 2.7 : Effect of Perfect/Imperfect Channel Estimate on QSM-SIMO-MBM scheme

2.9 Conclusion

In this paper, the application of quadrature dimension of the spatial constellation was investigated in a media-based modulation SIMO scheme. This is to improve the spectral efficiency of the scheme's coupled with improving the overall error performance of the system. The MC simulation results obtained revealed the improvement of 3.5dB, 2.5dB and 3.5dB at 6b/s/Hz, 8b/s/Hz and 10b/s/Hz, respectively with $m_{rf} = 2$. Likewise, an improvement of 6.5dB and 7dB at 10b/s/Hz and 12b/s/Hz, respectively was revealed with $m_{rf} = 4$ over the conventional SIMO-MBM of [11]. In addition, the effect of sub-optimal MAP selection algorithm was investigated in the proposed scheme employing the channel amplitude coupled with antenna correlation to select the best channel for transmission at every transmission instant. The MC simulation results show that the MAP selection algorithm further improves the proposed scheme's error performance, with the norm-correlation scheme being superior. The effect of imperfect channels was examined on the proposed scheme with the trade-off of 2dB in coding gain due to channel estimation errors which

further validate the novelty of the scheme. The error performance of QSM-MBM-SIMO methods based on large intelligent surfaces (LIS) can be investigated. Additionally, there are still unresolved research questions regarding the performance evolution of LIS-assisted Index Modulation with erroneous phase estimate at various fading channels.

2.10 References

- [1] A. Goldsmith, *Wireless Communications*: Cambridge university press, 2005.
- [2] W. Son, H. S Jang, and B. C Jung. "A pseudo-random beamforming technique for improving physical-layer security of MIMO cellular networks." *Entropy* 2019, 21, 1038; doi:10.3390/e21111038.
- [3] S. M Tseng, Y. F Chen, P. H Chiu, H. C Chi, "Jamming resilient cross-layer resource allocation in uplink HARQ-based SIMO OFDMA video transmission systems." *IEEE Access*. vol. 5, pp. 24908–24919, Oct. 2017.
- [4] H. Wang, Y. Fu, R. Song, Z. Shi, X. Sun. "Power Minimization Precoding in Uplink Multi-Antenna NOMA Systems With Jamming". *IEEE Trans. Green Commun. Netw.* vol.3, pp 591–602. Nov. 2019.
- [5] S. J. A. Goldsmith, N. Jindal and S. Vishwanath, "Capacity limits of MIMO channels," *IEEE Journal on Selected Areas in Communications*, vol. 21, pp. 684-702, June 2003.
- [6] H. Hass. R. Y. Mesleh, L. Yeonwoo and Y. Sangboh, "Interchannel Interference Avoidance in MIMO Transmission by Exploiting Spatial Information," in *Proceedings of the IEEE 16th International Symposium on Personal, Indoor and Mobile Radio Communications, (PIMRC 2005)*, pp. 141-145, Sep. 2005.
- [7] R. Y. Mesleh, H. Haas, S. Sinanovic, A. Chang Wook, and Y. Sangboh, "Spatial Modulation," *IEEE Transactions on Vehicular Technology*, vol. 57, no. 4, pp. 2228-2241, Jul. 2008.
- [8] N. R. Naidoo, H. Xu, T. Quazi, "Spatial modulation: optimal detector asymptotic performance and multiple-stage detection," *IET Communications*, vol. 5, no. 10, pp. 1368 - 1376, Jul. 2010.
- [9] Z. Pan, J. Luo, J. Lei, L. Wen, and C. Tang, "Uplink Spatial Modulation SCMA System," *IEEE Communications Letters*, Vol. 23, no. 1, pp. 184-187 Jan. 2019.

- [10] C. Zhong, X. Hu, X. Chen, D. W. K. Ng, and Z. Zhang, "Spatial modulation assisted multi-antenna non-orthogonal multiple access," *IEEE Wireless Commun.*, vol. 25, no. 2, pp. 61–67, Apr. 2018.
- [11] A. Bhowal, A. S. Sapre, R. Lalani and R. S Kshetrimayum, "Advanced spatial modulation for efficient MIMO-based B2B communications in sporting Activities," *IET Commun.*, Vol. 13 Iss. 20, pp. 3529-3536, Nov. 2019.
- [12] A. Bhowal and R. S Kshetrimayum, "Advanced Optical Spatial Modulation Techniques for FSO Communication," *IEEE Transactions on Communications*, vol. 69, no. 2, Feb. 2021
- [13] R. Mesleh, S. S. Ikki, and H. M. Aggoune, "Quadrature Spatial Modulation," *IEEE Transactions on Vehicular Technology*, vol. 64, no. 6, pp. 2738-2742, Jul. 2014.
- [14] R. Mesleh and S. S. Ikki, "A High Spectral Efficiency Spatial Modulation Technique," in *Proceedings of the 80th IEEE Vehicular Technology Conference (VTC Fall 2014)*, pp. 14-17, Sep. 2014.
- [15] S.Naidu, N. Pillay, H. Xu, "A Study of Quadrature Spatial Modulation," presented at the SATNAC, Western Cape, Aug. 2015.
- [16] A. Bhowal and R. S Kshetrimayum, "Optical Improved Quadrature Spatial Modulation for Cooperative Underwater Wireless Communication under Weak Oceanic Turbulence Conditions," *IET Optoelectron.*, Vol. 14 Iss. 6, pp. 434-439, September 2020
- [17] Y. Naresh and A. Chockalingam, "On Media-based Modulation using RF Mirrors," *IEEE Transactions on Vehicular Technology*, vol. 66, no. 6, pp. 4967 - 4983, Oct. 2016.
- [18] N. Pillay and H. Xu, "Quadrature spatial media-based modulation with RF mirrors," *IET Communication*, vol. 11, pp. 2440 - 2448, 2017.
- [19] R. Pillay, N. Pillay and H. Xu, "A Study of Single-Input Multiple-Output Media-based Modulation with RF Mirrors," presented at the SATNAC, Spain, 2017.
- [20] R. Rajashekar, K. V. S. Hari, and L. Hanzo, "Antenna Selection in Spatial Modulation Systems," *IEEE Wireless Communications Letters*, vol. 17, no. 3, pp. 521-524, Jan. 2013.

- [21] N. Pillay and H. Xu, "Comments on "Antenna Selection in Spatial Modulation Systems", *IEEE Wireless Communications Letters*, vol. 17, no. 9, pp. 1681-1683, Aug. 2013.
- [22] H. Xu, "Symbol error probability for generalized selection combining reception of M-QAM " *SAIEE Africa Research Journal*, vol. 100, no. 3, pp 68 - 71, Sep. 2009.
- [23] N. Pillay and H. Xu, "Low-complexity transmit antenna selection schemes for spatial modulation," *IET Communications*, vol. 9, no. 2, pp. 239-248, January. 2015.
- [24] N. Pillay, H. Xu, "Low Complexity Detection and Transmit Antenna Selection for Spatial Modulation," *SAIEE Africa Research Journal*, Vol. 105, no. 1, Mar. 2014.
- [25] W. Nan, L. Wenlong, M. Hongzhi, J. Minglu, and H. Xu, "Further Complexity Reduction Using Rotational Symmetry for EDAS in Spatial Modulation," *IEEE Communications Letters*, vol. 18, no. 10 pp. 1835-1838, Oct. 2014.
- [26] Z. Zhou, N. Ge, and X. Lin, "Reduced-Complexity Antenna Selection Schemes in Spatial Modulation," *IEEE Communications Letters*, vol. 18, no. 1, pp. 14-17, Jan. 2014.
- [27] J. Wu and C. Xiao, "Optimal diversity combining based on linear estimation of rician fading channels," in *IEEE Transactions on Communications*, vol. 56, no. 10, pp. 1612-1615, October 2008
- [28] W. Zhou, J. Wu and P. Fan, "Optimum designs OFR highmobility systems with imperfecr channel state information", *Proc. IEEE ICC*, pp. 5920-5925, Jun. 2014.
- [29] M. A. Mahamadu, J. Wu, Z. Ma, W. Zhou, Y. Tang and P. Fan, "Fundamental Tradeoff Between Doppler Diversity and Channel Estimation Errors in SIMO High Mobility Communication Systems," in *IEEE Access*, vol. 6, pp. 21867-21878, 2018.

Chapter 3

Journal Article 2

Journal Article 2

**Two-way Decode and Forward Quadrature Media-based
Modulation for Single-Input Multiple-Output Scheme**

Ayodeji James Bamisaye and Tahmid Quazi

Published: International Journal of Communication Systems

Vol.35, Iss 11, 2022; e5186. <https://doi.org/10.1002/dac.5186>

3.1 Abstract

The recently proposed Quadrature spatial modulation aided single-input multiple-output media-based modulation (QSM aided SIMO-MBM) improves the spectral efficiency, achieves a high data rate, and overall system error performance when compared with conventional single-input multiple-output media-based modulation (SIMO-MBM) and single-input multiple-output (SIMO) schemes. Cooperative Network (CN) involves collaboration among nodes to improve wireless network reliability, link quality, and spectral efficiency. This Paper investigates the performance of QSM aided SIMO-MBM in Cooperative Network (CN) by employing the decode and forward relaying technique, which utilizes two source nodes that simultaneously transmit a unique message block on the same time slot to the relay node, the relay node decodes the received message block from both transmitting nodes, before re-encoding and re-transmitting the decoded message block in the next time slot to the destinations in order to enhance the error performance of the QSM aided SIMO-MBM further. Each Node can decode the data of the other Node using network coding (NC) techniques. In NC, data is encoded and decoded to improve network throughput, complexity, robustness and lower delays; algebraic algorithms are applied to the detected message to accumulate the various transmissions. The theoretical average error probability of the proposed scheme was formulated using a lower bound technique, and the Monte Carlo simulation (MCS) results obtained validated the result. The MCS results achieved exhibit a significant improvement of 8 dB at 6 b/s/Hz for a BER of 10^{-5} , and 12 dB at 8 b/s/Hz for a BER of 10^{-5} over the conventional QSM aided SIMO-MBM scheme. Consequently, the obtained results show that the system configuration with $m_{rf} = 2$ outperforms the system configuration with $m_{rf} = 4$ for the proposed scheme.

3.2 Introduction

The demand for high-capacity transmission and effective link reliability in wireless communication has grown tremendously, and MIMO (multiple input multiple output) technologies have shown a lot of promise in terms of meeting this requirement.[1]. This has encouraged tremendous research in MIMO schemes [2-7].

An innovative form of MIMO scheme to consider is spatial modulation (SM) [2], which increases the energy efficiency [6-10] and improves the drawback of conventional MIMO schemes with the requirement of a single RF chain per transmission interval. However, SM still requires many transmit antennas to accomplish a high data rate limiting its practical implementation with reference to complexity. This brings about the introduction of generalized spatial modulation (GSM) [3].

GSM is an SM-based scheme that map bits of information to the index of a transmit antenna combination, allowing two transmit antennas to be employed at every transmission instant. This reduces the number of required antennas for transmission. Nevertheless, the GSM system performance is reduced when compared to SM due to average power effect [3]. This led to the introduction of quadrature spatial modulation (QSM) [5].

QSM is another form of innovative MIMO scheme, which conveys additional information by extending its spatial dimension to the in-phase and quadrature dimensions. In QSM, the APM symbols are decomposed into its real and imaginary components, which are respectively modulated into cosine and sine carriers. Hence, it made a single RF chain requirement possible, which is more energy-efficient than GSM and exhibits an improved error performance than SM and GSM [3,4], [11-17].

Media-based modulation (MBM) [18] has been proven as a more efficient technique to achieve a high data rate at the cost of low hardware complexity. This is accomplished by utilizing RF mirrors to produce various channel fade realizations, classified as mirror activation patterns (MAPs) [18].

Similarly, in MBM [10], a subset of channel realizations may be chosen from the unique channel perturbations. Also, the received constellation size is independent of the transmit power. An additional advantage of the MBM scheme is that placement of RF mirrors side-by-side is achievable. However, in conventional MIMO schemes, the transmit antennas must have a minimum distance between each other so as to achieve an independent fading.

The studies conducted by [18,19] respectively proposed MBM designed for the generalized SM (MBM-GSM) and quadrature SM (MBM-QSM). The proposed system in [18] utilizes the conventional GSM technique, which made use of the combination of transmit antenna to activate two transmit antennas at every instant of transmission with the spatial dimension to send information related to [4].

Likewise, in MBM-QSM [19], Single RF chain's requirement is achieved by modulating the decomposed APM symbol into in-phase and quadrature components which are respectively transmitted via the sine and cosine carriers. However, multiple RF chains is required in MBM-GSM

In [20], a SIMO-MBM scheme was proposed to obtain a high data rate at low hardware complexity. To attain the same spectral efficiency as SIMO-MBM, an SM system would need $2^{m_{rf}}$ transmit antennas, making SIMO-MBM more desirable with reference to the data rate.

In [21], a QSM aided SIMO-MBM scheme was proposed, achieving a higher data rate than SIMO-MBM coupled with maintaining the earlier stated benefits of QSM over SM, GSM, and traditional MIMO systems. This was achieved by employing RF mirrors to create various mirror activation pattern. Hence, achieving high data rate and improving the system performance.

In the literature, cooperative relay-based communication systems have shown tremendous promise in enhancing wireless link quality, reliability, and spectral efficiency. This is achieved by employing multiple relay nodes (active or passive nodes) as a virtual antenna to re-transmit user information [22-24].

Data transmission from various source nodes during the same time slot increases the throughput rate over the network by efficiently utilizing packet transmissions, i.e., by conveying more messages with fewer transmissions. Algebraic algorithms are employed to combine messages and forward the accumulated result to the destination. The received message is decoded at the destination using the same algorithm, and the destination nodes are synchronized with the transmitting node; this system is described as network coding (NC) [25]. Its primary objective is to achieve optimum utilization of network resource efficiency, computational efficiency, and robustness to network dynamics. Error-free transmission is assumed in wired networks [26], while multi-path fading of the signal can considerably affect the link quality, thereby resulting in transmission errors in wireless networks. Also faced in wireless channels is the interference; all these can be eliminated using network coding combined with cooperative relay-based communication. [25]

Typically, a relay system can either be an amplify-and-forward (AF) relay or a decode-and-forward (DF) relay. In AF, the signal received at the relay from the source is amplified and forwarded to the destination, while in DF, the signal received at the relay is decoded before transmission to the destination [22-23],[27], both schemes reduce spectral efficiency due to the communication between the source and the destination on two orthogonal time slots.

In [26-33], two-way relaying has been proven as a spectral efficient relaying scheme. This technique employs two or more source nodes, simultaneously transmitting a message block on the same time slot to the relay node. Each source node transmits its modulated message block towards the relay node, such that the relay node is the receiver. The relay node receives and computes the message from the source nodes and transmit them to the appropriate destination nodes.

Furthermore, whenever a message is sent from Node A and Node B to Node R, Node R receives it and decodes the message using ML; if the message arrives simultaneously through a different channel, ML will be applied to them independently to process the message. After that, the relay node estimates the received signal and applies the network coding principle (i.e. application of algebraic algorithms to schedule the data and accumulate the various transmissions) on the received messages. The message block of other Node can be obtained by each source node via reversing the operation performed at the relay.[20]. This is graphically illustrated in Figure 3.1.

In the study presented in [24], in order to improve the error performance of the traditional SM system with numerous source nodes, a two-way relaying system was investigated in SM. Similarly, in [28], the two-way DF relaying technique is investigated in QSM, employing two source nodes and a relay node, which decode the transmitted message block from both source nodes and re-transmit the decoded message block to the final destination node. This exhibits a significant improvement of 9dB at 10^{-5} over the conventional QSM and one-way DF-QSM relaying system in terms of error performance. As mentioned earlier, QSM aided SIMO-MBM exhibits several advantages over SM, GSM, QSM, and SIMO-MBM, such as the requirement of fewer transmit antennas to achieve a high data rate. Moreover all the previous works didn't consider QSM, MBM and Network coding in a SIMO system, which we are considering in this scheme. Hence, two-way DF-QSM aided SIMO-MBM is expected to outperform SIMO-MBM coupled with QSM aided SIMO-MBM with reference to error performance. This motivates us to examine a novel two-way DF-QSM aided SIMO-MBM.

Contributions: The Paper has the following contributions:

- a) We investigate the two-way DF-QSM aided SIMO-MBM relaying technique with two source nodes.

b) We formulate the proposed scheme's theoretical analysis and validate the results with the MCS results achieved.

The following is the rest of the paper's structure: The system model for the proposed scheme is presented in section 2. In sections 3 and 4, the proposed scheme's performance analysis and numerical analysis are shown, respectively, while section 5 presented the resulting conclusions.

Notation: Vectors/matrices are denoted by bold italic lowercase/uppercase symbols, while regular letters represent scalar quantities. $\|\cdot\|_F$ signifies Frobenius norm, $Q(\cdot)$ depicts the Gaussian Q-function, $\underset{w}{\operatorname{argmin}}(\cdot)\backslash\underset{w}{\operatorname{argmax}}(\cdot)$ illustrates the minimum/maximum value of an argument in relation to w , $\binom{\cdot}{\cdot}$ denotes the binomial coefficient, $|\cdot|$ signifies the Euclidean norm, \oplus represents the XOR operator, $E\{\cdot\}$ is the expectation operator and $[\cdot]^T$ represents transpose.

3.3 System Model

Two-time slots were employed to complete a data transmission in the proposed two-way DF QSM aided SIMO-MBM. The first phase or time slot is the transmission phase while the second phase is the relaying phase. In the transmission phase, both source nodes (Node A and Node B) transmit its message blocks \mathbf{x}_A and \mathbf{x}_B to the relay node (Node R), simultaneously.

At the relay node (Node R), the network coding principle i.e, Node R XORed the received bits from Node A and Node B, was applied to the detected message to pre-code the estimated bits, which generates a new message block \mathbf{x}_R . This is transmitted to both source nodes (Node A and Node B), simultaneously in the relaying phase, such that Node R is the source node, while Node A and Node B represent the destination nodes.

Node R is the receiver when Nodes A and B transmit; Node R is the transmitter when Nodes A and B receive, which means all the nodes can send and receive messages. The received signal at the relay node is decoded, employing a maximum-likelihood (ML) detection algorithm and a network coding principle to formulate a new message block.

The system model of the proposed scheme is presented in Figure 3.1, which consists of two source nodes (Nodes A and Node B), relaying information via Node R. Node A, Node B, and Node R are equipped with N_{T_A} , N_{T_B} and N_{T_R} transmit antennas, respectively, coupled with the same number of RF chains. Likewise, the number of receive antennas is denoted as N_{R_A} , N_{R_B} , N_{R_R} for Node A, Node B and Node R, respectively, coupled with the same number of RF chains. The QSM aided SIMO-MBM model is employed to transmit the message block. Such that the spectral efficiency

is $m = (\log_2 M + 2mrf)$ b/s/Hz, where mrf and M represent the number of RF mirrors and the M -QAM modulation order respectively.

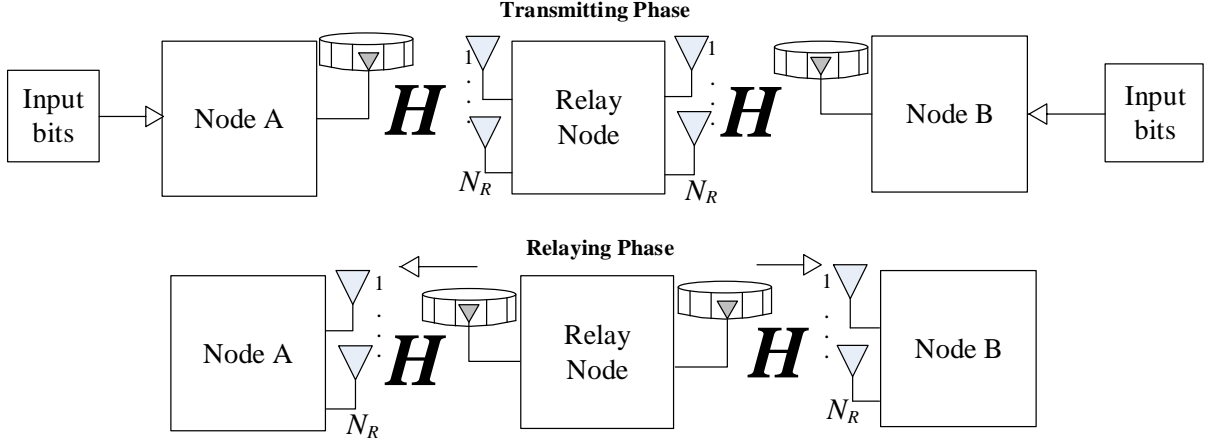


Figure 3.1 The System model of the proposed two-way DF-QSM-SIMO-MBM relaying system

3.3.1 Phase 1: Transmission Phase

Taking into consideration an illustration of a system with the following settings at Node A and Node B: $M = 4$, $N_T = 1$, and $m_{rf} = 4$, i.e. $N_m = 2^{m_{rf}} = 8$. It generates 10 b/s/Hz spectral efficiency. Thus, in order to transmit the decomposed modulated symbol, the RF mirrors are activated using the unique MAP indices of each transmitting unit.

The modulated symbol is conveyed through the $\mathbf{H}_j = [\mathbf{h}_1 \mathbf{h}_2 \cdots \mathbf{h}_{N_m}]$, $j \in [1: N_m]$ channel, which is independent and identically distributed (i.i.d) as $CN(0, 1)$ with $N_R \times N_m$ dimension and additive white Gaussian noise (AWGN) \mathbf{n} of dimension $N_R \times 1$. Hence, \mathbf{y}_R which represent the received signal vector can be composed as:

$$\mathbf{y}_R = \sqrt{\rho_A} \left(\mathbf{H}_j \mathbf{e}_{\ell_{RA}} \mathbf{x}_{ARe}^q + \mathbf{H}_j \mathbf{e}_{\ell_{IA}} \mathbf{x}_{AIm}^q \right) + \sqrt{\rho_B} \left(\mathbf{H}_j \mathbf{e}_{\ell_{RB}} \mathbf{x}_{BRe}^q + \mathbf{H}_j \mathbf{e}_{\ell_{IB}} \mathbf{x}_{BIm}^q \right) + \mathbf{n} \quad (3.1)$$

where ρ_A and ρ_B signifies the average SNR corresponding to the transmission from Node A and Node B, respectively. Also $x_q = \mathbf{x}_{ARe}^q + i\mathbf{x}_{AIm}^q$, $q \in [1: M]$ and $x_q = \mathbf{x}_{BRe}^q + i\mathbf{x}_{BIm}^q$, $q \in [1: M]$ respectively indicates the APM symbol in Nodes A and Nodes B, $\ell_{RA}, \ell_{RB}, \ell_{IA}$ and ℓ_{IB} are the

corresponding active RF mirror used to transmit the decomposed symbol, $\mathbf{e}_{\ell_{RA}}, \mathbf{e}_{\ell_{RB}}, \mathbf{e}_{\ell_{IA}}$ and $\mathbf{e}_{\ell_{IB}}$ are the $N_m \times 1$ vector with ℓ^{th} in Node A and Node B, the non-zero position equivalent to the selected MAP, set to unity.

The message block is optimally detected, using the maximum likelihood (ML) detector at the relay. The ML detector is defined as:

$$\begin{aligned}
 [\hat{\mathbf{x}}_A^q, \hat{\mathbf{x}}_B^q] = & \underset{\substack{\mathbf{x}_A \in \mathbf{X}_A \\ \mathbf{x}_B \in \mathbf{X}_B}}{\text{argmin}} \left\| \mathbf{y}_R \right. \\
 & - \left(\sqrt{\rho_A} \left(\mathbf{H}_j \mathbf{e}_{\ell_{RA}} \mathbf{x}_{ARe}^q + \mathbf{H}_j \mathbf{e}_{\ell_{IA}} \mathbf{x}_{AIIm}^q \right) \right. \\
 & \left. \left. + \sqrt{\rho_B} \left(\mathbf{H}_j \mathbf{e}_{\ell_{RB}} \mathbf{x}_{BRe}^q + \mathbf{H}_j \mathbf{e}_{\ell_{IB}} \mathbf{x}_{BIIm}^q \right) \right) \right\|_F^2
 \end{aligned} \tag{3.2}$$

where \mathbf{X}_A and \mathbf{X}_B are the set of all possible transmission vectors corresponding to Node A and Node B, respectively.

3.3.2 Phase 2: Relaying Phase

The estimated bits are pre-coded employing an XOR operation to generate the bits $\mathbf{D} = [D_1, \dots, D_m]$ using [28]:

$$\mathbf{D} = \hat{\mathbf{a}} \oplus \hat{\mathbf{b}} \tag{3.3}$$

where $\hat{\mathbf{a}}$ and $\hat{\mathbf{b}}$ are the estimated bits for Node A and Node B, respectively at Node R. The vector \mathbf{D} bits modulate the block \mathbf{x}_R , which is forwarded to both nodes (Node A and Node B) at the second time slot. This is sent via a Rayleigh frequency-flat fading channel represented as complex channel matrices to Node A and Node B of dimension $N_{RA} \times N_{TR}$ and $N_{RB} \times N_{TR}$, respectively, with i.i.d entries as CN (0,1). The message block is received in the presence of AWGN \mathbf{n}_A and \mathbf{n}_B for Node A and Node B, respectively, with i.i.d entries as CN (0,1) of dimension $N_{RA} \times 1$ and $N_{RB} \times 1$, respectively. The $N_{RA} \times 1$ and $N_{RB} \times 1$ received signal vectors \mathbf{y}_A and \mathbf{y}_B at Node A and Node B, respectively, can be written as:

$$\mathbf{y}_A = \sqrt{\rho} \left(\mathbf{H}_j \mathbf{e}_{\ell_{RA}} \mathbf{x}_{ARe}^q + \mathbf{H}_j \mathbf{e}_{\ell_{IA}} \mathbf{x}_{AIIm}^q \right) + \mathbf{n} \tag{3.4}$$

$$\mathbf{y}_B = \sqrt{\rho}(\mathbf{H}_j \mathbf{e}_{\ell_R} \mathbf{x}_{B_{Re}}^q + \mathbf{H}_j \mathbf{e}_{\ell_I} \mathbf{x}_{B_{Im}}^q) + \mathbf{n} \quad (3.5)$$

Where ρ represent the SNR. ML detector is implemented on the received signals at Node A and Node B for detected vectors estimation as:

$$[\hat{\ell}, \hat{j}, \mathbf{x}_{A_{Re}}^q, \mathbf{x}_{A_{Im}}^q] = \underset{\substack{q \in [1:M] \\ \ell \in [1:N_m]}}{\operatorname{argmin}} \left(\|\mathbf{y}_A - \sqrt{\rho}(\mathbf{H}_j \mathbf{e}_{\ell_R} \mathbf{x}_{A_{Re}}^q + \mathbf{H}_j \mathbf{e}_{\ell_I} \mathbf{x}_{A_{Im}}^q)\|_F^2 \right) \quad (3.6)$$

$$[\hat{\ell}, \hat{j}, \mathbf{x}_{B_{Re}}^q, \mathbf{x}_{B_{Im}}^q] = \underset{\substack{q \in [1:M] \\ \ell \in [1:N_m]}}{\operatorname{argmin}} \left(\|\mathbf{y}_B - \sqrt{\rho}(\mathbf{H}_j \mathbf{e}_{\ell_R} \mathbf{x}_{B_{Re}}^q + \mathbf{H}_j \mathbf{e}_{\ell_I} \mathbf{x}_{B_{Im}}^q)\|_F^2 \right) \quad (3.7)$$

The detected vector (Eqns. 3.6, 3.7) is mapped to the corresponding bit block for each Node. Let \mathbf{D}_a represent the obtained bits block at Node A and \mathbf{D}_b is the obtained bits block at Node B. An estimated form of the transmitted bits can be extracted from the other Node by performing an XOR operation with its transmitted bits, such that [28]:

$$\mathbf{r}_A = \mathbf{D}_a \oplus \mathbf{a} \quad (3.8)$$

$$\mathbf{r}_B = \mathbf{D}_b \oplus \mathbf{b} \quad (3.9)$$

where \mathbf{r}_A is the estimated form of \mathbf{b} obtained at Node A and \mathbf{r}_B is the estimated form of \mathbf{a} obtained at Node B, thus, estimating the $2m$ bits. Figure 3.2 shows the scheme flowchart for transmission and relay phase.

3.4 Performance Analysis

The average BER analysis for the proposed system is formulated based on the average BER analysis for QSM aided SIMO-MBM in [21], with few adjustments to derive the theoretical bound. The average BER for the proposed system is given as:

$$\begin{aligned} P_e &\geq 1 - ((1 - P_a)(1 - P_b)) \\ &= P_a + P_b - P_a P_b \end{aligned} \quad (3.10)$$

where P_e is segmented into two; the first part i.e P_a is the antenna index's bit error probability estimation provided the APM symbol is correctly detected, while the second part has P_b as the estimated symbol's bit error probability provided the antenna index is correctly detected.

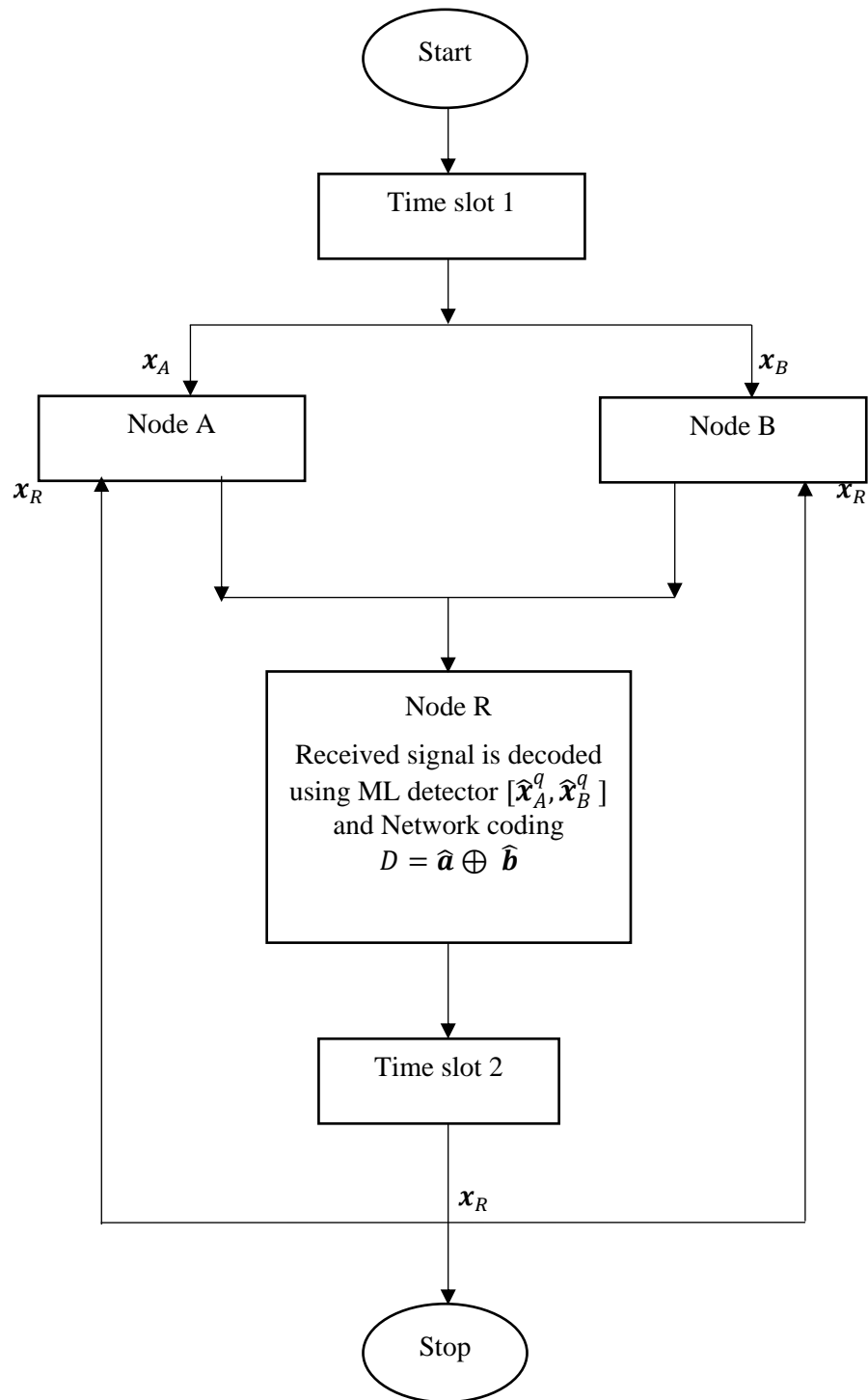


Figure 3.2. Flow chart for the two-way DF-QSM aided SIMO-MBM Implementation.

For the proposed system, the Node A side is regarded as both Node A and Node B are identical. However, the antenna error needs adjustment because multiple RF mirrors convey the APM symbol. The error is modified based on the active antennas as $P_a = 2P_a$ utilizing an average SNR $\frac{\rho}{N_m}$. Hence, $P_e \geq 2P_a + P_b - 2P_aP_b$

Hence, P_a can be computed by employing a union bound on PEP as:

$$P_a \leq \sum_{q=1}^M \sum_{j=1}^{N_m} \sum_{\hat{j}=1}^{N_m} \frac{N(j, \hat{j}) \mu^{N_R} \sum_{k=0}^{N_R-1} \binom{N_R-1+k}{k} [1-\mu]^k}{N_m^2 M} \quad (3.11)$$

where $\mu = \frac{1}{2} \left(1 - \sqrt{\frac{\gamma}{\gamma+1}} \right)$, $N(j, \hat{j})$ correspond to the number of bit errors between the transmit antenna j and the transmit antenna estimation \hat{j} , while $\gamma = \frac{\rho}{N_m} |x_q|^2$.

Utilizing square M -QAM, P_b is calculated analogous to [30]: as:

$$P_b = \frac{1}{\log_2 M} \left(\frac{a}{c} \left[\frac{1}{2} \left(\frac{2}{b\rho+2} \right)^{N_R} - \frac{a}{2} \left(\frac{1}{b\rho+1} \right)^{N_R} + (1 - a) \sum_{i=1}^{c-1} \left(\frac{2\sin^2\theta}{b\rho+2\sin^2\theta} \right)^{N_R} + \sum_{i=c}^{2c-1} \left(\frac{2\sin^2\theta}{b\rho+2\sin^2\theta} \right)^{N_R} \right] \right) \quad (3.12)$$

where $a = 1 - \frac{1}{\sqrt{M}}$, $b = \frac{3}{M-1}$, $\theta = \frac{i\pi}{4c}$, $\rho = \frac{\rho}{4}$ and c is the number of summations $c > 10$, for the trapezoidal approximation of the Q-function to achieve convergence [30]:

3.5 Numerical Analysis and Discussion

The system performance and MCS results obtained for the two-way DF-QSM aided SIMO-MBM system is described in this section. The average BER against the SNR in dB is considered. I assumed a flat-fading Rayleigh channel and full knowledge of channel at the receiver.

The notation (N_T, N_R, M, m_{rf}) is employed for the two-way DF-QSM aided SIMO-MBM system, and QSM aided SIMO-MBM. In all cases, ML detection is employed, and two source nodes are employed for two-way DF-QSM aided SIMO-MBM. The theoretical ABER results expressed in (Eqn. 3.10) and MCS results obtained for the proposed system (two-way DF-QSM aided SIMO-MBM) are also shown in Figure 3.3. The average theoretical result obtained shows a close match with the MCS result, verifying the theoretical expression. The setting of the system configuration using 4 receive antennas with 4-QAM and 16-QAM is employed, alongside 2 and 4 RF mirrors with spectral efficiency of 6 b/s/Hz, 8 b/s/Hz and 10 b/s/Hz.

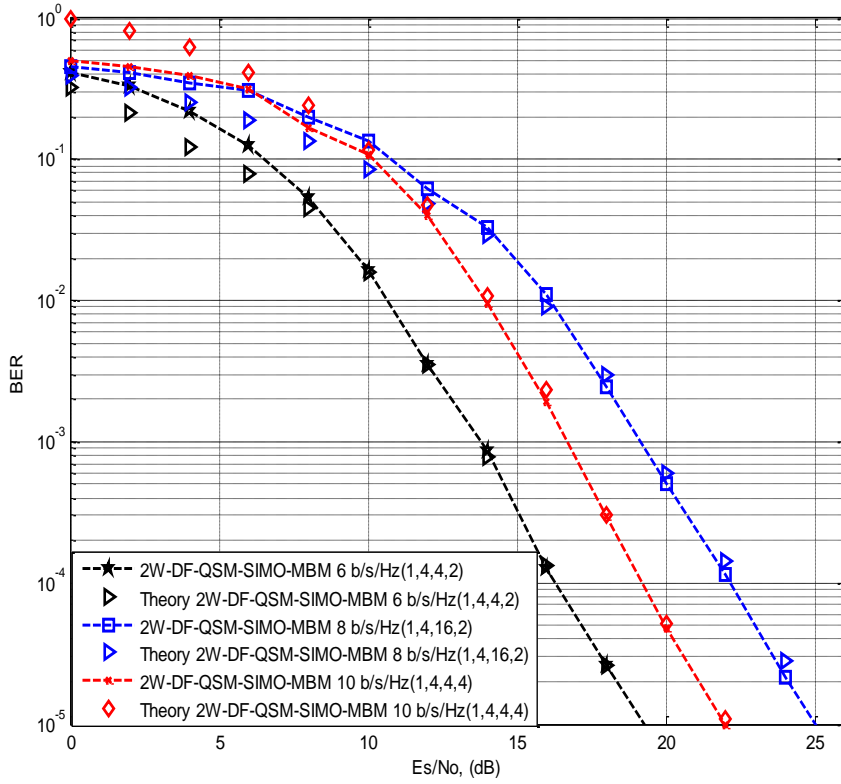


Figure 3.3 BER performance of 2W-DF-QSM-SIMO-MBM.

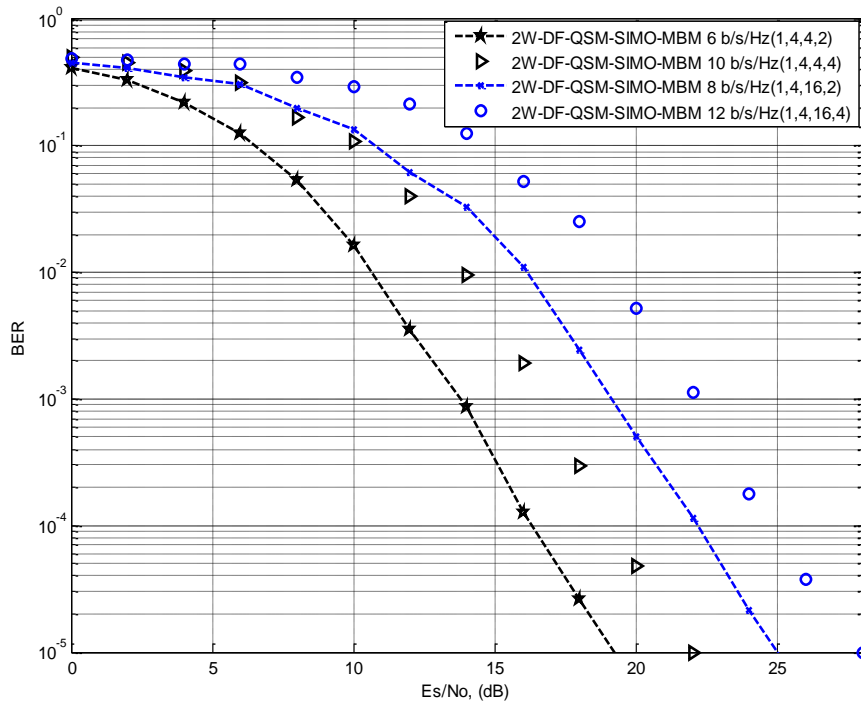


Figure 3.4 BER performance comparison of 2W-DF-QSM-MBM-SIMO for $m_{rf} = 2$ and $m_{rf} = 4$, respectively

Furthermore, it is evident from the MCS results shown in Figure 3.4 that two-way DF-QSM aided SIMO-MBM with $m_{rf} = 2$ achieves an improved system performance of approximately 3dB at 10^{-5} when compared with $m_{rf} = 4$.

Similarly, in Figure 3.5, the comparison of the performance between the proposed two-way DF-QSM aided SIMO-MBM system and the conventional QSM aided SIMO-MBM [21] is presented. Based on the MCS results obtained, it is evident that exploiting the quadrature dimension of the spatial constellation coupled with two-way relay transmission improves the scheme's system performance.

A SNR gain of 8 dB and 12 dB is achieved for the 6 b/s/Hz and 8 b/s/Hz two-way DF-QSM aided SIMO-MBM, respectively at a BER of 10^{-5} over the conventional QSM aided SIMO-MBM [21]. In the two-way DF-QSM-MBM-SIMO, two source nodes are considered; hence, the system's spectral efficiency is doubled i.e., 2m bits (Eqns. 3.8 and 3.9). Therefore, doubling the spectral efficiency required for the conventional QSM aided SIMO-MBM (Figure. 3.5). Consequently, this is accomplished by maximizing the systems' transmit and cooperative diversity and utilizing the QSM aided MBM as the adopted modulation at all nodes in the two-way relay system. The effect of imperfect channels and abridging algorithm technique proposed by [36], which is able to vertically reduce the size of network traffic dataset without affecting its statistical characteristics can be considered with the proposed scheme for future work.

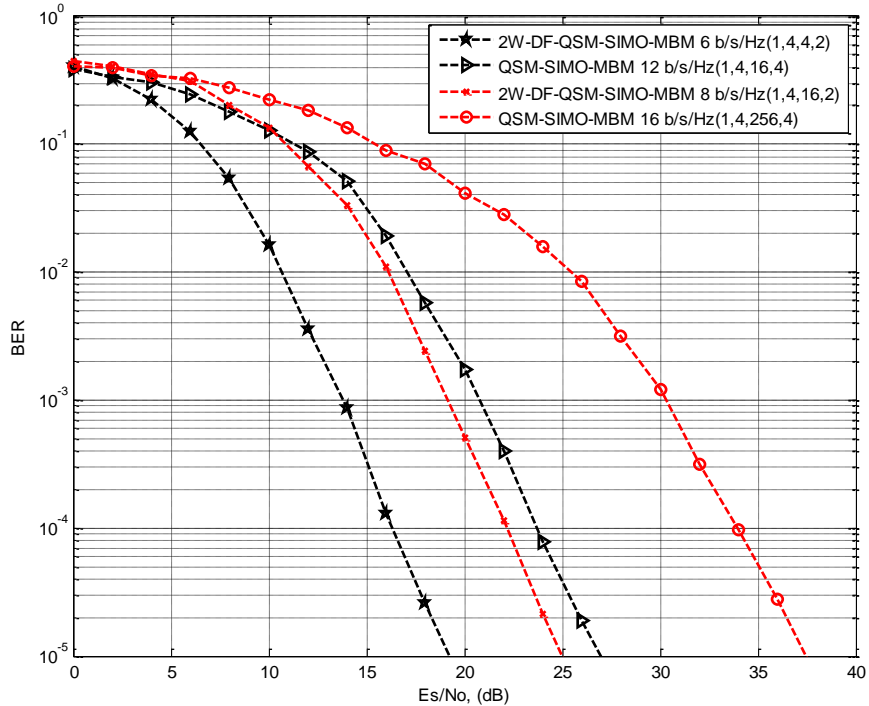


Figure 3.5 BER performance comparison of 2W-DF-QSM-MBM-SIMO and QSM aided SIMO-MBM.

3.6 Conclusion

The two-way DF scheme was investigated with QSM aided SIMO-MBM to improve the reliability of the conventional system. The decode and forward relaying technique was utilized; this was achieved by employing a relaying node, which received the message signal from two source nodes, decoded the received signal using network coding techniques, and then re-transmitted the message to its destination. The MCS results obtained revealed the improvement of 8 dB and 12 dB at 6b/s/Hz and 8b/s/Hz, respectively at a BER of 10^{-5} , over the conventional QSM aided SIMO-MBM. Likewise, the result obtained exhibits that the system configuration with $m_{rf} = 2$ outperform the configuration with $m_{rf} = 4$ for the proposed scheme. This Paper assumed full channel knowledge.

3.7 References

- [1] A. Goldsmith. "Wireless communications," Cambridge University Press, 2005.
- [2] R. Mesleh, H. Haas, H. Sinanovic, A. Chang Wook, and Y. Sangboh. "Spatial modulation," *IEEE Transactions on Vehicular Technology*, vol. 57, no. 4, pp. 2228-2241, Jul. 2008.
- [3] A. Younis, N. Serafimovski, R. Mesleh, and H. Haas. "Generalised spatial modulation," In: Proc. conference record of the forty fourth asilomar conference on signals, systems and computers. Pacific Grove, CA, USA, pp. 1498-1502, Nov. 2010.
- [4] F. Jinlin, H. Chunping, X. Wei, Y. Lei, and H. Yonghong "Generalised spatial modulation with multiple active transmit antennas," In: Proc. IEEE GLOBECOM Workshops (GC Workshops), Miami, FL, USA: IEEE, pp. 839-844, Dec. 2010.
- [5] R. Mesleh, S. Ikki, and H. Aggoune. "Quadrature spatial modulation," *IEEE Transactions on Vehicular Technology*, vol. 64, no. 6, pp. 2738-2742, Jun. 2015.
- [6] A. Saeed., H. Xu, and T. Quazi, "Alamouti Space-Time Block Coded Hierarchical Modulation with Signal Space Diversity and MRC Reception in Nakagami-m Fading Channel" IET proceedings Communications, vol 8, No 4, pp:516-524, Mar, 2014.
- [7] A. Saeed, T. Quazi, and H. Xu., "Hierarchical Modulated QAM with Signal Space Diversity and MRC Reception in Nakagami-m fading channels". IET proceedings Communications. vol 7, No 12, pp:1296-1303, Aug, 2013.
- [8] X.Q. Jiang, H. Hai, J. Hou, J. Li, and W. Duan, "Euclidean-geometrybased space-time block coded spatial modulation," *IEEE J. Sel. Topics Signal Process.*, vol. 13, no. 6, pp. 1301–1311, Oct. 2019.
- [9] X. Q. Jiang, M. Wen, H. Hai, J. Li, and S. Kim, "Secrecy-enhancing scheme for spatial modulation," *IEEE Commun. Lett.*, vol. 22, no. 3, pp. 550–553, Mar. 2018.
- [10] M. Chu, R. Qiu and X. -Q. Jiang, "Spectrum-Energy Efficiency Tradeoff in Decode-and-Forward Two-Way Multi-Relay Networks," *IEEE Access*, vol. 9, pp. 16825-16836, Jan. 2021

- [11] T. L. Narasimhan, P. Raviteja, and A. Chockalingam, "Generalized Spatial Modulation in Large-Scale Multiuser MIMO Systems" *IEEE transactions on wireless communications*, vol. 14, no. 7, pp 3764- 3779, July 2015.
- [12] W. Qu , M. Zhang, X. Cheng and P. Ju "Generalized Spatial Modulation With Transmit Antenna Grouping for Massive MIMO" *IEEE Access*. volume 5. pp 26798-26807, May 2017
- [13] N. R. Naidoo, H. Xu, T. Quazi, "Spatial modulation: optimal detector asymptotic performance and multiple-stage detection," *IET Communications*, vol. 5, no. 10, pp. 1368 - 1376, Jul. 2010.
- [14] C. Zhong, X. Hu, X. Chen, D. W. K. Ng, and Z. Zhang, "Spatial modulation assisted multi-antenna non-orthogonal multiple access," *IEEE Wireless Commun.*, vol. 25, no. 2, pp. 61–67, Apr. 2018.
- [15] M. Wen , B. Zheng, K. Jin Kim, M. Renzo, T. A. Tsiftsis, K. Chen , and N. Al-Dhahir " Survey on Spatial Modulation in Emerging Wireless Systems: Research Progresses and Applications" *IEEE Journal on selected areas in communications*, vol. 37, no. 9, pp 1949-1972, September, 2019.
- [16] H. Niu, X. Lei, Y. Xiao, Y. Li and W. Xiang, "Performance Analysis and Optimization of Secure Generalized Spatial Modulation," *IEEE Transactions on Communications*, vol. 68, no. 7, pp. 4451-4460, July 2020, doi: 10.1109/TCOMM.2020.2983368.
- [17] S. Guo , H. Zhang , P. Zhang, S. Dang, C. Liang, and M. Alouini, " Signal Shaping for Generalized Spatial Modulation and Generalized Quadrature Spatial Modulation" *IEEE Transactions On Wireless Communications*, vol. 18, no. 8, pp 4047-4059, August 2019.
- [18] Y. Naresh and A. Chockalingam, "On Media-based Modulation using RF Mirrors," *IEEE Transactions on Vehicular Technology*, vol. 66, no. 6, pp. 4967 - 4983, Oct. 2016.
- [19] N. Pillay and H. Xu, "Quadrature spatial media-based modulation with RF mirrors," *IET Communication*, vol. 11, pp. 2440 - 2448, Nov. 2017.
- [20] R. Pillay, N. Pillay, and H. Xu, "A Study of Single-Input Multiple-Output Media-based Modulation with RF Mirrors," presented at the SATNAC, Spain, Sept. 2017.

- [21] A. J Bamisaye and T. Quazi, "Quadrature Spatial Modulation-aided Single-Input Multiple-Output media-based Modulation," *International Journal of Communication Systems*.vol. 34, no.11, May 2021; e4883. <https://doi.org/10.1002/dac.4883>.
- [22] Z. He, H. Shen, W. Xu, and C. Zhao, "Energy efficient joint power optimization for full-duplex relaying," *IEEE Access*, vol. 7, pp. 137040–137047, Jan. 2019.
- [23] K. Singh, M.-L. Ku, and C.-M. Yu, "Joint subcarrier pairing and power allocation for achieving energy-efficient decode-and-forward relay networks," in *Proc. IEEE 89th Veh. Technol. Conf. (VTC-Spring)*, Kuala Lumpur, Malaysia, , pp. 1–6, Apr. 2019.
- [24] Y. Li, M. Daneshmand, and W. Duan "A cooperative relay method and performance for wireless networks," In: *Proc. 2nd international symposium on intelligence information processing and trusted computing*, Hubei, pp. 31-34, Dec. 2011.
- [25] R. Ahlswede, N. Cai, S.-Y. R. Li, and R.W. Yeung, "Network information flow," *IEEE Trans. Inform. Theory*, vol. 46, no. 4, pp. 1204–1216, Jul. 2000.
- [26] R. Koetter and M. Médard, "An algebraic approach to network coding," *IEEE/ACM Trans. Netw.*, vol. 11, no. 5, pp. 782-795, Oct.2003
- [27] X. Cheng et al., "Cooperative MIMO Channel Modeling and Multi-Link Spatial Correlation Properties," in *IEEE Journal on Selected Areas in Communications*, vol. 30, no. 2, pp. 388-396, February 2012. doi: 10.1109/JSAC.2012.120218.
- [28] S. Althunibat and R. Mesleh "Performance analysis of quadrature spatial modulation in two-way relaying cooperative networks," *IET Communications*, vol. 12, no. 4, pp. 466-472, Mar. 2018.
- [29] A. Koc, I. Altunbas, and E. Basar "Two-way full-duplex spatial modulation systems with wireless powered AF relaying," *IEEE Wireless Communications Letters*, vol. 7, no. 3, pp. 444-447, Jun. 2018.
- [30] B. Rankov and A. Wittneben "Achievable rate regions for the two-way relay channel," In: *Proc. IEEE international symposiumon information theory*, Seattle, WA, pp. 1668-1672, Dec. 2006.

- [31] H. Ju, E. Oh, and D. Hong. "Catching resource-devouring worms in next-generation wireless relay systems: Two-way relay and full-duplex relay," *IEEE Communications Magazine*, vol. 47, no. 9, pp. 58-65, Oct. 2009.
- [32] N. R. Naidoo, H. Xu, and T. Quazi, "Spatial modulation: optimal detector asymptotic performance and multiple-stage detection," *IET Communications*, vol. 5, no. 10, pp. 1368 - 1376, Jul. 2010.
- [33] Y. Naresh and A. Chockalingam, "Performance of Media-Based Modulation in Two-Way Full-Duplex Relaying Networks," 2019 IEEE 30th Annual International Symposium on Personal, Indoor and Mobile Radio Communications (PIMRC), pp. 1-6, 2019.
- [34] Y. Naresh and A. Chockalingam, "Performance of full-duplex decode and-forward relaying with media-based modulation," *IEEE Trans. Veh. Tech.*, vol. 68, no. 2, pp. 1510-1524, Feb. 2019.
- [35] Y. Ye, L. Shi, X. Chu, H. Zhang and G. Lu, "On the Outage Performance of SWIPT-Based Three-Step Two-Way DF Relay Networks," *IEEE Transactions on Vehicular Technology*, vol. 68, no. 3, pp. 3016-3021, March 2019.
- [36] S. Garg, R. Singh, M.S Obaidat, V.K Bhalla, & B. Sharma, "Statistical vertical reduction-based data abridging technique for big network traffic dataset". *International Journal of Communication Systems*. vol. 33 no.4, March 2020: e4249.

Chapter 4

Journal Article 3

Journal Article 3

Application of Golden Code Orthogonal Super-Symbol in Media-Based Modulation for Single-Input Multiple- Output Schemes

Ayodeji James Bamisaye and Tahmid Quazi

Published: Journal of Telecommunications and information Technology.
2/2022, pp 43-48. <https://doi.org/10.26636/jtit.2022.158921>

4.1 Abstract

The media-based modulation (MBM) scheme can achieve significant throughput, increase spectrum efficiency, and enhance the performance of bit-error-rate (BER). In this paper, the application of MBM, employing radio frequency (RF) mirrors and Golden code, is investigated in the single-input multiple-output (GC-SIMO). The purpose is to improve hardware complexity of the system, maximizing the linear relationship between RF mirrors and the spectral efficiency in MBM to obtain a high data rate at a reduced hardware complexity. The orthogonal pairs of the super-symbol in the GC scheme's encoder are employed, transmitted via different RF mirror at a different time slot to achieve full rate full diversity. In the results of MCS obtained, at a BER of 10^{-5} , the GC-SIMO-MBM exhibits a significant performance of approximately 7dB and 6.5 dB SNR gain for 4 b/s/Hz and 6 b/s/Hz, respectively, compared to GC-SIMO. The derived theoretical average error probability of the proposed scheme is validated by the results of the Monte Carlo simulation

4.2 Introduction

Recently, there has been a massive increase in the requirement for high bit rate in wireless communication. This led to multiple-input multiple-output (MIMO) systems, which have shown great promise regarding high transmission capacity and improved link reliability as the prospect of wireless communication [1-6]

MIMO systems split signals into bit streams for high data rate realization via the simultaneous transmission of information to multiple receivers. An iconic example of MIMO to consider is spatial modulation (SM) [7], a unique MIMO scheme, which employs innovatively transmit antennas for high data rate accomplishment.

The basic idea of Spatial Modulation (SM) is to convey information using both the amplitude/phase modulation (APM) and transmit antenna index. For example, a conventional MIMO system with 4 transmit antennas and 4 quadrature amplitude modulation (4-QAM) modulation order yields a data rate of 2 b/s/Hz while the same configuration in an SM system yields a data rate of 4 b/s/Hz. Similarly, the involvement of a single radio frequency (RF) chain in SM improves on the major setbacks experienced in the conventional MIMO system, for example, inter-antenna synchronization (IAS) and inter-channel interference (ICI) [7-11]. The improvements recorded in SM scheme have produced a great deal of research in MIMO systems [12-13].

Spatial diversity is a technique to improve link reliability through the channel's variation in frequency, time, and space with numerous copies of data received at the receiver. An example to consider is space-time block code (STBC) [14-16], a transmit diversity scheme, which employs precoding technique to send multiple copies of data from the obtainable transmit antennas to optimize the SNR and transmitting power with the suitable phase and amplitude. Two time-slots are required to transmit two symbols; hence, the data rate remains unchanged [14-15]. There is an improvement in the reliability of the link because of the transmitted redundant copies of data over an independent channel to the receiver. Furthermore, signal space diversity (SSD) [17-18] is another example, which achieves diversity via transmitting the in-phase and quadrature of the rotated multi-dimension signal to the receiver in an independent fading channel. Hence, achieving improved link reliability at no additional cost of hardware complexity, bandwidth, and transmit power.

For the next generation of wireless communication systems; energy efficiency, spectrum efficiency and complexity of the system are essential in supporting the demand for multimedia services and applications. [19-21] proposed Media-based modulation (MBM) to enhance high data rate transmission. Due to hardware and performance advantages of MBM, it has attracted recent research attention [22-25]. In the index modulation (IM) family [26], MBM has emerged as a promising technique, exhibiting greater benefits over the existing IM systems like frequency-domain (FD) IM (FD-IM) [26-27], space domain IM (SD-IM), also referred to as spatial modulation (SM) [8, 28] and time-domain IM (TD-IM) [29-30].

MBM exhibits a better performance when compared with conventional modulation schemes [14],[21],[23],[31]. Likewise, investigations of MBM in MIMO and multiuser settings also established improved performance of MBM [12],[24]. In addition, MBM [24], [32-34] can further improve link reliability at a lower hardware complexity.

MBM employing radio frequency (RF) mirrors reduce the imposed hardware complexity when compared to other spatial multiplexing techniques. This is due to the linear correlation between the spectral efficiency and the number of RF mirrors, which is achieved by creating different channel fade realizations via the RF mirrors, known as mirror activation patterns (MAPs) [24]. This is evident in [33], a SIMO aided MBM (SIMO-MBM) scheme, where the linear correlation between the spectral efficiency and the number of RF mirrors (m_{rf}) reduces the imposed system complexity. Considering an example of an equivalent SM system, which would require $2^{m_{rf}}$ transmit antennas to achieve the same spectral efficiency as SIMO-MBM. Consequently, in terms of data rate and hardware complexity, SIMO-MBM is more expedient than SM.

In MBM, the RF mirrors can be positioned side-by-side and the received constellation size is independent of the transmit power; while in conventional MIMO schemes, transmit antennas are adequately separated so as to achieve an independent fading. Thus, a large increase in spectral efficiency is easily realizable in MBM schemes [35-36].

In the literature [37-41], Golden code (GC) has been introduced as a scheme, which achieves a full rate full diversity employing precoding technique, considering different transmit antennas are employed at various time slots based on the idea of space time label diversity. In [38], GC modulation was investigated in single input multiple output (SIMO) systems, maintaining the same bandwidth efficiency, if a pair of super-symbols is transmitted coupled with an extra diversity gain been achieved. The computation complexity (CC) imposed in the GC-SIMO scheme of [37] is reduced by transmitting only the orthogonal pairs in the encoder, such that two symbols are

transmitted in total. This still achieves the extra diversity gain when compared to the conventional SIMO system.

Similarly, in [42], the MBM technique was investigated in GC modulation. The scheme employs four complex symbols to output the super-symbols termed the Golden codewords via the encoder. The super-symbols are transmitted via four independent transmit antennas in different time slots, such that four symbols are transmitted in total, achieving full rate and full diversity, considering each pair of these super-symbols are transmitted via multi-active transmit antennas and in a different time slot. However, the system complexity imposed in [42] is high, limiting practical implementation.

Considering MBM achieves a high data rate at a reduced hardware complexity. Therefore, incorporating the MBM technique in the GC-SIMO scheme employs only the super-symbol orthogonal pairs, i.e., only two symbols as against 4 in [42] in the encoder will achieve a high data rate similar to [37], at a reduced hardware complexity. This is my motivation in proposing media-based Golden codeword modulation for SIMO system termed GC-SIMO-MBM.

This paper presents the following contributions: a) we examine RF mirror-based MBM in a GC-SIMO scheme. b) Formulation of the theoretical ABEP for the proposed system (GC-SIMO-MBM) to be validated by the results of the monte carlo simulation.

The rest of the paper is structured in this order: The system model of the proposed GC-SIMO-MBM scheme is presented in section 2, the analysis of the average bit error rate (BER) and numerical analysis of the proposed scheme are shown in section 3 and section 4 respectively, while the conclusion drawn is presented in section 5.

Notation: Scalar quantities are represented by regular letters while vectors/matrices are indicated by Bold italic lowercase/uppercase symbols. $\|\cdot\|_F$ symbolises Frobenius norm, $Q(\cdot)$ denotes the Gaussian Q-function, $\underset{w}{\operatorname{argmin}}(\cdot)/\underset{w}{\operatorname{argmax}}(\cdot)$ signifies the minimum/maximum rate of an argument with reference to w , the binomial coefficient is represented by $\binom{\cdot}{\cdot}$, i is a complex number, the real component of the complex number is given by $R\{\cdot\}$, $|\cdot|$ signifies the Euclidean norm, $[\cdot]^T$ represent transpose and $\lfloor \cdot \rfloor$ indicates the closest integer to a lesser extent than the input argument.

4.3 System Model

In this segment, the concept of the Golden code is presented, thereafter, the system model of the proposed system is discussed.

4.3.1 A. The Golden Code

The Golden code exhibits full rate full diversity, employing precoding technique. The Golden code encoder employs 4 unique complex symbols to output 4 super-symbols, which are transmitted via unique independent transmit antennas in two-time slots. The Golden codeword matrix is given as [37, 42]:

$$\mathbf{X} = \begin{bmatrix} \alpha(x_1 + x_2\theta) \frac{1}{\sqrt{5}} & \gamma \bar{\alpha}(x_3 + x_4\bar{\theta}) \frac{1}{\sqrt{5}} \\ \alpha(x_3 + x_4\theta) \frac{1}{\sqrt{5}} & \bar{\alpha}(x_1 + x_2\bar{\theta}) \frac{1}{\sqrt{5}} \end{bmatrix}$$

where $\theta = \frac{1+\frac{1}{\sqrt{5}}}{2}$, $\bar{\theta} = 1 - \theta$, $\alpha = 1 + j\bar{\theta}$, $\bar{\alpha} = 1 + j(1 - \bar{\theta})$ and $\gamma = j$. Four super-symbols $\left(\alpha(x_1 + x_2\theta) \frac{1}{\sqrt{5}}, \gamma \bar{\alpha}(x_3 + x_4\bar{\theta}) \frac{1}{\sqrt{5}}, \alpha(x_3 + x_4\theta) \frac{1}{\sqrt{5}} \text{ and } \bar{\alpha}(x_1 + x_2\bar{\theta}) \frac{1}{\sqrt{5}} \right)$ are generated referred to as Golden codeword, which form two pairs of super-symbols $\left\{ \alpha(x_1 + x_2\theta) \frac{1}{\sqrt{5}}, \bar{\alpha}(x_1 + x_2\bar{\theta}) \frac{1}{\sqrt{5}} \right\}$ and $\left\{ \alpha(x_3 + x_4\theta) \frac{1}{\sqrt{5}}, \gamma \bar{\alpha}(x_3 + x_4\bar{\theta}) \frac{1}{\sqrt{5}} \right\}$. The pair $\left\{ \alpha(x_1 + x_2\theta) \frac{1}{\sqrt{5}}, \bar{\alpha}(x_1 + x_2\bar{\theta}) \frac{1}{\sqrt{5}} \right\}$ is employed for transmission in the proposed system.

4.3.2 B . Proposed GC-SIMO-MBM

System Model of the Proposed GC-SIMO-MBM scheme is shown in figure 4.1. The spectral efficiency associated with the proposed GC-SIMO-MBM scheme is: $m = \log_2(M) + m_{rf}$ b/s/Hz, where M and m_{rf} represents the amplitude/phase modulation (APM) constellation size and the number of RF mirrors at the transmitting unit, respectively.

In the proposed GC-SIMO-MBM, the input bit $\log_2(M)$ is fed into the mapper Ω_1 and Ω_2 to map the $\log_2(M)$ bits onto the constellation points from the signal set of $\alpha(x_1 + x_2\theta)^{\frac{1}{\sqrt{5}}}$ and $\bar{\alpha}(x_1 + x_2\bar{\theta})^{\frac{1}{\sqrt{5}}}$ in the Argand plane, which yields two super-symbols x_q^1 and x_q^2 . In addition, the m_{rf} bit chooses the RF mirror to be used for transmission. The number of available RF mirrors m_{rf} , yields the mirror activation pattern (MAP), such that $N_m = 2^{m_{rf}}$, for example, if $m_{rf} = 2$, hence, $N_m = 4$.

The modulated symbol is conveyed across a channel \mathbf{H}_i of magnitude $N_R \times N_m$ in the presence of additive white Gaussian noise (AWGN) \mathbf{n}_i of magnitude $N_R \times 1$, \mathbf{e}_{ℓ_i} is an $N_m \times 1$ vector. A Rayleigh frequency-flat fading channel is assumed. Therefore, the received signal vector \mathbf{y}_i can be written as:

$$\mathbf{y}_i = \mathbf{H}_i x_q^i \mathbf{e}_{\ell_i} + \mathbf{n}_i \quad (4.1)$$

where $i \in [1:2]$, the corresponding transmit antenna employed to transmit the modulated symbol is represented by ℓ_i , while \mathbf{H}_i is the i^{th} column of the channel matrix, which is independent and identically distributed (i.i.d) complex Gaussian random variables distributed as $CN(0,1)$.

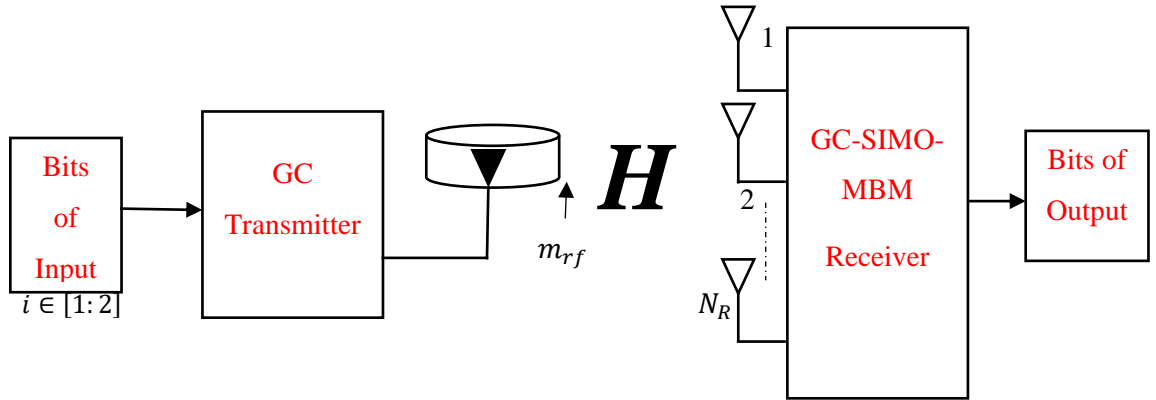


Figure 4.1 System Model of the Proposed GC-SIMO-MBM

4.4 Maximum Likelihood (ML) Detector

Utilizing the ML detector at the receiver, the received signal vector \mathbf{y}_i is detected optimally which examines the total signal space of M^2 constellation points combined with all possible transmit antenna index. The ML detector can be defined as:

$$[\hat{\ell}_1, \dots, \hat{\ell}_i, x_{\hat{q}}^i] = \underset{\ell \in [1:i]}{\operatorname{argmin}} \left(\|\mathbf{y}_i - \mathbf{H}_i x_{\hat{q}}^i \mathbf{e}_{\ell_i}\|_F^2 \right) \quad (4.2)$$

4.5 Performance Analysis of GC-SIMO-MBM

The average BER for the proposed GC-SIMO-MBM is formulated in this section. Similar to [27], the ABEP is defined as:

$$P_e \leq \frac{1}{2N_m M^2 m} \sum_{q=1}^{N_m M^2} \sum_{\hat{q} \neq q}^{N_m M^2} N(i, \hat{i}) P(\mathbf{X}_q \rightarrow \mathbf{X}_{\hat{q}}) \quad (4.3)$$

where $P(\mathbf{X}_q \rightarrow \mathbf{X}_{\hat{q}})$ symbolizes the pairwise error probability (PEP) of $\mathbf{X}_{\hat{q}}$ is detected at the receiver given that \mathbf{X}_q is transmitted, $\mathbf{X}_q = (x_q^1, x_q^2)$ and $\mathbf{X}_{\hat{q}} = (x_{\hat{q}}^1, x_{\hat{q}}^2)$, $N(i, \hat{i})$ stand for the bit error connected with the PEP event. Similar to [31], the conditional PEP may be defined as:

$$\begin{aligned} P(\mathbf{X}_q \rightarrow \mathbf{X}_{\hat{q}} | \mathbf{H}_i) &= P \left(\|\mathbf{y}_i - \mathbf{H}_i x_q^i \mathbf{e}_{\ell_i}\|_F < \|\mathbf{y}_i - \mathbf{H}_i x_{\hat{q}}^i \mathbf{e}_{\ell_i}\|_F | \mathbf{H}_i \right) \\ &= P \left(\sum_{i=1}^2 \|\mathbf{H}_i x_q^i \mathbf{e}_{\ell_i} - \mathbf{H}_i x_{\hat{q}}^i \mathbf{e}_{\ell_i}\|_F^2 < \sum_{i=1}^2 \|\mathbf{n}\|_F^2 \right) \\ &= Q \left(\sum_{i=1}^2 \alpha_i \right) \end{aligned} \quad (4.4)$$

where α_i is central chi-squared distribution with $2N_R$ degrees of freedom defined as:

$$\frac{\rho}{2} \|\mathbf{H}_i\|_F^2 |d_x^i|^2 = \sum_{k=1}^{2N_R} \alpha_i^2 \text{ with } N(0, \sigma^2), \sigma^2 = \frac{\rho}{4} |d_x^i|^2.$$

Evaluating the probability density function (PDF) of α_i^2 , employing $f_{\alpha_i}(\alpha_i) = \frac{\alpha_i^{N_R-1} e^{-\alpha_i/2\sigma^2}}{(2\sigma^2)^{N_R} (N_R-1)!}$ similar to the PEP derivation of the GC-SIMO of [37], coupled with the trapezoidal approximation

of the Q-function given in [17], it may be validated that the PEP for GC-SIMO-MBM can be defined as:

$$\frac{1}{4n} \left[\frac{1}{2} \prod_{i=1}^2 \left(\frac{\rho}{4} |d_x^i|^2 \right)^{-N_R} + \sum_{k=1}^{n-1} \prod_{i=1}^2 \left(\frac{\rho}{4} \frac{|d_x^i|^2}{u_k} \right)^{-N_R} \right] \quad (4.5)$$

where ρ represent the signal-to-noise ratio (SNR), $n > 10$ for trapezoidal approximation convergence of the Q-function [11], $i \in [1:2], k \in [1:2N_R]$, $u_k = \sin^2\left(\frac{k\pi}{2n}\right)$ and $|d_x^i|^2 = |x_q^i - x_{\hat{q}}^i|^2$.

4.6 Numerical Analysis and Discussion

The results of the MCS obtained for the proposed GC-SIMO-MBM scheme is presented in this section. Average BER vs average SNR in dB is considered. Likewise, the result of the evaluated theoretical ABEP is presented. In all cases, ML detector is utilized. The notation (N_T, N_R, M, m_{rf}) is employed for GC-SIMO-MBM and SIMO-MBM scheme.

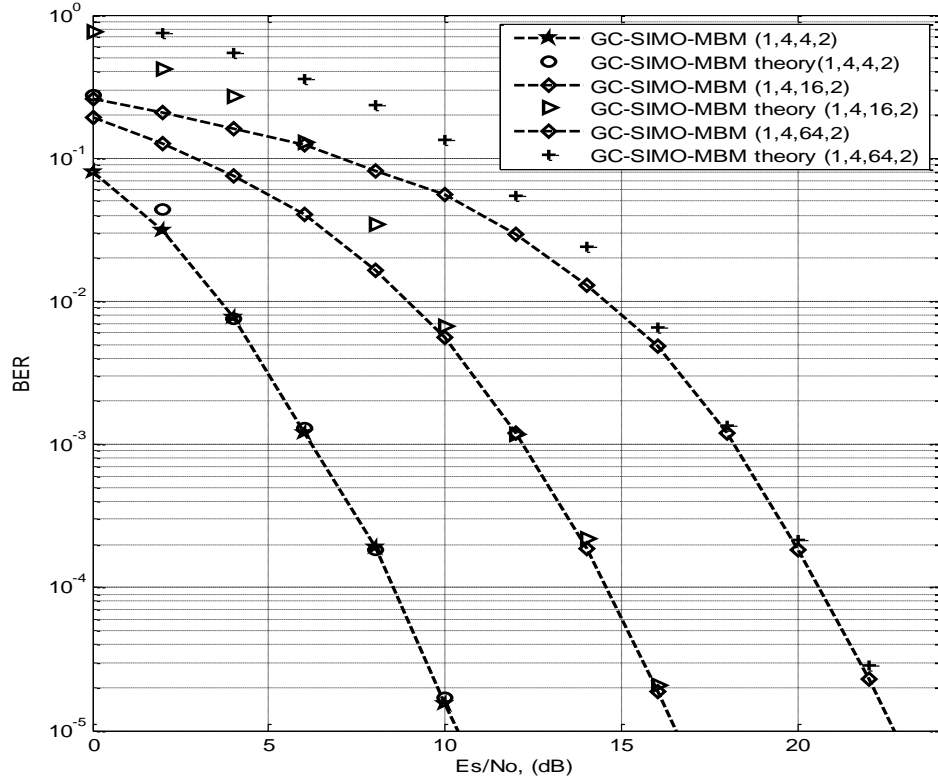


Figure. 4.2 Performance analysis validation for GC-SIMO-MBM for 4 b/s/Hz, 6 b/s/Hz and 8 b/s/Hz, respectively.

In Figure. 4.2, the GC-SIMO-MBM scheme is equipped with a configuration setting of 1×4 4-QAM, 1×4 16-QAM and 1×4 64-QAM, both with 2 RF mirrors around each transmit antenna, i.e. $m_{rf} = 2$. This yields a spectral efficiency of 4 b/s/Hz, 6 b/s/Hz and 8 b/s/Hz, respectively. The results of MC simulation obtained showed a close match with the average theoretical analysis at the high SNR region, validating the proposed scheme.

Figures 4.3(a) and 4.3(b) presents the performance comparison between the GC modulation of [37], SIMO-MBM and the proposed GC-SIMO-MBM system with the same spectral efficiency of 4 b/s/Hz and 6 b/s/Hz, respectively. The Monte Carlo simulation results revealed that GC-SIMO-MBM outperforms its counterpart in 4 b/s/Hz and 6 b/s/Hz, respectively.

It is obvious from the results of MC simulation obtained that utilizing the MBM technique based on RF mirrors improves the system's error performance at a reduced hardware complexity. At a BER of 10^{-5} , the GC-SIMO-MBM exhibits a significant performance of approximately 7dB and 6.5 dB SNR gain for 4 b/s/Hz and 6 b/s/Hz, respectively, compared to GC-SIMO of [27]. Likewise, GC-SIMO-MBM outperform SIMO-MBM by 5 dB and 3.5 dB in 4 b/s/Hz and 6 b/s/Hz, respectively. The notation (N_T, N_R, M) is employed for GC modulation of [37].

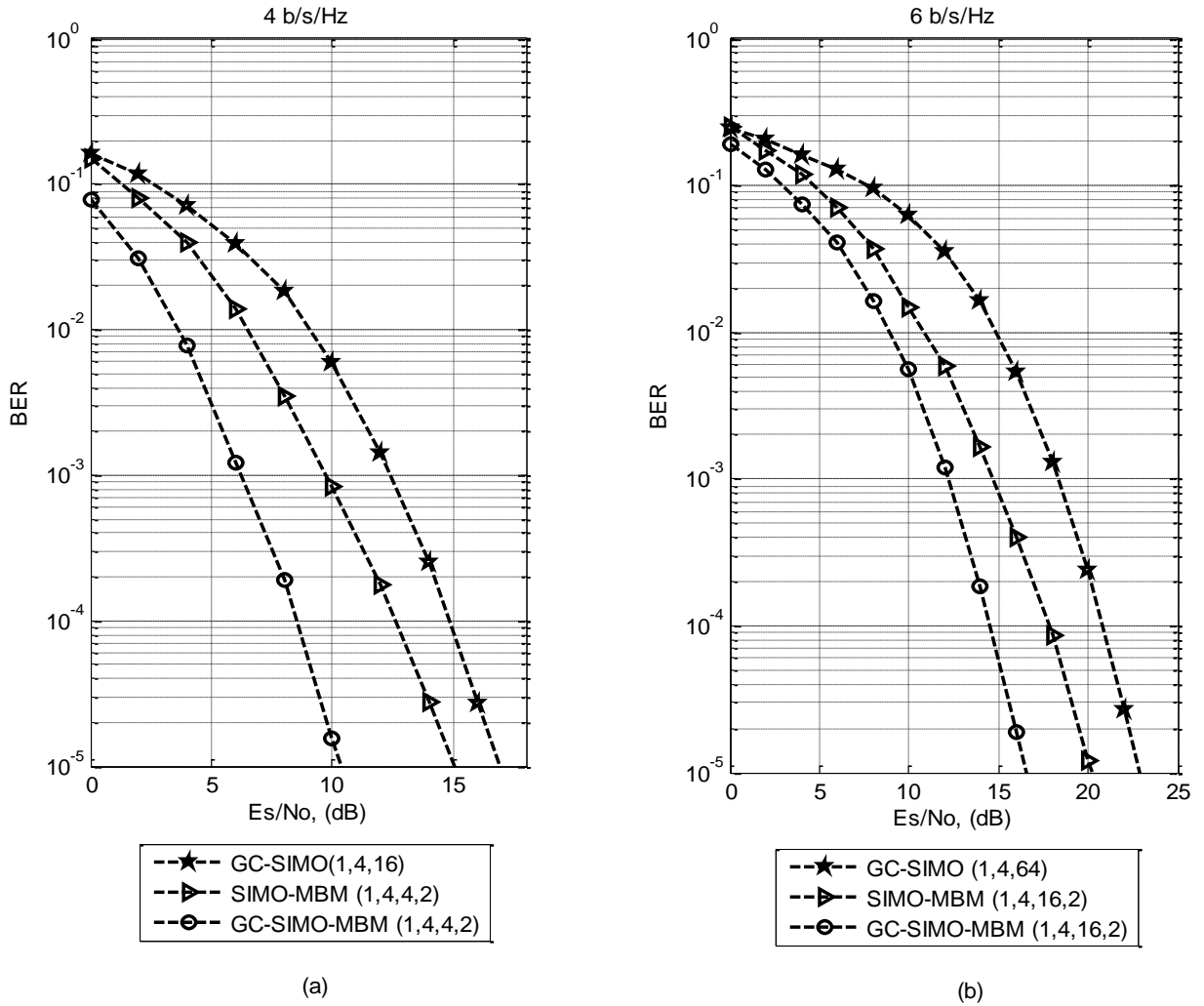


Figure 4.3 Performance comparison of GC-SIMO-MBM, GC-SIMO and SIMO-MBM for 4 b/s/Hz and 6 b/s/Hz, respectively.

4.7 Conclusion

In this paper, media-based modulation was examined in the GC-SIMO scheme, based on the RF mirror to improve its error performance, and enhance spectral efficiency. The topology based on the GC-SIMO-MBM technique demonstrates an enhanced error performance compared to the SIMO-MBM and GC-SIMO of the same spectral efficiency. Results of Monte Carlo Simulation indicate that the GC-SIMO-MBM shows a significant performance of approximately 7dB and 6.5 dB SNR gain for 4 b/s/Hz and 6 b/s/Hz, respectively, compared to GC-SIMO at a BER of 10^{-5} . The proposed GC-SIMO-MBM system validated by theoretical and numerical results has shown that the scheme is capable of significantly improving the system's hardware complexity,

maximizing the linear relationship between RF mirrors and the spectral efficiency in MBM to accomplish a high data rate at a reduced hardware complexity by employing the orthogonal pairs of the super-symbol in the GC scheme's encoder and transmitted via different RF mirror at a different time slot to achieve full rate full diversity.

4.8 References

- [1] A. Goldsmith "Wireless Communicatios",1st ed., New York: Cambridge University Press, 2005.
- [2] S. Patel, T. Quazi, and H. Xu, "High-rate uncoded space-time labelling diversity with low-complexity detection", *Int. J. of Commun. Syst.*, vol. 33, no. 14, e4520, 2020 .
- [3] T. Quazi and H. Xu, "SSD enhanced uncoded space-time labeling diversity", *Int. J. of Commun. Syst.*, vol. 31, no. 11, e3592, 2018.
- [4] A. Evans, T. Quazi, and H. Xu, "BER performance of a maximum ratio transmission enhanced hierarchical quadrature amplitude modulation (MRT-HQAM) system over Rayleigh fading channels", *IET Commun.*, vol. 10, no. 17, pp. 2473-2479, 2016.
- [5] T. Quazi and H. Xu, "Simple UEP mechanism for multimedia traffic using the Alamouti structure with hierarchical modulation and signal space diversity", *IET Commun.*, vol. 8, no. 17, pp. 3128-3135, 2014.
- [6] S. Solwa, M. K. Elmezughi, A. J. Bamisaye, D. Ayanda, A. Almaktoof, and M. T. E. Kahn, "Genetic algorithm-based uncoded M-ary phase shift keying space-time labelling diversity with three transmit antennas for future wireless networks", in *Proc. of the 9th Int. Conf. on Elec. and Electron. Engin. ICEEE2022*, Alanya, Turkey, 2022, pp. 423-428.
- [7] N. R Naidoo, H., Xu and T. Quazi, "Spatial modulation: optimal detector asymptotic performance and multiple-stage detection," *IET Communications*, vol. 5, pp. 1368 - 1376, Aug. 2019.
- [8] R. Y. Mesleh, H. Haas, S. Sinanovic, C. W. Ahn and S. Yun, "Spatial Modulation,"*IEEE Transactions on Vehicular Technology*, vol. 57, no. 4, pp. 2228-2241, July 2008.
- [9] Z. Pan, J. Luo, J. Lei, L. Wen and C. Tang, "Uplink Spatial Modulation SCMA System," *IEEE Communications Letters*, vol. 23, no. 1, pp. 184-187, Jan. 2019.
- [10] C. Zhong, X. Hu, X. Chen, D. W. K. Ng and Z. Zhang, "Spatial Modulation Assisted Multi-Antenna Non-Orthogonal Multiple Access,"*IEEE Wireless Communications*, vol. 25, no. 2, pp. 61-67, April 2018.

- [11] A. Khalid, T. Quazi, H. Xu, and S. Patel, "Performance analysis of M -APSK generalised spatial modulation with constellation reassignment", *Int. J. of Commun. Syst.*, vol. 33, no. 14, e4497, 2020.
- [12] A. Bhowal, R. Lalani, A.S Sapre, R and R.S Kshetrimayum. "Advanced spatial modulation for efficient MIMO-based B2B communications in sporting Activities," *IET Comm.*, Vol. 13 Is. 20, pp. 3529-3536, 2019.
- [13] A. Bhowal and R.S Kshetrimayum. "Advanced Optical Spatial Modulation Techniques for FSO Communication," *IEEE Transactions on Communications*, vol. 69, no. 2, pp. 1163-1174, Feb. 2021.
- [14] T. Liu, "Analysis of the Alamouti STBC MIMO System With Spatial Division Multiplexing Over the Rayleigh Fading Channel," *IEEE Transactions on Wireless Communications*, vol. 14, no. 9, pp. 5156-5170, Sept. 2015.
- [15] E. Basar, U Aygolu, E. Panayirci, and H.V Poor. "Space-Time Block Coded Spatial Modulation," *IEEE Transactions on Wireless Communications*, vol. 59, pp. 823-832, 2011.
- [16] A. Saeed, H. Xu, T. Quazi, "Alamouti Space-Time Block Coded Hierarchical Modulation with Signal Space Diversity and MRC Reception in Nakagami- m Fading Channel. In: IET proceedings Communications, vol 8, No 4, pp:516-524, Mar, 2014.
- [17] J. Boutros and E. Viterbo, "Signal space diversity: a power- and bandwidth-efficient diversity technique for the Rayleigh fading channel," *IEEE Transactions on Information Theory*, vol. 44, no. 4, pp. 1453-1467, July 1998.
- [18] A. Saeed, T. Quazi, Hongjun Xu, "Hierarchical Modulated QAM with Signal Space Diversity and MRC Reception in Nakagami- m fading channels. In: IET proceedings Communications. vol 7, No 12, pp:1296-1303, Aug, 2013
- [19] A. K Khandani. "Media-based modulaiton: Converting static Rayleigh fading to awgn," in *2014 IEEE International Symposium on Information Theory*, Honolulu, HI, USA, pp. 1549–1553, June 2014.

- [20] T. Mao, Q. Wang, Z. Wang, Z and S. Chen. “Novel index modulation techniques: A survey,” *IEEE Communicatons Surveys and Tutorials*, Early Access, vol. 21, no. 1, pp. 315-348, Firstquarter 2019.
- [21] Y. Naresh, and A. Chockalingam, “On Media-Based Modulation Using RF Mirrors” *IEEE Transactions on Vehicular Technology*, Vol. 66, No. 6, pp 4967-4983, June 2017
- [22] E. Seifi, M. Atamanesh and A. K. Khandani, "Media-based MIMO: Outperforming known limits in wireless," 2016 IEEE International Conference on Communications (ICC), pp.1-7, 2016.
- [23] E. Seifi, M. Atamanesh, and A. K Khandani. “Performance evaluation of media-based modulation in comparison with spatial modulation and legacy SISO/MIMO,” in *Proc. Biennial Symp. Commun.*, pp. 1–6, 2016.
- [24] Y. Naresh and A. Chockalingam.. “On media-based modulation using RF mirrors,” *IEEE Trans. Veh. Tech.*, vol. 66, no. 6, pp. 4967–4983, June 2017.
- [25] Y. Naresh and A. Chockalingam. “A low-complexity maximum likelihood detector for differential media-based modulation,” *IEEE Commun. Lett.*, vol. 21, no. 10, pp. 2158–2161, Oct. 2017.
- [26] E. Basar “Index modulation techniques for 5G wireless networks,” *IEEE Commun. Mag.*, vol. 54, no. 7, pp. 168–175, July 2016.
- [27] M. Wen, E. Basar, Q. Li, B. Zheng, and M. Zhang,. “Multiple-mode orthogonal frequency division multiplexing with index modulation,” *IEEE Trans. Commun.*, vol. 65, no. 9, pp. 3892–3906, Sept. 2017.
- [28] M.D Renzo, H. Haas and P.M Grant. “Spatial modulation for multipleantenna wireless systems: A survey,” *IEEE Commun. Mag.*, vol. 49, no. 12, pp. 182–191, Dec. 2011.
- [29] M. Nakao, T. Ishihara and S. Sugiura, "Single-Carrier Frequency-Domain Equalization With Index Modulation," *IEEE Communications Letters*, vol. 21, no. 2, pp. 298-301, Feb. 2017.

- [30] M. Nakao, T. Ishihara, and S. Sugiura.. “Dual-mode time-domain index modulation for Nyquist-criterion and faster-than-Nyquist single-carrier transmissions,” *IEEE Access*, vol. 5, pp. 27659–27667, Nov. 2017.
- [31] Y. Naresh and A. Chockalingam. “Performance Analysis of Media-Based Modulation With Imperfect Channel State Information” *IEEE Trans. Veh. Technol.*, vol. 67, no. 5, pp. 4192–4207, May. 2018.
- [32] N. Pillay and H. Xu. "Quadrature Spatial Media-based Modulation with RF Mirrors," *IET Communications*, vol. 11, pp. 2440-2448, Nov. 2017.
- [33] R. Pillay, N. Pillay, and H. Xu. "A Study of Single-Input Multiple-Output Media-based Modulation with RF Mirrors," in *Proceedings of the Southern Africa Telecommunication Networks and Applications Conference (SATNAC)*, pp. 20-25, 2017.
- [34] T. Mao, Q. Wang, M. Wen and Z. Wang, "Secure Single-Input-Multiple-Output Media-Based Modulation," *IEEE Transactions on Vehicular Technology*, vol. 69, no. 4, pp. 4105-4117, April 2020.
- [35] A.J Bamisaye and T. Quazi “Two-way Decode and Forward Quadrature Media-based Modulation for Single-Input Multiple-Output Scheme” *International Journal of Communication System* 2022;e5186. <https://doi.org/10.1002/dac.5186>.
- [36] A.J Bamisaye and T. Quazi. “Quadrature spatial modulation-aided single-input multiple output- media-based modulation”. *International Journal of Communication System* Vol.34, no 11, 2021;e4883. <https://doi.org/10.1002/dac.4883>
- [37] H. Xu, and N. Pillay. ."Golden Codeword based Modulation Schemes for Single-Input Multiple-Output Systems", *International journal of Communication. Systems*, pp. 1-12, April 2019.
- [38] L. Luzzi, G. R. Othman, J. Belfiore and E. Viterbo, "Golden Space–Time Block-Coded Modulation," *IEEE Transactions on Information Theory*, vol. 55, no. 2, pp. 584-597, Feb. 2009.

- [39] J. Belfiore, G. Rekaya, and E. Viterbo. "The Golden Code: A 2×2 Full-Rate Space-Time Code with Nonvanishing Determinants," *IEEE Transactions on Information Theory*, vol. 51, no. 4, pp. 1432-1436, April 2005.
- [40] H. Xu and N. Pillay. "The Component-Interleaved Golden Code and Its Low-Complexity Detection," *IEEE Access*, vol. 8, pp. 59550–59558, March 2020.
- [41] H. Xu and N. Pillay. "Multiple Complex Symbol Golden Code," *IEEE Access*, vol. 8, pp. 103576–103584, May, 2020.
- [42] N. Pillay and H. Xu. "RF Mirror Media-based Modulation for Golden Codes," *Journal of telecommunication electronic and computer engineering*, vol. 10, no.3, pp. 21-24., Aug. 2018.

Chapter 5

Conclusion

5.1 Conclusion

QSM is a form of innovative MIMO scheme, which conveys additional information by extending its spatial dimension to the in-phase and quadrature dimensions. In QSM, the APM symbols are decomposed into its real and imaginary components, which are respectively modulated into cosine and sine carriers. Hence, it made a single RF chain requirement possible, which is more energy-efficient than GSM and exhibits an improved error performance than SM and GSM.

Media-based modulation (MBM) has been proven as a more efficient technique to achieve a high data rate at the cost of low hardware complexity. This is accomplished by utilizing RF mirrors to produce various channel fade realizations, classified as mirror activation patterns (MAPs). In MBM, a subset of channel realizations may be chosen from the unique channel perturbations. Also, the received constellation size is independent of the transmit power. An additional advantage of the MBM scheme is that placement of RF mirrors side-by-side is achievable.

Single-input multiple-output media-based modulation (SIMO-MBM) improves the limitation of single-input multiple-output (SIMO) systems by minimizing the required number of antennas to achieve a high data rate and enhanced error performance.

In this thesis, the application of quadrature dimension of the spatial constellation was investigated in a media-based modulation SIMO scheme by decomposing the amplitude/phase modulation (APM) symbol into real and imaginary components similar to quadrature spatial modulation (QSM). This is to improve the spectral efficiency of the scheme's coupled with improving the overall error performance of the system and to achieve a higher data rate. The MCS results obtained revealed the improvement of 3.5dB, 2.5dB and 3.5dB at 6b/s/Hz, 8b/s/Hz and 10b/s/Hz, respectively at BER of 10^{-5} with $m_{rf} = 2$. Likewise, an improvement of 6.5dB and 7dB at 10b/s/Hz and 12b/s/Hz, respectively at BER of 10^{-5} was revealed with $m_{rf} = 4$ over the conventional SIMO-MBM system. In addition, the effect of sub-optimal MAP selection algorithm was investigated in the proposed scheme employing the channel amplitude coupled with antenna correlation to select the best channel for transmission at every transmission instant. The MCS results show that the MAP selection algorithm further improves the proposed scheme's error performance, with the norm-correlation scheme being superior.

Furthermore, cooperative relay-based communication systems have shown tremendous promise in enhancing wireless link quality, reliability, and spectral efficiency. This is achieved by employing multiple relay nodes (active or passive nodes) as a virtual antenna to re-transmit user

information. Two-way relaying has been proven as a spectral efficient relaying scheme. This technique employs two or more source nodes, simultaneously transmitting a message block on the same time slot to the relay node. Each source node transmits its modulated message block towards the relay node, such that the relay node is the receiver. The relay node receives and computes the message from the source nodes and transmit them to the appropriate destination nodes. The two-way DF scheme was investigated with QSM aided SIMO-MBM to improve the reliability of the QSM aided SIMO-MBM system. The decode and forward relaying technique was utilized; this was achieved by employing a relaying node, which received the message signal from two source nodes, decoded the received signal using network coding techniques, and then re-transmitted the message to its destination.

The MCS results obtained revealed the improvement of 8 dB and 12 dB at 6b/s/Hz and 8b/s/Hz, respectively at a BER of 10^{-5} , over the conventional QSM aided SIMO-MBM. Likewise, the result obtained exhibits that the system configuration with $m_{rf} = 2$ outperform the configuration with $m_{rf} = 4$ for the proposed scheme. This thesis assumed full channel knowledge.

Golden code (GC) has been introduced as a scheme, which achieves a full rate full diversity employing precoding technique, considering different transmit antennas are employed at different time slots based on the concept of space time label diversity. Media-based modulation was examined in the GC-SIMO scheme, based on the RF mirror to improve its error performance, and enhance spectral efficiency. The topology based on the GC-SIMO-MBM technique demonstrates an enhanced error performance compared to the SIMO-MBM and GC-SIMO of the same spectral efficiency.

Results of MCS indicate that the GC-SIMO-MBM shows a significant performance of approximately 7dB and 6.5 dB SNR gain for 4 b/s/Hz and 6 b/s/Hz, respectively, compared to GC-SIMO at a BER of 10^{-5} . The proposed GC-SIMO-MBM system validated by theoretical and numerical results has shown that the scheme is capable of significantly improving the system's hardware complexity, maximizing the linear relationship between RF mirrors and the spectral efficiency in MBM to accomplish a high data rate at a reduced hardware complexity by employing the orthogonal pairs of the super-symbol in the GC scheme's encoder and transmitted via different RF mirror at a different time slot to achieve full rate full diversity.

The effect of imperfect channel estimation on the proposed QSM aided SIMO-MBM scheme was investigated, with a trade-off of 2dB in coding gain due to channel estimation errors. A similar

conclusion is expected in the systems studied in journals 2 and 3 since the methodology of the schemes is the same, however the verification of this is left as future work.

5.2 Summary of Contributions and Results

The following are a summary of the major research contributions and findings provided in this thesis:

- a. Chapter 2 Investigated RF mirror-based MBM in a SIMO-based QSM system, by decomposing the APM symbol prior to transmission and employing unique (different) RF mirrors to transmit the decomposed APM symbol in a SIMO scheme.

From the MC simulation results achieved, it is apparent that utilizing the quadrature dimension of the spatial constellation improves the scheme's system performance. At a BER of 10^{-5} , an SNR gain of approximately 3.5dB, 2.5dB and 3.5dB at 6b/s/Hz, 8b/s/Hz and 10b/s/Hz, respectively with $m_{rf} = 2$ at BER of 10^{-5} . Likewise, an improvement of 6.5dB and 7dB at 10b/s/Hz and 12b/s/Hz, respectively was revealed with $m_{rf} = 4$ over the conventional SIMO-MBM system. Thus, this is achieved by maximizing the system's transmit diversity via employing the quadrature dimension of the APM symbol.

The performance comparison between QSM aided SIMO-MBM with different configuration settings ($m_{rf} = 2$ and $m_{rf} = 4$) are considered, respectively. The MCS results revealed that the configuration settings with $m_{rf} = 2$ exhibits an improved system performance compared with its counterparts. The proposed system equipped with $m_{rf} = 2$ outperforms its counterpart equipped with $m_{rf} = 4$ by an SNR gain of approximately 3dB for 4-QAM, 2dB for 16-QAM and 1dB for 64-QAM, respectively

- b. The theoretical ABEP is formulated for QSM aided SIMO-MBM to be validated by the simulation results.

The MC simulation results achieved show a tight fit in the higher SNR region with the average theoretical result achieved confirming the theoretical expression.

- c. To further improve QSM aided SIMO-MBM error performance, the impact of MAP selection based on processing the channel amplitude and antenna correlation to remove the imperfect channel(s) at each transmission instance is studied on the QSM aided SIMO-MBM scheme.

The MCS results achieved for the QSM aided SIMO-MBM scheme with the MAP selection algorithm exhibit superior performance than the traditional SIMO-MBM scheme. However, QSM aided SIMO-MBM beats all other schemes when using the MAP selection algorithm, which is based on antenna norm-correlation with approximately 4dB and 5.5dB with respect to conventional QSM aided SIMO-MBM and SIMO-MBM, respectively.

This is because the amplitude of the MAPs is maximized while the correlations between the MAPs are minimized.

- d. Investigation of the impact of imperfect channel estimation on the proposed QSM aided SIMO-MBM.
- e. Chapter 3 proposed a two-way DF-QSM aided SIMO-MBM relaying technique with two source nodes.

It is evident from the MCS results that two-way DF-QSM aided SIMO-MBM with $m_{rf} = 2$ achieves an improved system performance of approximately 3dB at 10^{-5} when compared with $m_{rf} = 4$. Similarly, based on the MCS results obtained, it is evident that exploiting the quadrature dimension of the spatial constellation coupled with two-way relay transmission improves the scheme's system performance. A SNR gain of 8 dB and 12 dB is achieved for the 6 b/s/Hz and 8 b/s/Hz two-way DF-QSM aided SIMO-MBM, respectively at a BER of 10^{-5} over QSM aided SIMO-MBM. In the two-way DF-QSM-MBM-SIMO, two source nodes are considered; hence, the system's spectral efficiency is doubled i.e., 2m bits. Therefore, doubling the spectral efficiency required for the conventional QSM aided SIMO-MBM. Consequently, this is accomplished by maximizing the systems' transmit and cooperative diversity and utilizing the QSM aided MBM as the adopted modulation at all nodes in the two-way relay system.

- f. Theoretical analysis formulation for DF-QSM aided SIMO-MBM and validation of the results with the MCS results obtained.

The average theoretical result obtained shows a close match with the MCS result, verifying the theoretical expression.

- g. Chapter 4 investigated RF mirror-based MBM in a GC-SIMO system. The MCS showed that GC-SIMO-MBM outperforms its counterpart in 4 b/s/Hz and 6 b/s/Hz, respectively. It is obvious from the results of MC simulation obtained that utilizing the MBM system based on RF mirrors improves the system's error performance at a reduced hardware complexity. At a BER of 10^{-5} , the GC-SIMO-MBM exhibits a significant performance of approximately 7dB

and 6.5 dB SNR gain for 4 b/s/Hz and 6 b/s/Hz, respectively, compared to GC-SIMO. Likewise, GC-SIMO-MBM outperform SIMO-MBM by 5 dB and 3.5 dB in 4 b/s/Hz and 6 b/s/Hz, respectively.

- h. The theoretical average bit error probability (ABEP) formulation for GC-SIMO-MBM to be validated by the simulation results obtained.

The results of MC simulation obtained showed a close match with the average theoretical analysis at the high SNR region, validating the proposed scheme.

5.3 Suggestion for further research

The investigation of the effect of IChE on systems 2 and 3 can be done.

The error performance of QSM-MBM methods based on large intelligent surfaces (LIS) can be investigated. Additionally, there are still unresolved research questions regarding the performance evolution of LIS-assisted Index Modulation with erroneous phase estimate at various fading channels.

The impact of near-optimal or sub-optimal detector can also be considered on QSM aided SIMO-MBM and DF-QSM-SIMO-MBM.

The influence of different channel imperfections couple with near-optimal or sub-optimal detector can be studied on QSM aided SIMO-MBM and DF-QSM-SIMO-MBM with two-way relaying for future work.

